Controlling the position and the electronic structure of quantum dots

Armando Rastelli

HFP | Institute of Semiconductor and Solid State Physics

Institute of Semiconductor and Solid State Physics,
Johannes Kepler University Linz (Austria)

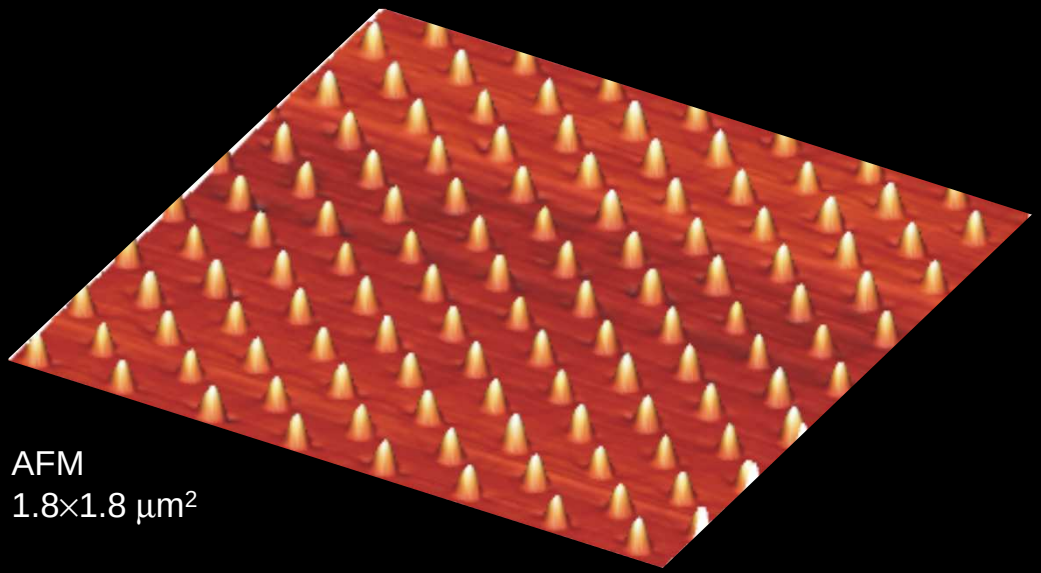

AFM
1.8×1.8 μm²

Outline

1. Introduction:

1.1 Quantum dots: basic properties

1.2 Methods to obtain QDs via self-assembly

1.3 Some applications of ensembles and of single epitaxial QDs

1.4 Why do controlled position and electronic properties matter?

2. Approaches to position QDs

2.1 Top-down: Lateral confinement in QWs

2.1.a Deep etching

2.1.b Shallow etching

2.1.c Selective annealing

2.1.d Selective diffusion

2.1.e Electrical gating

2.2 Bottom-up + Top down

2.2.a QD location followed by device fabrication

2.2.b In-situ lithography

Outline

2.3 Top down + Bottom-up
- 2.3.a SK growth on mesas
- 2.3.b SK growth on buried stressors
- 2.3.c SK growth in grooves and pits
- 2.3.d Lattice-matched heterostructure grown on pits
- 2.2.e Self-limited growth of pits + filling

3. Post-growth control of electronic structure of single QDs
- 3.1 Post-growth thermal treatment (irreversible)
- 3.2 Electric fields – quantum confined Stark effect
- 3.3 Piezoelectric-induced strain
- 3.4 Combination of strain and electric field
- 3.5 Full-control of in-plane stress in QD matrix

1.1 What is a semiconductor quantum dot (QD)?

A system confining the motion of charge carriers in all directions in regions of space sufficiently small to make quantization effects significant

➡ Solid-state realization of the "quantum box" concept

in 1D: potential well (see, e.g. L.I. Schiff, *Quantum mechanics,* McGraw-Hill, 1952)

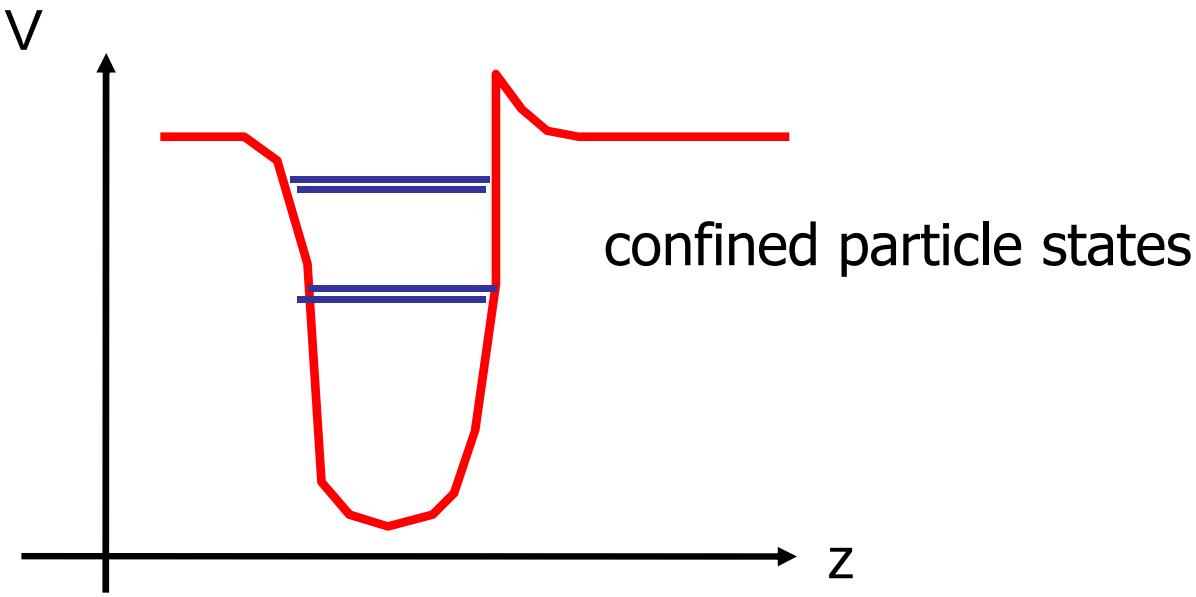

In a semiconductor, the potential profile depends on the used materials, strain... and is different for electrons and holes

How small should a quantum dot be?

Approximation: cubic box with infinitely deep barriers

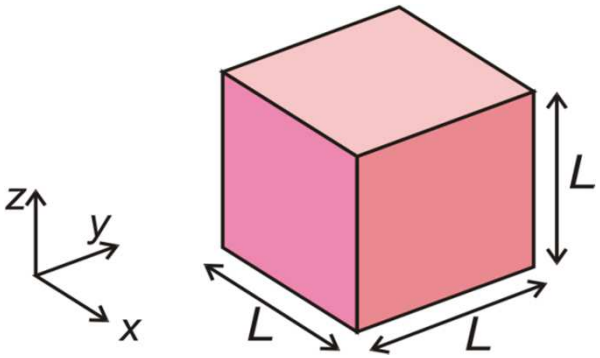

$$V(x,y,z)=\begin{cases}0 & 0 < x,y,z < L \\ \infty & \text{otherwise}\end{cases}$$

Schrödinger equation for the envelope wave-function:

$$\left[-\frac{\hbar^2}{2m^*}\nabla^2+V(\vec{r})\right]\psi(\vec{r})=E\psi(\vec{r})$$

m^*: effective mass of electron or hole

Eigenvalues:

$$E(n_x,n_y,n_z)=\frac{\pi^2\hbar^2}{2m^*L^2}(n_x^2+n_y^2+n_z^2) \qquad n_x,n_y,n_z=1,2,3,\ldots$$

How small should a quantum dot be?

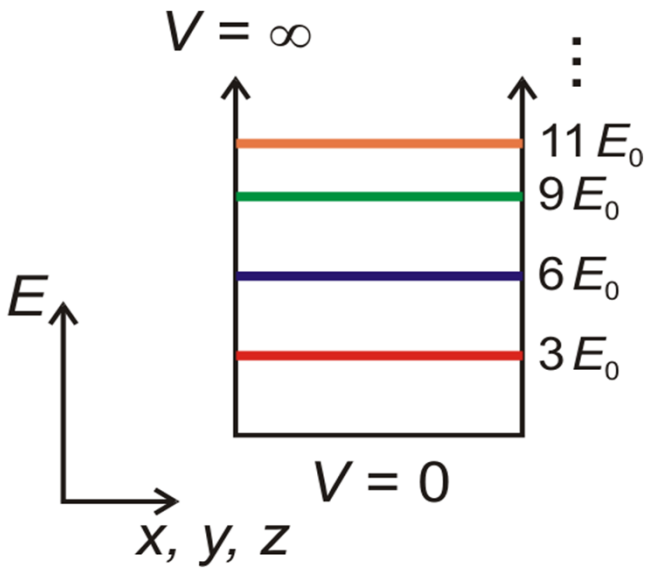

$$E_0 = \frac{\pi^2 \hbar^2}{2m^* L^2}$$

for electrons in GaAs
$m_e^* \sim 0.063\, m_0$

One possible criterion to say that effects of confinement are significant: level separation >> $K_B T$

➡ $3E_0 >> K_B T \quad L << \pi\hbar \sqrt{\frac{3}{2m^* K_B T}} \sim 26\ nm$ (for GaAs at T=300 K)

Similar conclusion can be reached by asking that $L <$ de Broglie wavelength

➡ **Nanostructures required!**

Optically active QDs

- QDs based on direct-bandgap materials (strong interband transitions)
- Both electrons and holes are confined inside the QD volume

Fluorescence image of CdSe QDs in solution with size 2-6 nm

Colloidal QDs: Nanocrystals made via chemical synthesis

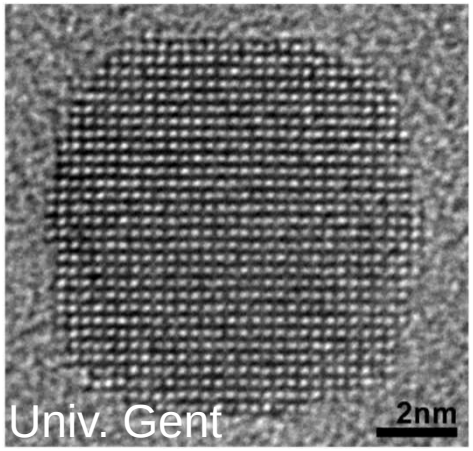

PbSe nanocrystal

Quantum dots ~ "artificial atoms"

- Strong size dependence of energy spectum ➡ widely and ~continuously tunable emission wavelength with even a single material
- Can be "trapped" and used for devices easier than real atoms

Application: now in Quantum-dot displays!

1.2.a Stranski-Krastanow growth mode

Lattice mismatched heteroepitaxy (easiest way to obtain quantum dots)

e.g. Ge/Si – lattice mismatch $\varepsilon=(a_{Ge}-a_{Si})/a_{Si}$ = 4.2%

InAs/GaAs – mismatch 7%…

Ge source

Si source

Stranski-Krastanow growth mode:

Spontaneous formation of 3D islands

on top of thin wetting layer (WL)

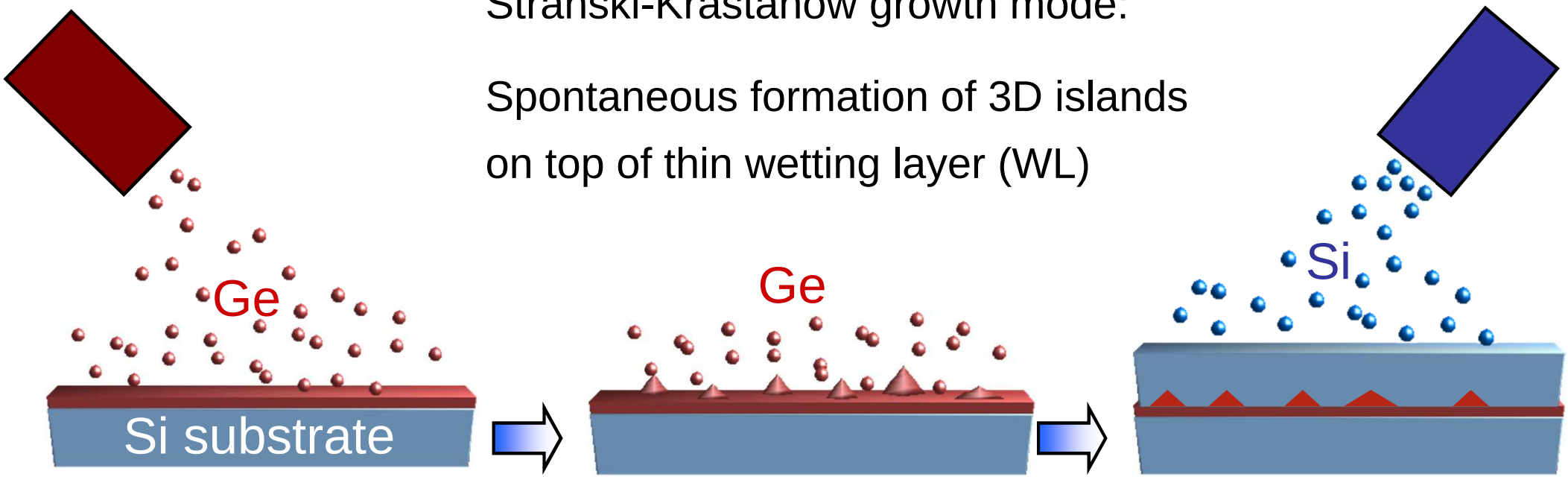

Substrate: single crystal with clean surface

Environment: for MBE ultra-high vacuum (p~10^{-13} bar)

Note: in the initial SK paper there was no elastic stress

[4] I. N. Stranski and Von L. Krastanow, Akad. Wiss. Lit. Mainz Math.-Natur. Kl. IIb **146**, 797 (1939).

VOLUME 64, NUMBER 16 PHYSICAL REVIEW LETTERS 16 APRIL 1990

Dislocation-Free Stranski-Krastanow Growth of Ge on Si(100)

D. J. Eaglesham and M. Cerullo

AT&T Bell Laboratories, 600 Mountain Avenue, Murray Hill, New Jersey 07974

(Received 27 December 1989)

We show that the islands formed in Stranski-Krastanow (SK) growth of Ge on Si(100) are initially *dislocation-free*. Island formation in true SK growth should be driven by strain relaxation in large, dislocated islands. Coherent SK growth is explained in terms of *elastic* deformation around the islands, which partially accommodates mismatch. The limiting critical thickness, h_c, of coherent SK islands is shown to be higher than that for 2D growth. We demonstrate growth of dislocation-free Ge islands on Si to a thickness of $\approx$ 500 Å, 50× higher than h_c for 2D Ge/Si epitaxy.

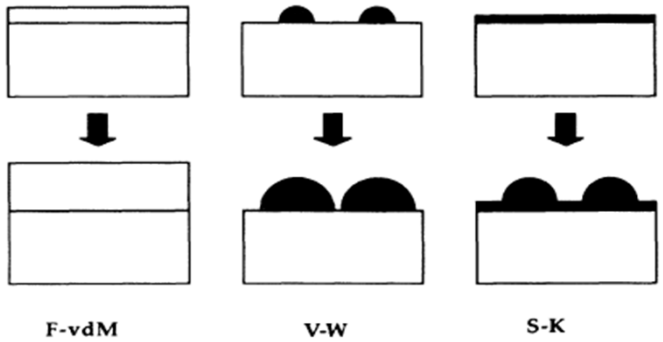

FIG. 1. Schematic diagram of the three possible growth modes: Frank–van der Merwe, Volmer-Weber, and Stranski-Krastinov. Where interface energy alone is sufficient to cause island formation, VW growth will occur; SK growth is uniquely confined to systems where the island strain energy is lowered by misfit dislocations underneath the islands.

500°C, 3 ML Ge

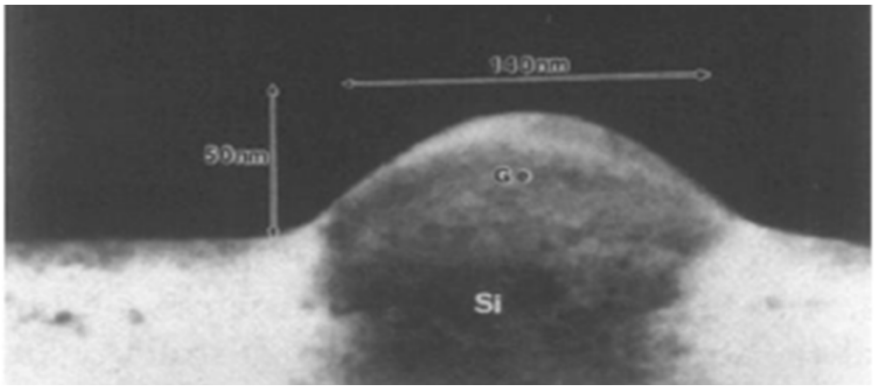

FIG. 4. Plan-view and cross-section TEM images of large coherent SK islands close to their maximum size prior to dislocation introduction. (a) Bright-field image near the {202} Bragg position showing characteristic "bend-contour" contrast due to dome-shaped deformation of the substrate around the island. (b) (400) dark-field image; note strong strain contrast around island.

Recent review on Ge/Si: J.-N. Aqua, I. Berbezier, L. Favre, T. Frisch, A. Ronda, Phys. Rep. 522, 59–189 (2013)

Similarities among different material systems

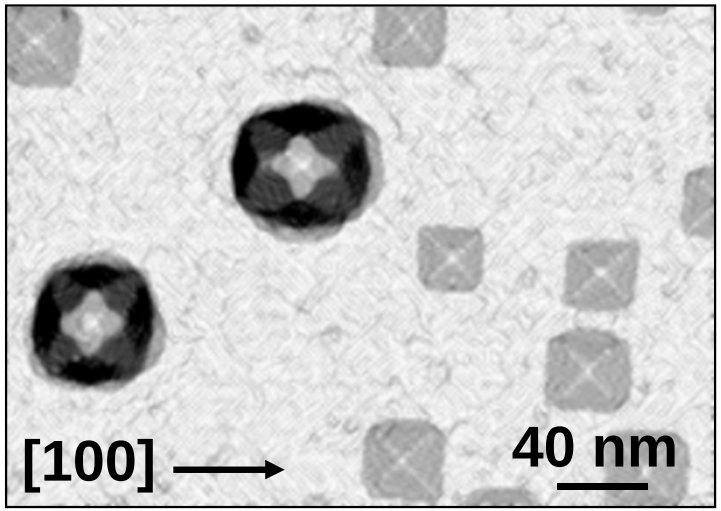

7 ML Ge/Si(001) @ 550°C

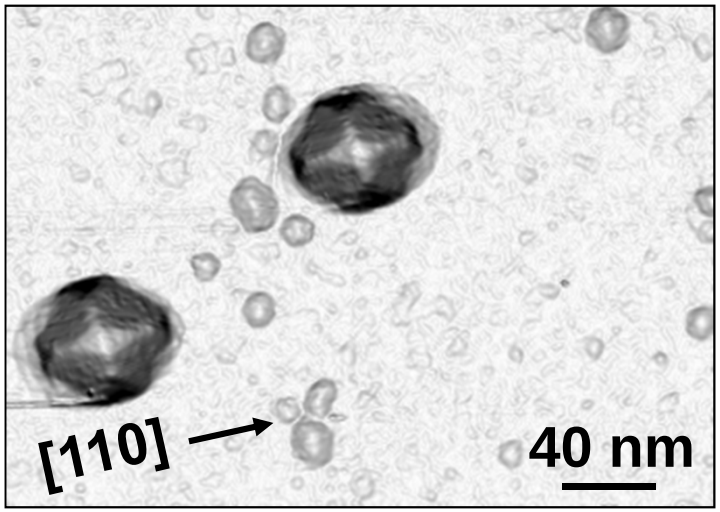

1.8 ML InAs/GaAs(001) @ 500°C

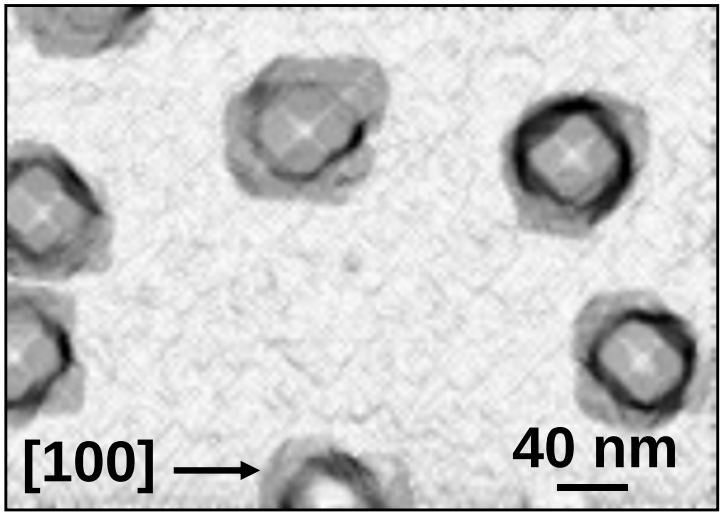

+1 ML Si cap @ 450°C

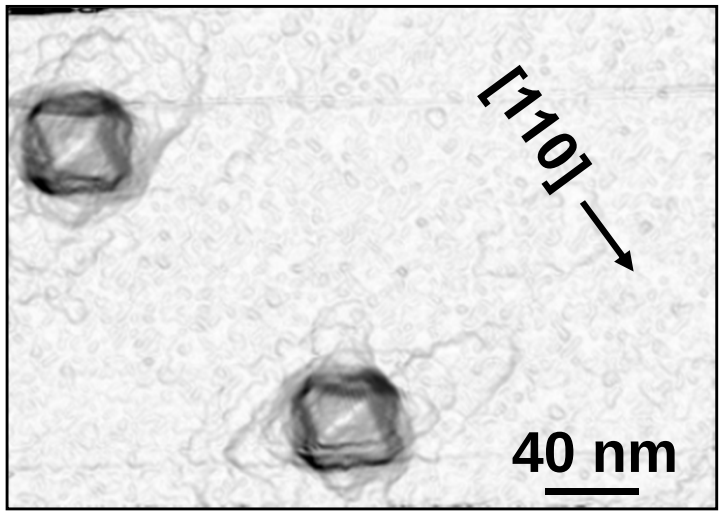

+1 ML GaAs cap @ 460°C

During capping under usual conditions islands intermix and get shallower

G. Costantini, A. Rastelli, *et al.* APL 85, 5673 (2004), JCG 278, 38 (2005); PRL 96, 226106 (2006); P. Kratzer *et al.* PRB 73, 205347 (2006)

1.2.b Droplet epitaxy

When lattice mismatch is small, nanostructures can be obtained via alternative methods. Most prominent: droplet epitaxy.
Example: GaAs QDs on AlGaAs (lattice mismatch ~0.1%)

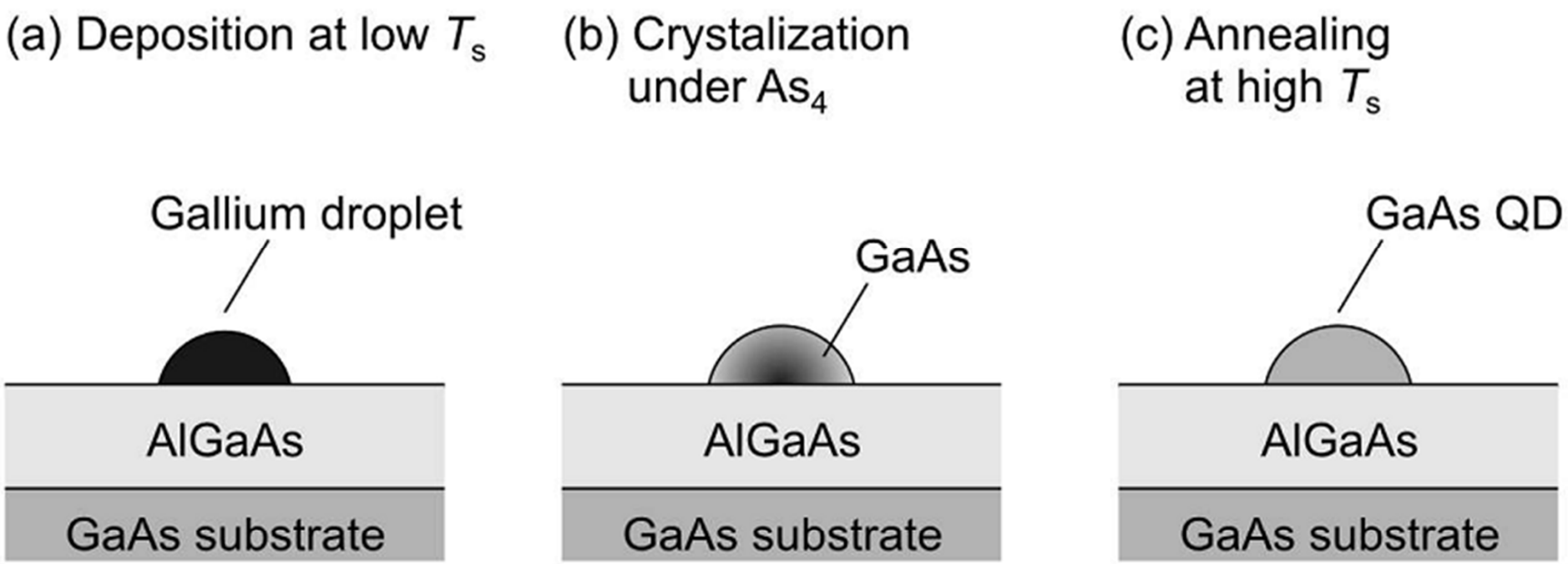

K. Watanabe, N. Koguchi, Y. Gotoh, Jpn. J. Appl. Phys. **39**, 79 (2000)
T. Mano, K. Watanabe, S. Tsukamoto, N. Koguchi, H. Fujioka, M. Oshima, C.D. Lee, J.Y. Leem, H.J. Lee, S.K. Noh, Appl. Phys. Lett. **76**, 3543 (2000)
M. Yamagiwa, T. Mano, T. Kuroda, T. Tateno, K. Sakoda, G. Kido, N. Koguchi, F. Minami, Appl. Phys. Lett. **89**, 113115 (2006). DOI

1.2.c Droplet etching and overgrowth

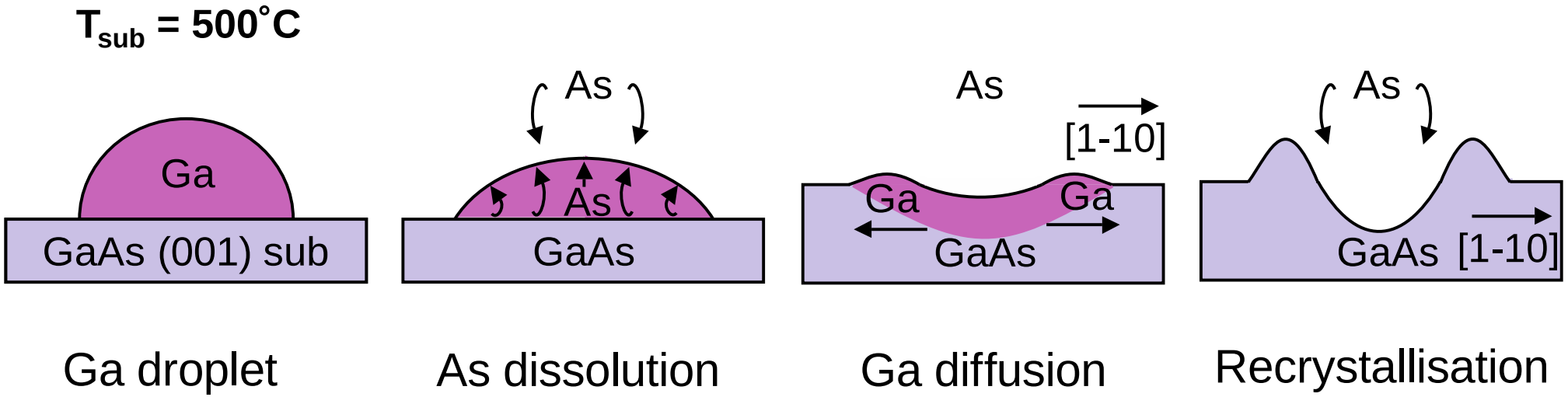

E. Zallo *et al.*, *J. Cryst. Growth* 338, 232 (2012)

First report on nanoholes: Z. Wang et al. APL 90, 113120 (2007)
For a different method to make nanoholes see A. Rastelli et al. Phys. Rev. Lett. 92, 166104 (2004)

1.2.c Droplet etching and overgrowth

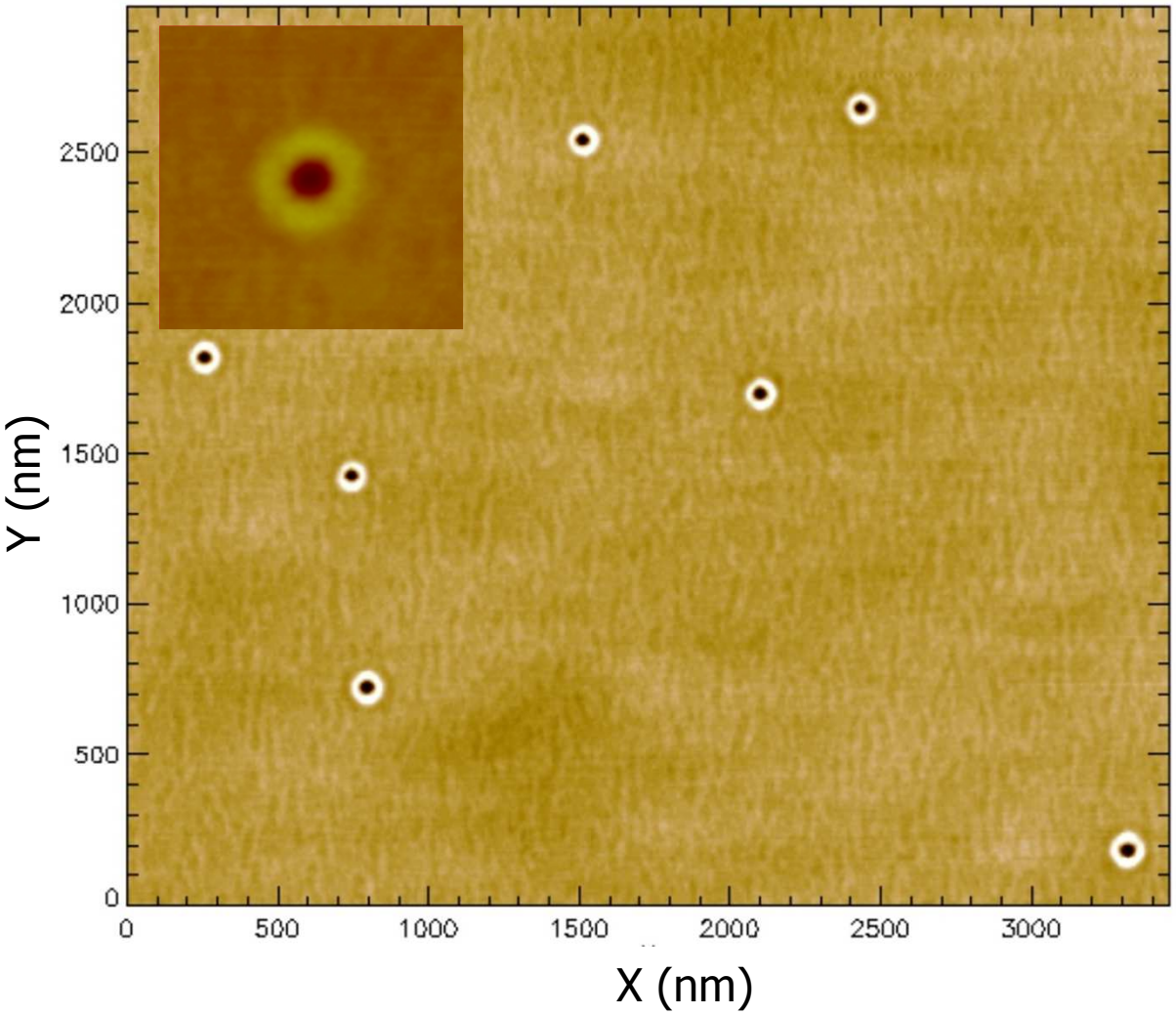

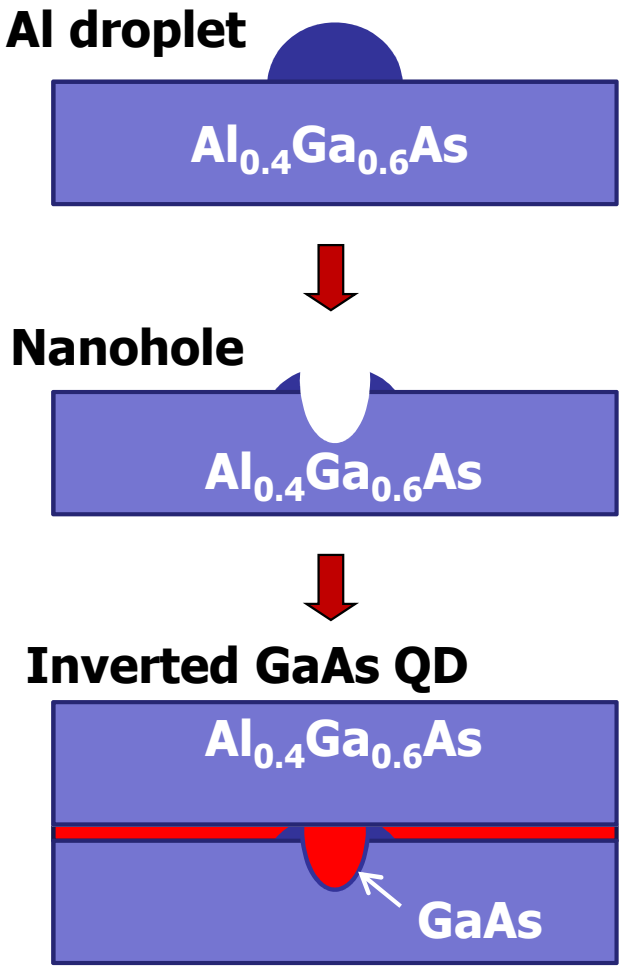

Annealing step with no As supply

Y. Huo, A. Rastelli, O. Schmidt, APL 102, 152105 (2013)
Y. Huo, V. Krapek, A. Rastelli, O.G. Schmidt, PRB 90, 041304(R)
First report on nanoholes: Z. Wang et al. APL 90, 113120 (2007)

1.3 Epitaxial QDs and their applications

Example: InGaAs QDs on GaAs(001) substrates

Atomic force microscopy topograph of QDs on surface

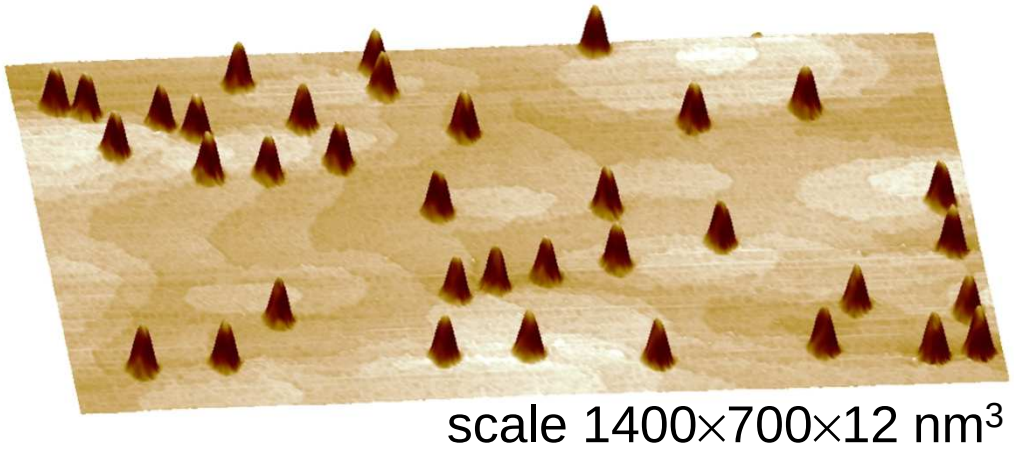

scale 1400×700×12 nm^3

Transmission electron micrograph of a QD embedded in GaAs matrix

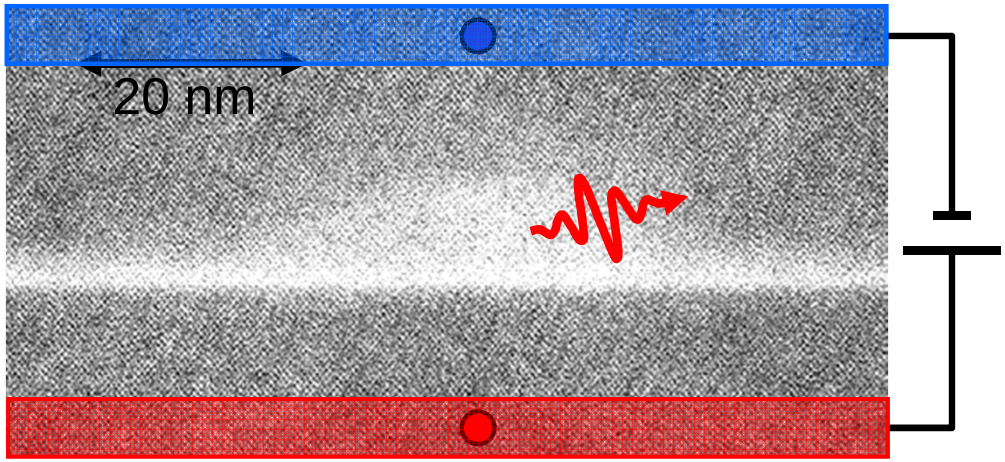

Key features of epitaxial self-assembled QDs:

- Fully compatible with optoelectronic devices by proper doping of the matrix (barrier) material, enabling electrical injection
- Random position on the substrate
- Shape/size/composition fluctuations → each QD has its own energy spectrum

Applications of ensembles of QDs

Optical data communication and chip-to-chip interconnects

Diode lasers with QDs replacing QWs in active region: improved performance (e.g. temperature stability) and wider range of accessible wavelengths.

N. Kirstädter et al. Electron. Lett. 30, 1416 (1994)

Emission spectrum of InGaAs/GaAs(001) QDs

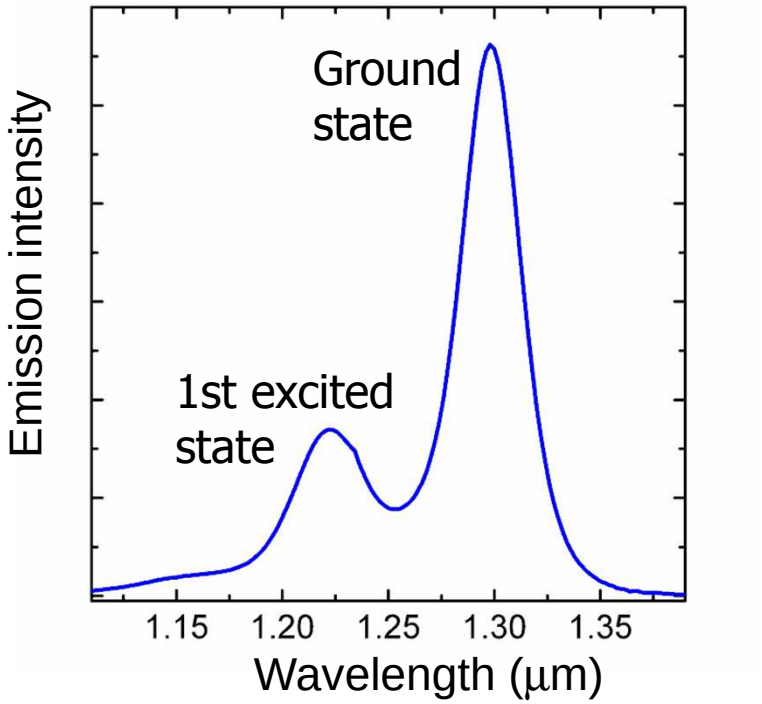

Attenuation of telecom optical fibers

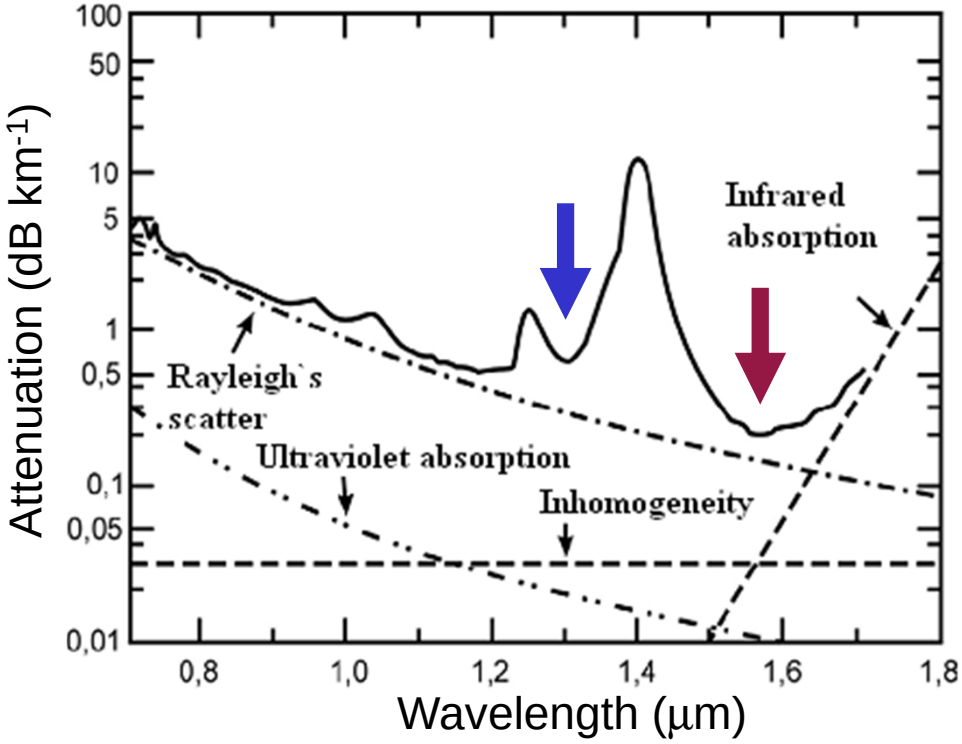

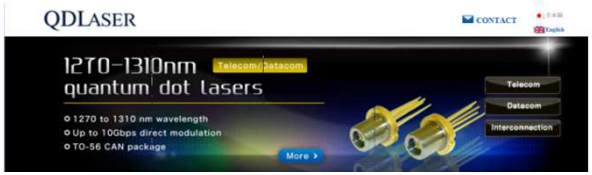

Envisioned applications of single QDs

Secure data communication via quantum cryptography

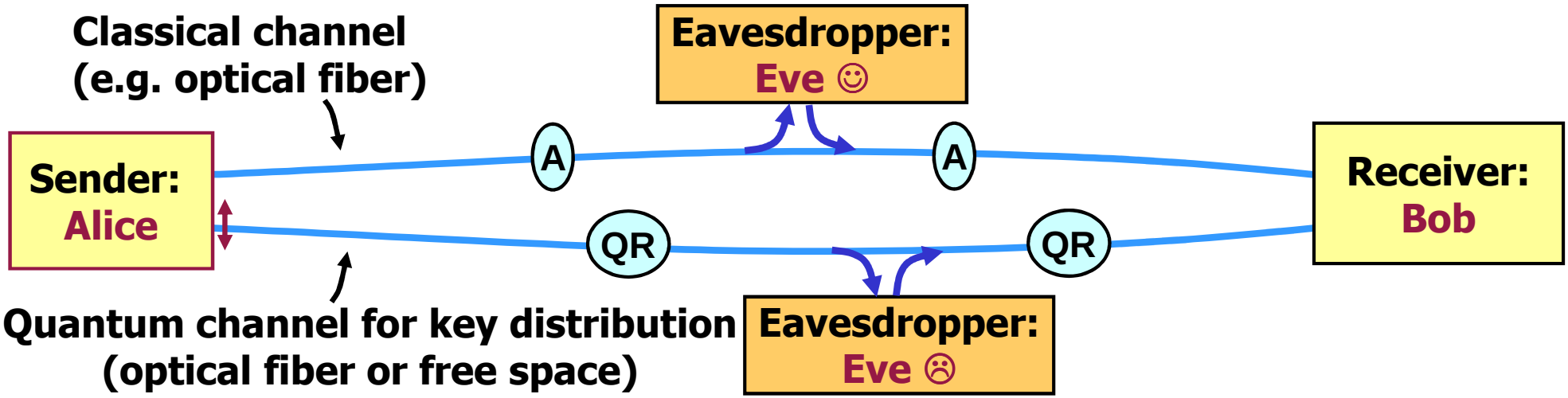

See Mark Fox, *Quantum Optics – An Introduction,* Oxford Univ. Press (2006)

QDs as sources of single photons on demand

Electrically Driven Single-Photon Source

Zhiliang Yuan,[1] Beata E. Kardynal,[1] R. Mark Stevenson,[1]
Andrew J. Shields,[1]* Charlene J. Lobo,[2] Ken Cooper,[2]
Neil S. Beattie,[1,2] David A. Ritchie,[2] Michael Pepper[1,2]

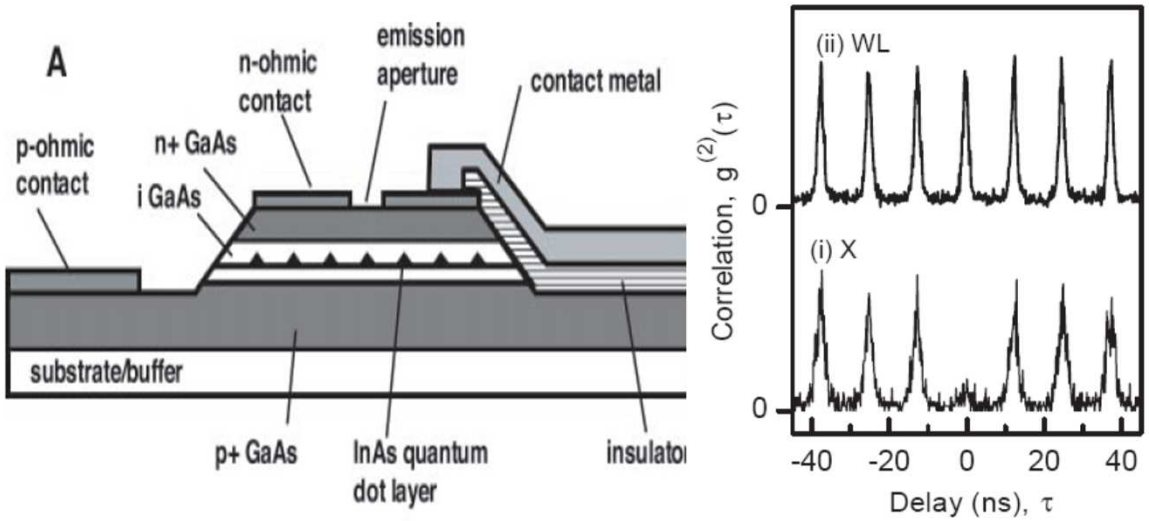

Science **295,** 102 (2002)

See also P. Michler et al., Science **290,** 2282 (2000)

Optical transitions in QDs generally have higher oscillator strengths (faster spontaneous emission) than real atoms

⇩

QDs as sources of photons at high repetition rates

EL of a QD in RC-LED driven at 1 GHz

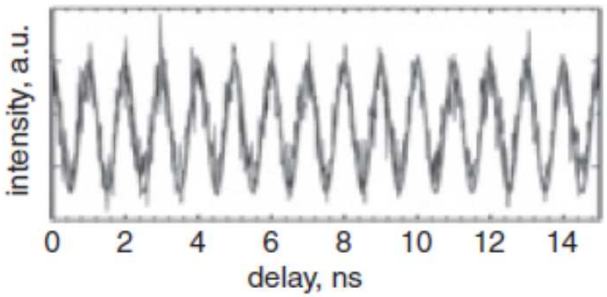

A. Lochmann *et al* Electron. Lett. **45,** 566 (2009)

See also S. Reitzenstein *et al* APL **96**, 011107 (2010)

Applications of single QDs

Advantages of QDs over other systems: compatible with well established semiconductor processing → can be easily embedded in photonic structures

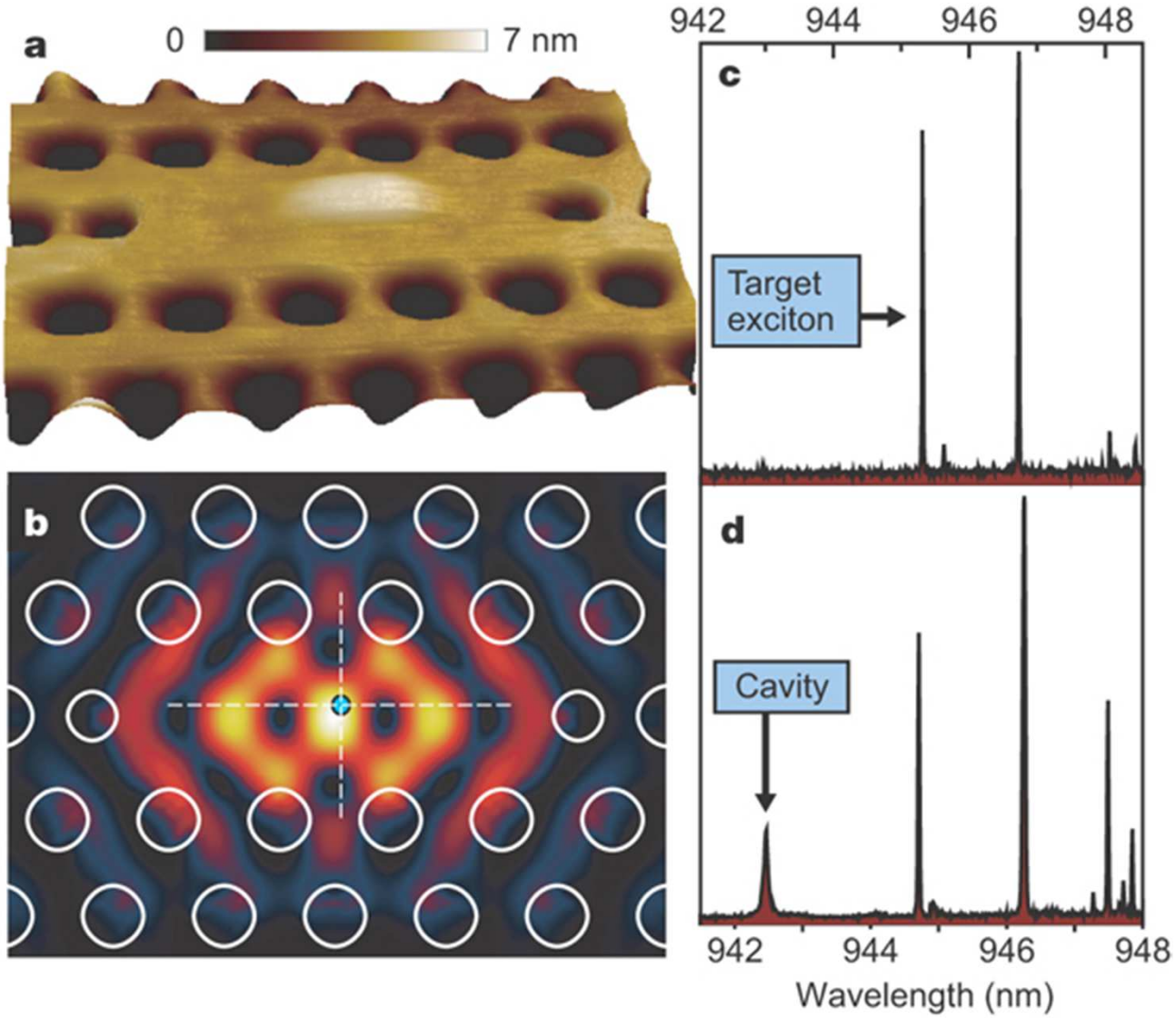

Problems for scalability:

- Random position (stochastic nucleation!)
- Variable emission spectra due to fluctuating structural properties (stochastic processes occurring during growth!)

***K. Hennessy et al,* *Nature* 445, 896-899 (2007)**

Random position, structural differences, anisotropies

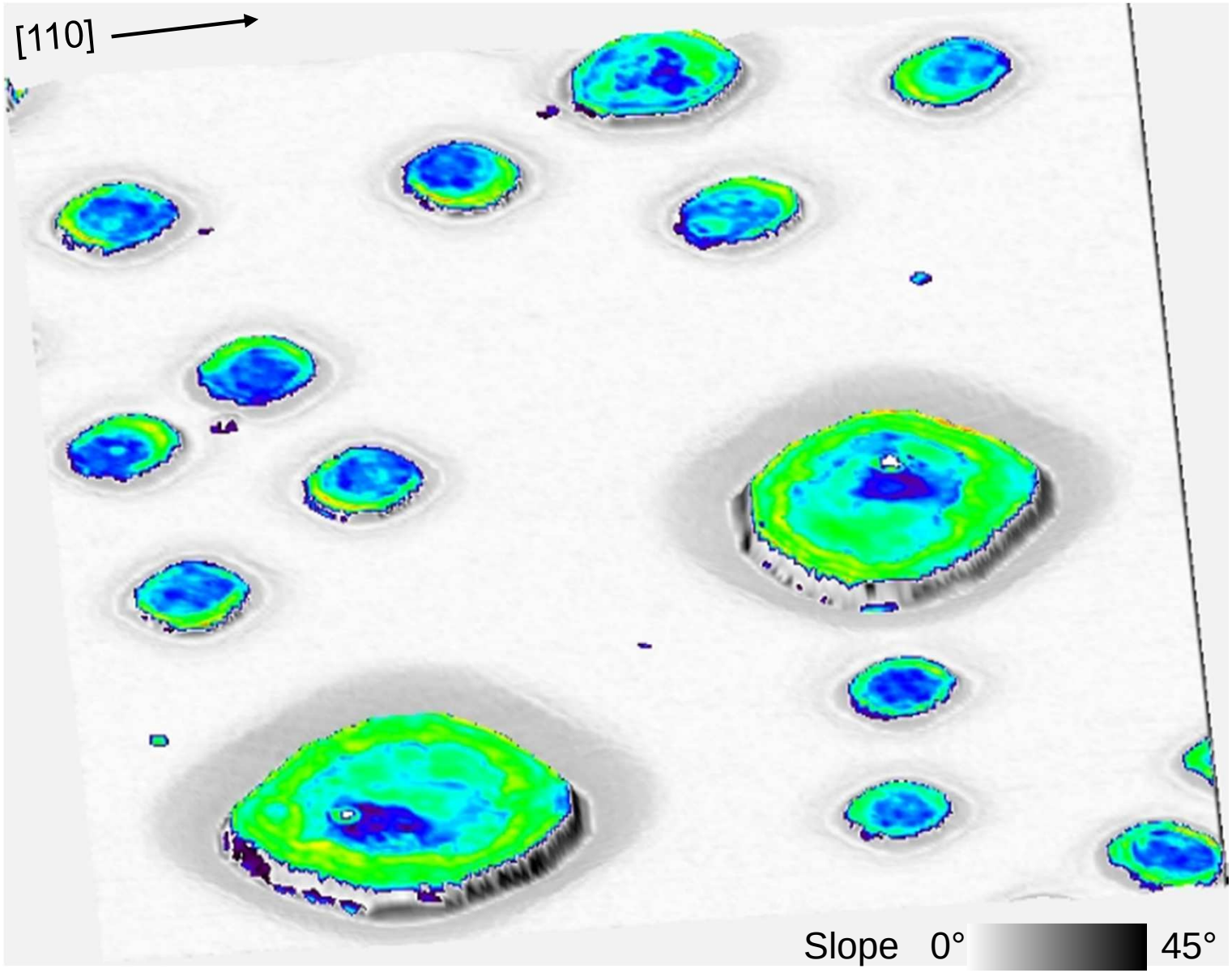

3D composition profiles of SiGe dots obtained by AFM combined with selective etching.

Similar trends seen for InGaAs QDs

Horizontal slices spaced 3 nm in vertical direction

Local Ge fraction x

0.3 — 0.43

AFM Scale:
1670 x 2150 x 107 nm^3

A. Rastelli, M. Stoffel *et al.* Nano Lett. 8, 1404 (2008)

How to access single QDs?

For optically active QDs, photoluminescence spectroscopy of single QDs at low temperature

Focused laser beam

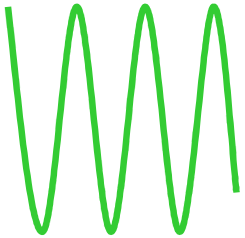

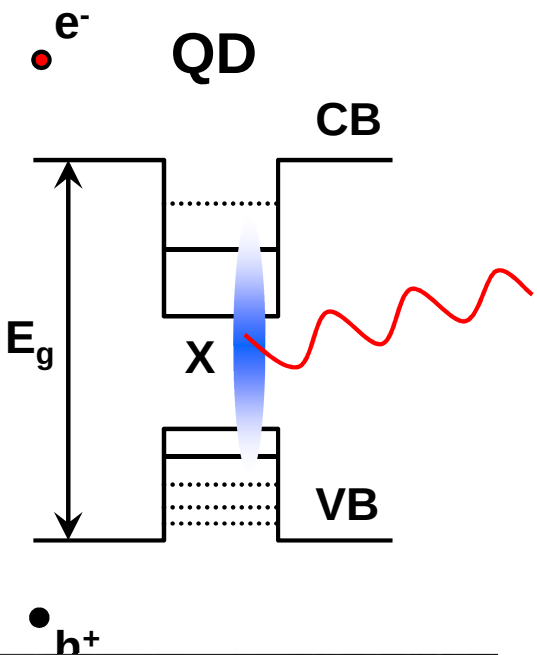

Spectrometer+ Detector

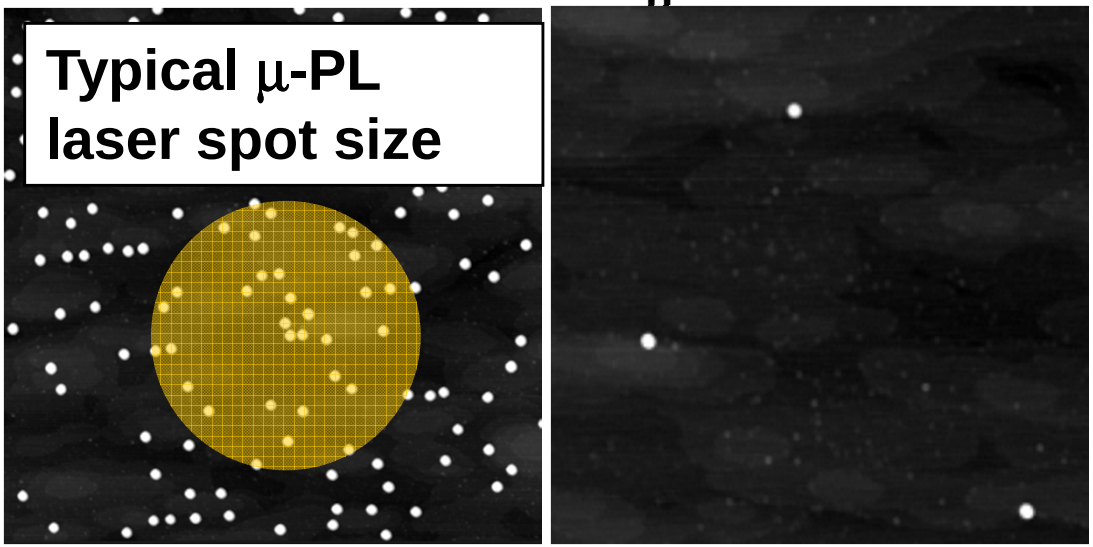

For single QD spectroscopy, densities <10^8 cm^{-2} desired

InAs/GaAs QDs AFM 2×2 μm^2

Problem: artificial atoms are not natural atoms

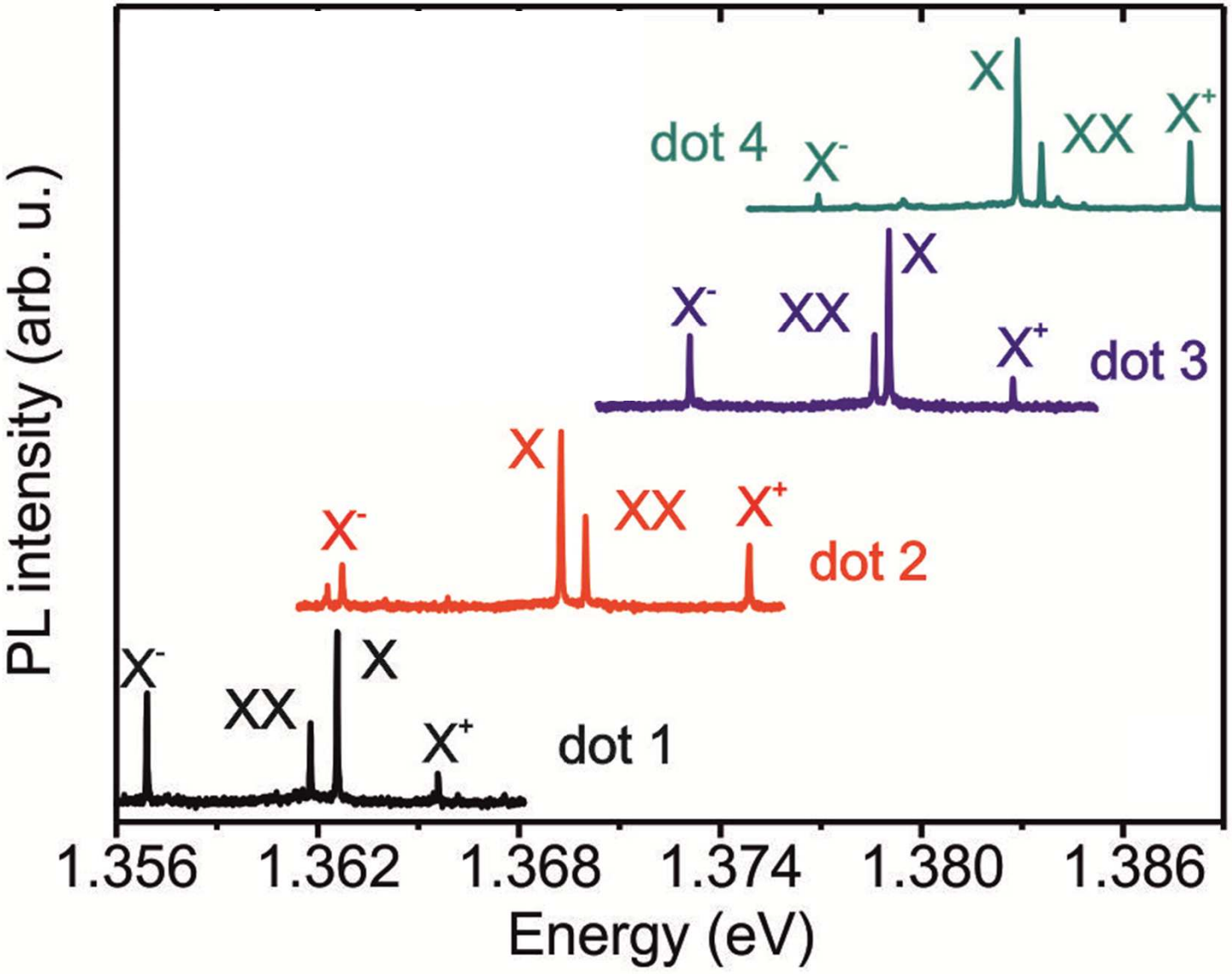

QD potential varies from QD to QD due to size, shape, composition fluctuations

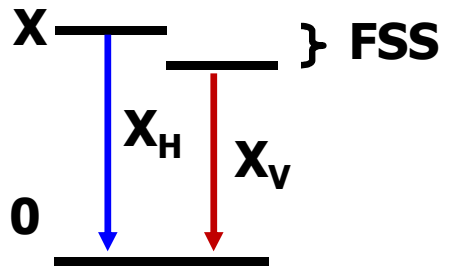

QD **anisotropy** leads to broked degeneracies in excitonic emission preventing some application

Longstanding problem… M. Bayer, et al., Phys. Rev. B 65, 195315 (2002)
R. Trotta, E. Zallo, E. Magerl, O. G. Schmidt, A. Rastelli, Phys. Rev. B (2013)

1.4 Why do controlled position and electronic properties matter?

Position control:

- Indispensable for placing emitter in micro-/nano-photonic device
- Indispensable for electrical contacting
- Prerequisite towards scalability (long-term)

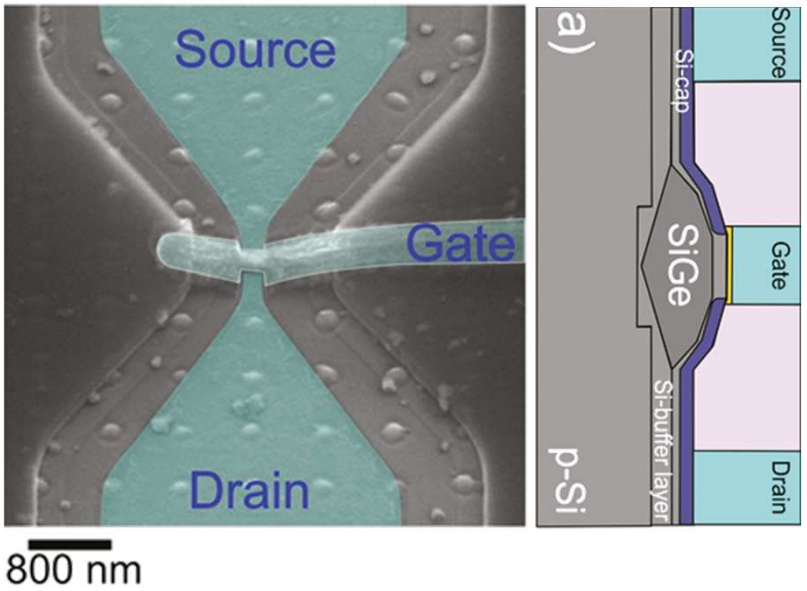

N. Hrauda et al., Nano Letters 11, 2875 (2011)

Electronic structure control:

- Indispensable for advanced quantum optics experiments
- Indispensable for interfacing two or more QDs
- Prerequisite for scalability

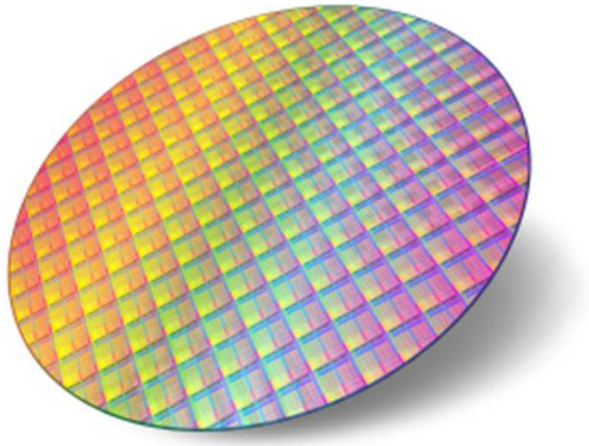

2. Approaches to position QDs

Top-down ("brute force", little freedom left to nature):

- Mostly based on lithographic approaches, etching, implantation…
- Absolute position on a substrate → fully scalable*
- Generally used for most consumer electronics → Just perfect for classical devices
- Crystal defects introduced during processing deleterious for applications in the quantum regime (Single quanta are fragile)

*Fluctuations in structural properties may still lead to unacceptable spread in electronic structure (problem encountered also in classical devices)

Bottom-up (nature does most of the job)

- Based on self-assembly
- Random or short-scale order → not scalable
- Crystal defects can be avoided → Nanostructures just perfect for ensemble applications and for most fundamental studies of single-objects (also in the quantum regime)

2. Approaches to position QDs

Bottom-up + Top down

- QDs are self-assembled and device is positioned around them
- Control on relative position between QD and device → Scalability can be reached if absolute position on substrate is not required
- Crystal defects can be avoided → Nanostructures just perfect for proof-of-principle experiments

Top-down + Bottom-up (+Top-down)

- QDs self-assemble at predefined positions on a substrate
- Absolute position on a substrate → fully scalable
- Crystal defects can be (in principle) avoided → that's the solution!?

2.1 Top-down: lateral confinement in QW

Quantum well (QW) provides confinement along growth direction

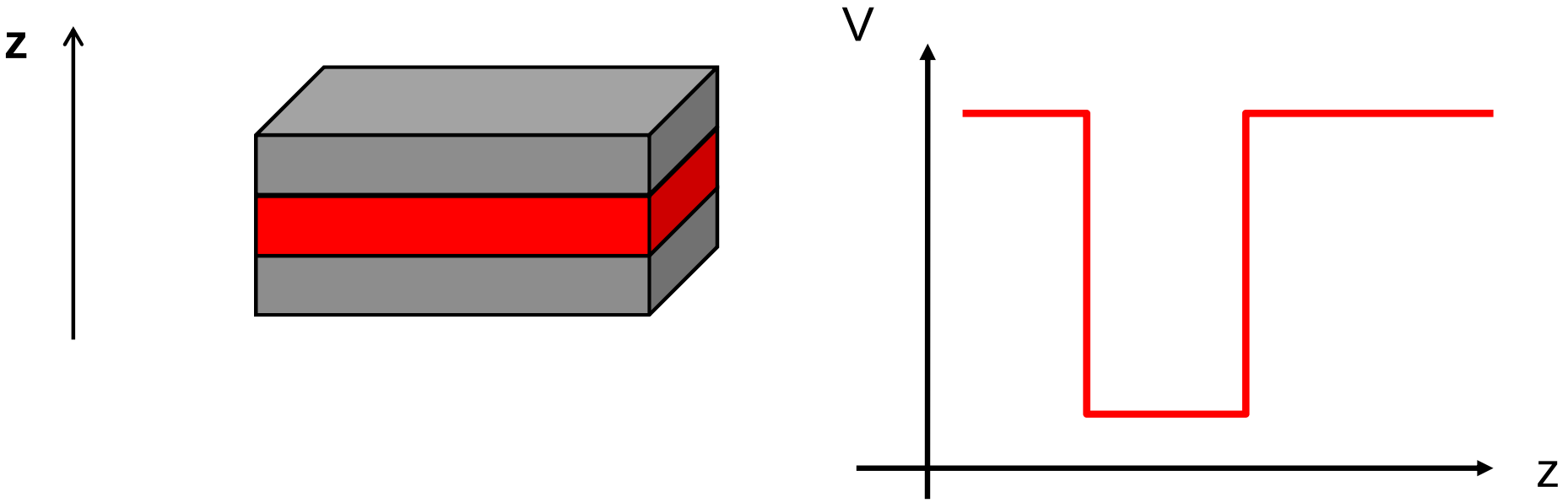

By introducing also lateral confinement, a QD can be obtained. Note: the lateral dimensions must be of the order of a few 10 nm (depending on material and temperature)!

2.1.a Lateral confinement in QW by deep etching

Quantum well provides confinement along growth direction

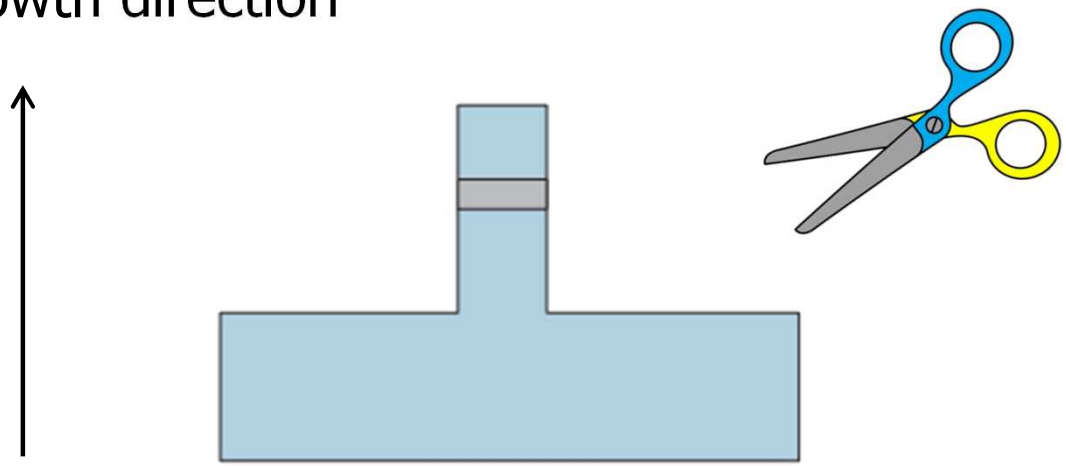

(a) Deeply etched QW

Lateral confinement provided by deep etching (carriers are trapped by the semiconductor-air interface). Barrier about 5 eV

→ Poor optical properties due to recombination of carriers at surface states

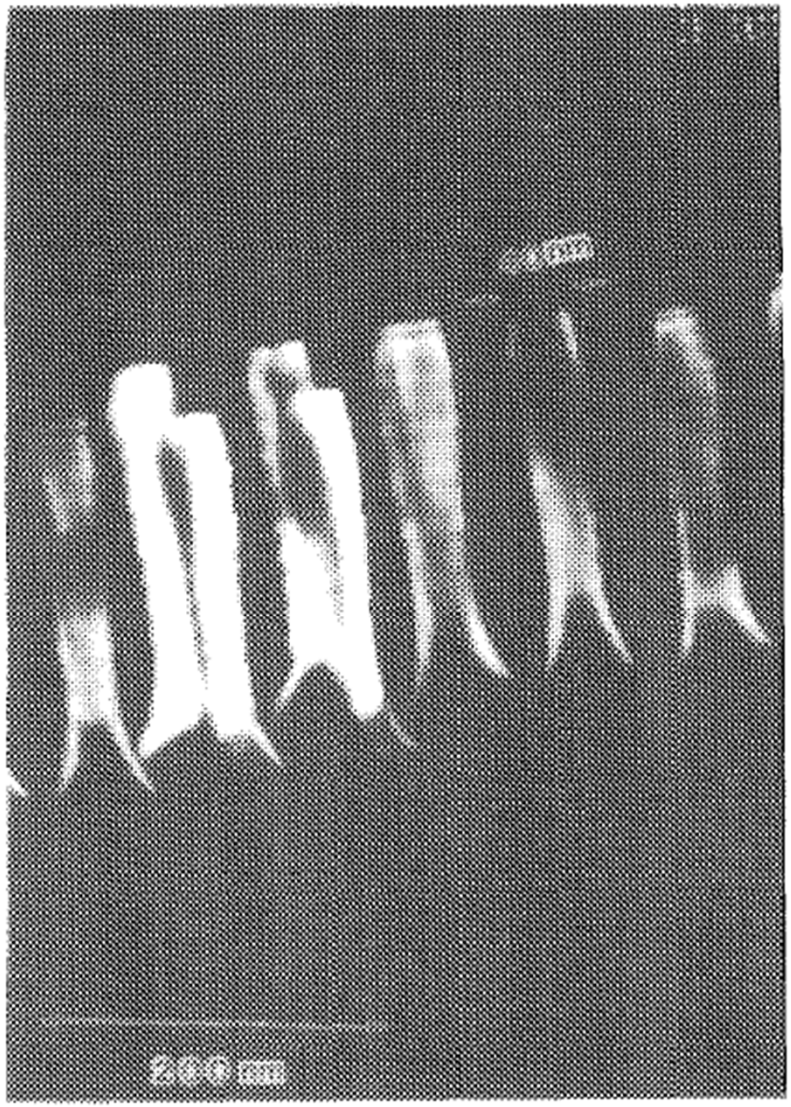

From A. Scherer et al. Appl. Phys. Lett. 49, 1284 (1986)

FIG. 3. REM image of columns etched into multiple quantum well material.

2.1.a Lateral confinement in QW by deep etching

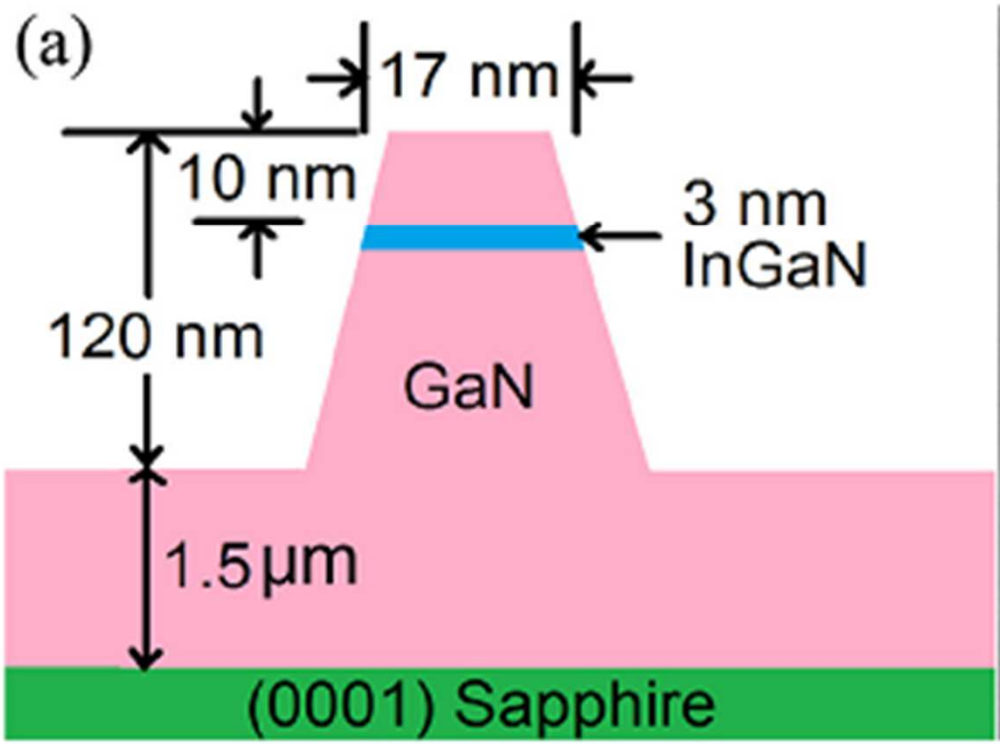

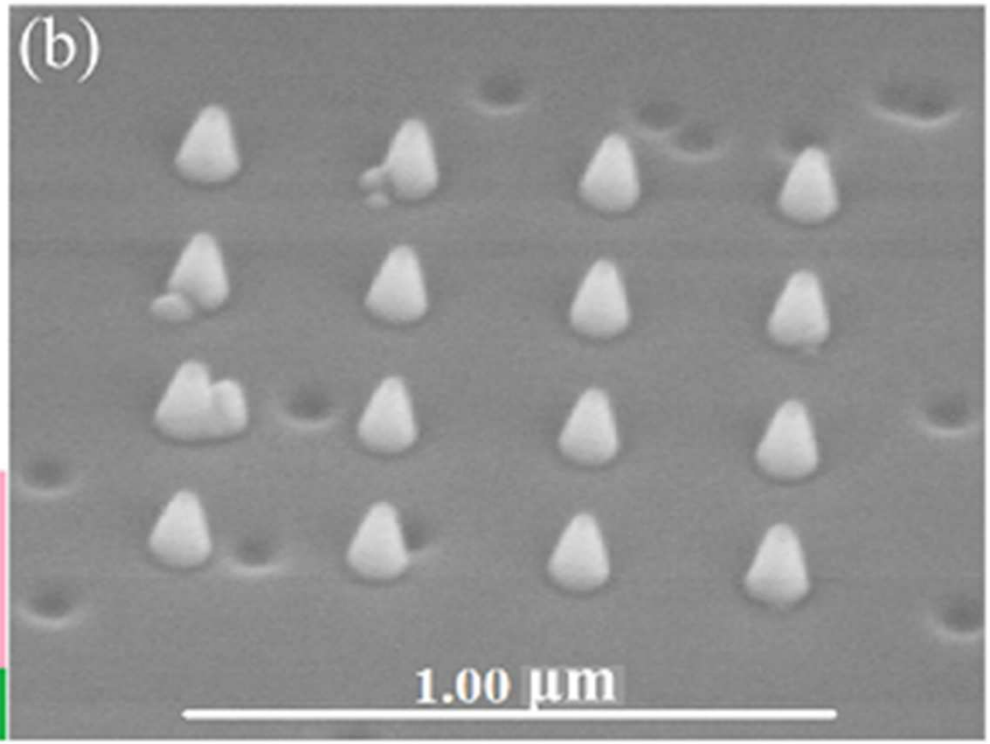

Same approach with InGaN/GaN QDs (lower effects produced by surfaces). Single photon emission observed but broad emission

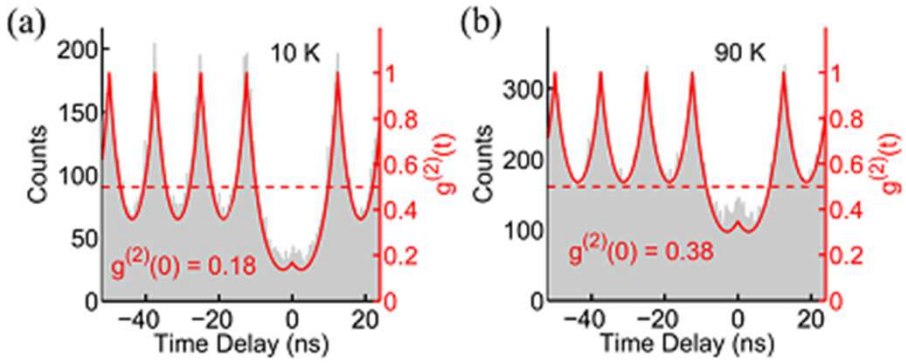

L. Zhang et al. Appl. Phys. Lett.103, 192114 (2013))

2.1.b Lateral confinement in QW by shallow etching

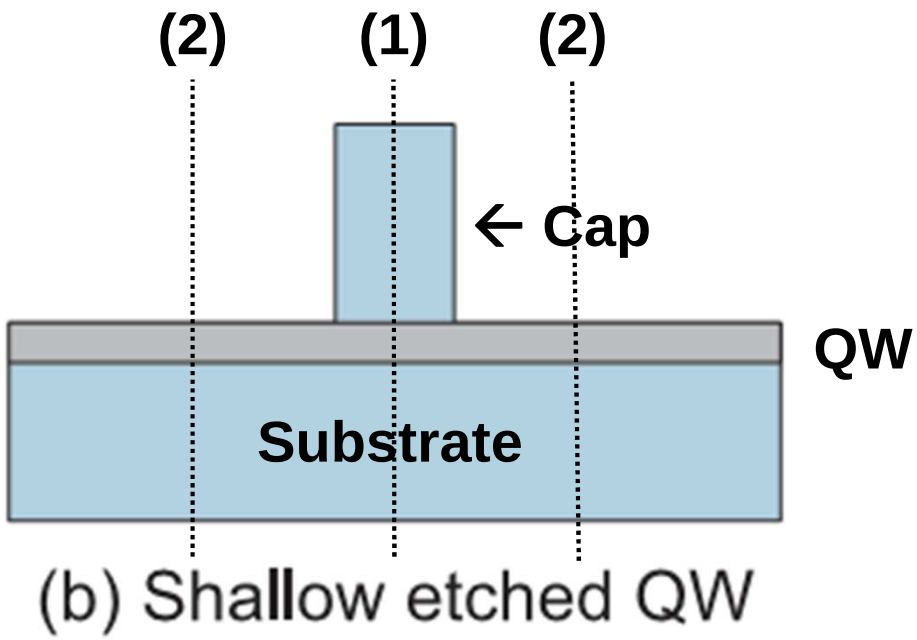

(b) Shallow etched QW

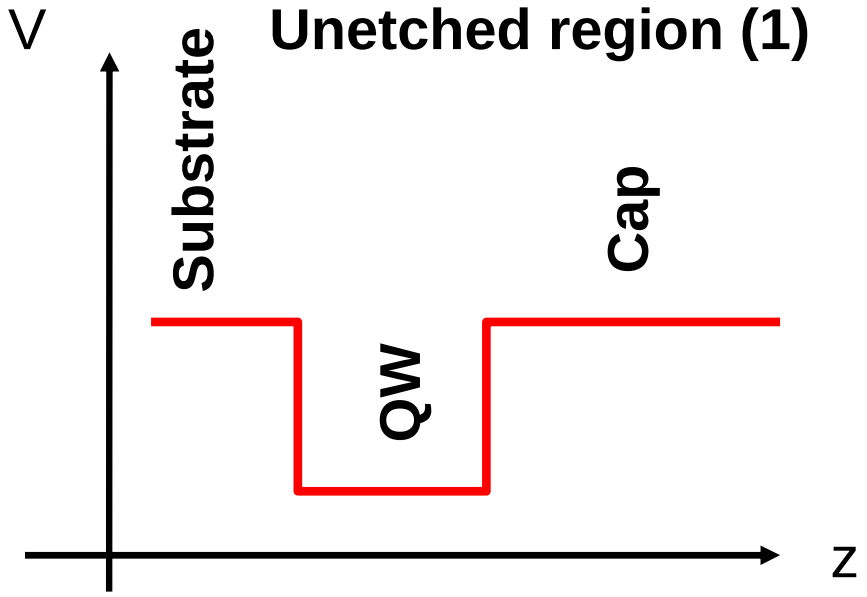

Difference in vertical confinement produces lateral confinement. You can't explain this classically, but it's easy to see by solving the Schrödinger equation separating vertical and lateral motion.

→ Weaker confinement compared to deep etch

→ Improved optical properties, but still not great

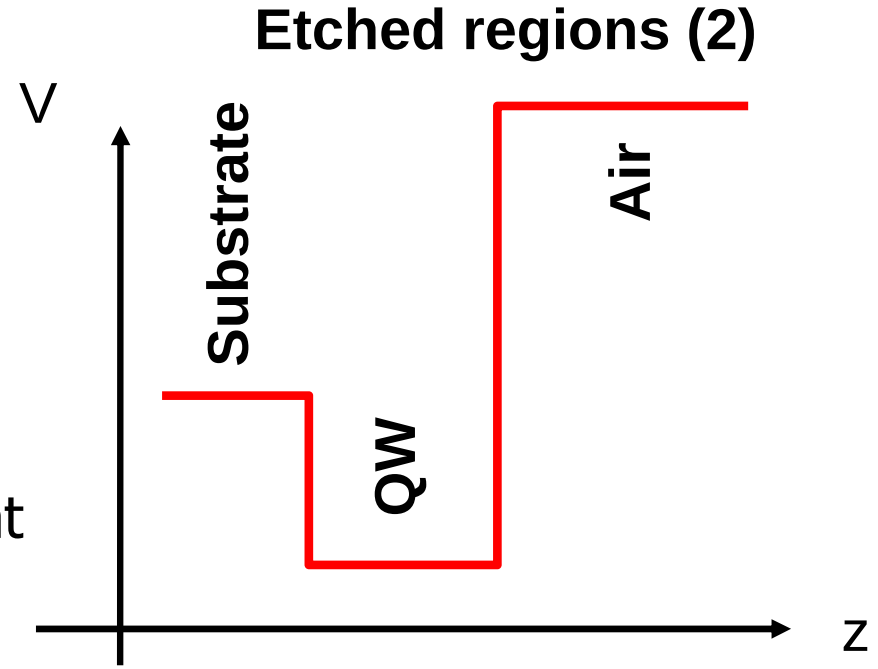

See Appl. Phys. Lett. 61, 1199 (1992)

2.1.c Lateral confinement in QW by selective annealing

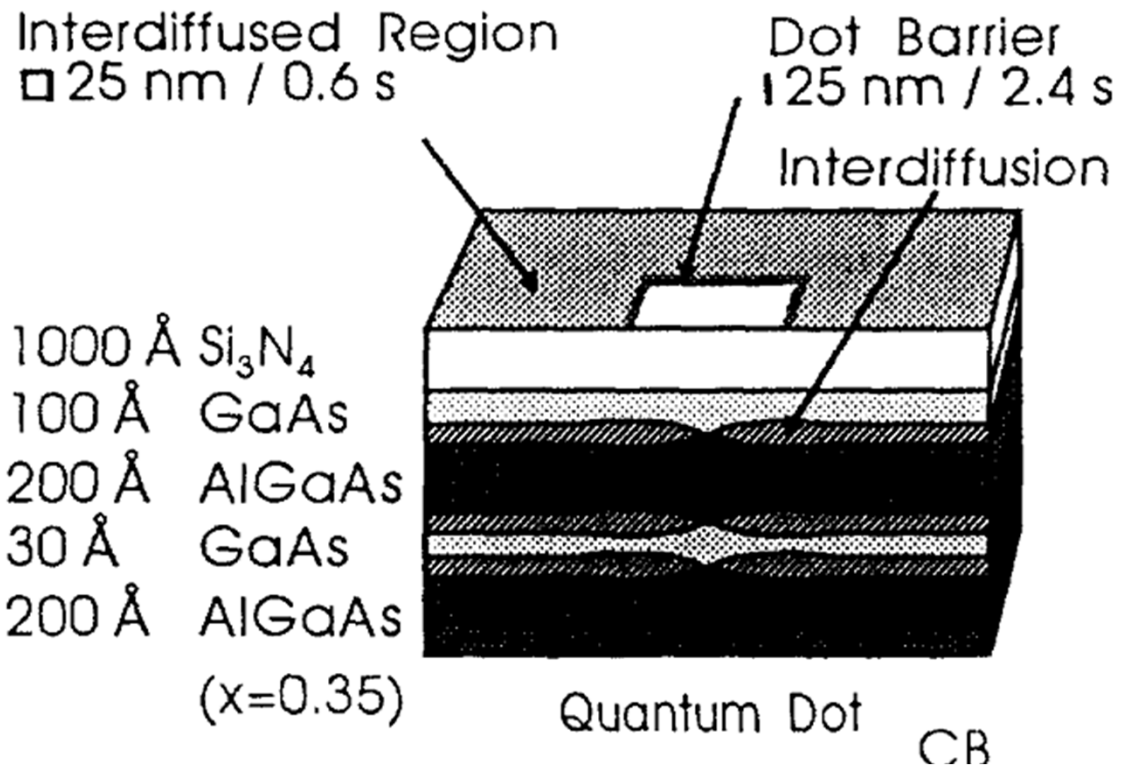

Not annealed region

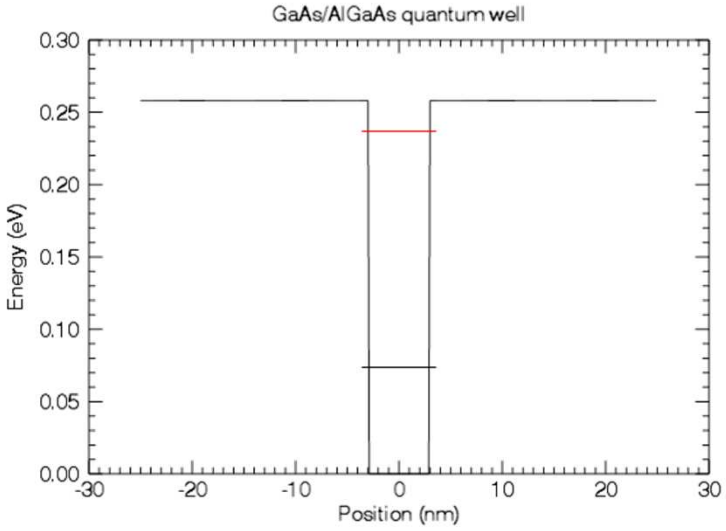

Annealed regions

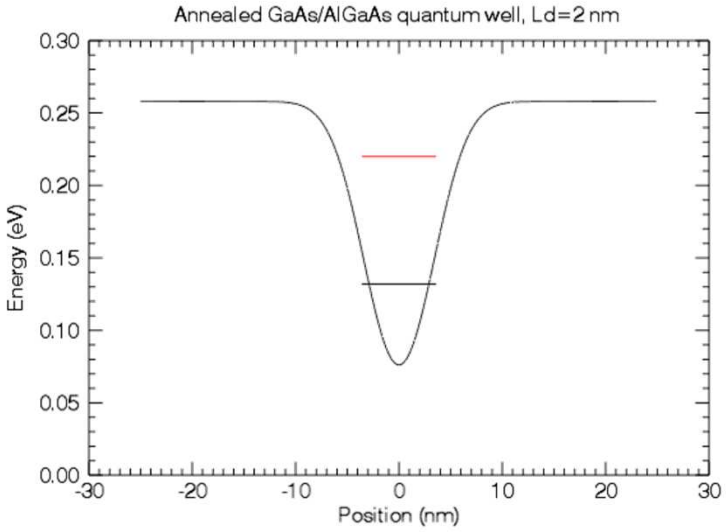

Local heating promotes interdiffusion and bandgap shift → lateral and vertical modulation of confinement potential
→ Relatively week confinement

See K. Brunner et al., Phys. Rev. Lett. 69, 3216–3219 (1992)

2.1.d Lateral confinement in QW by selective diffusion

Selective hydrogen irradiation of diluted GaAsN

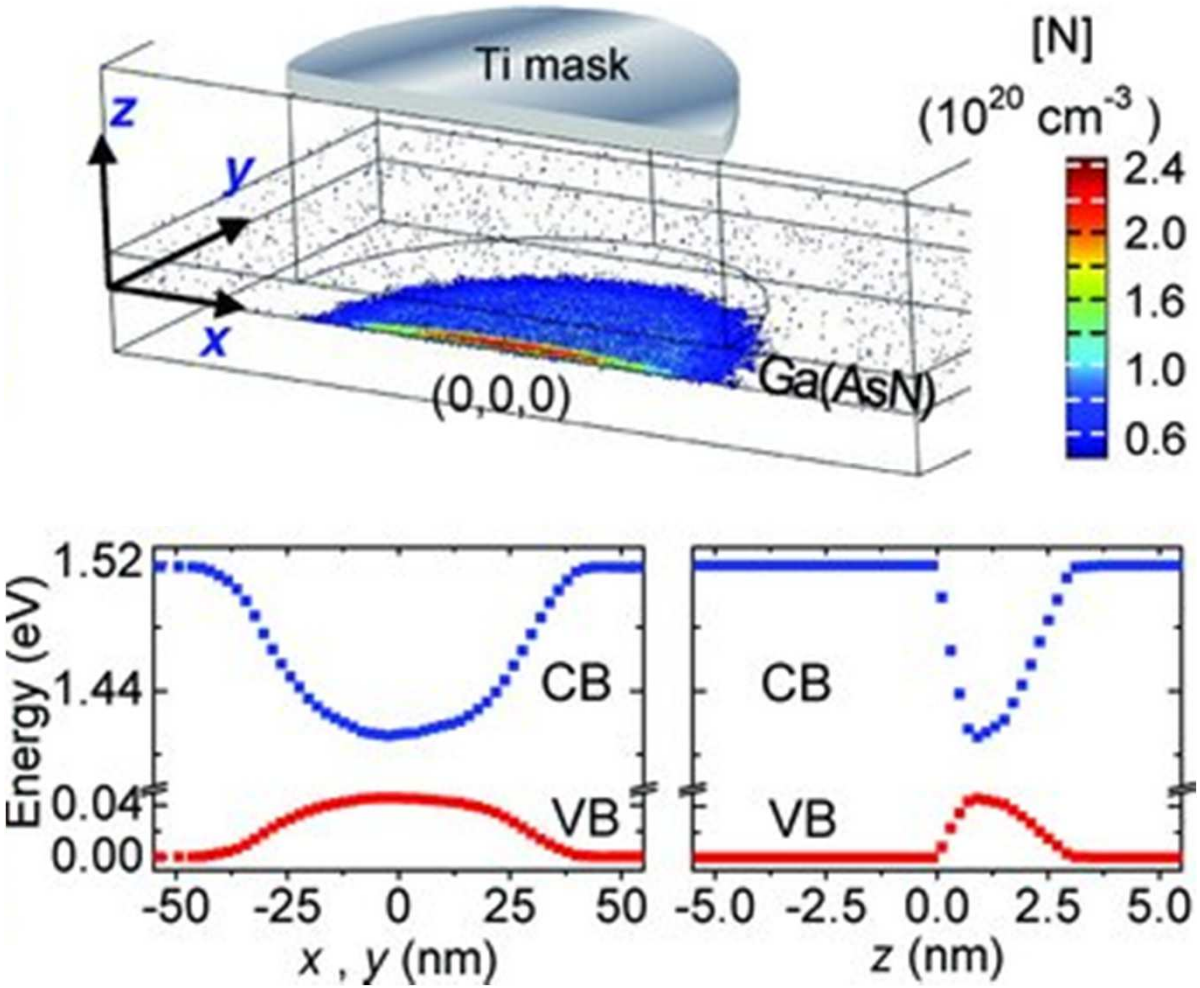

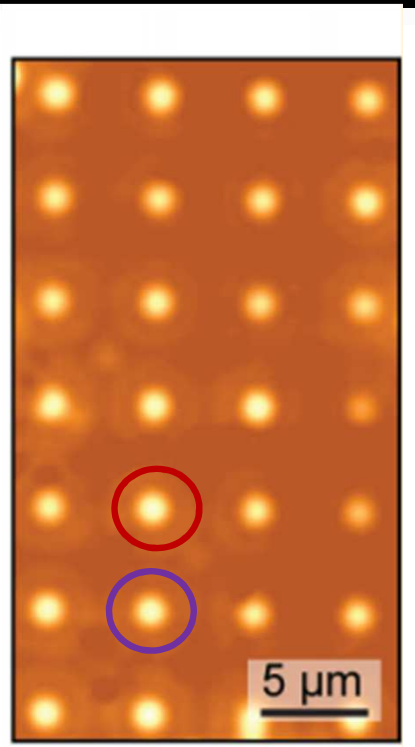

µ-PL

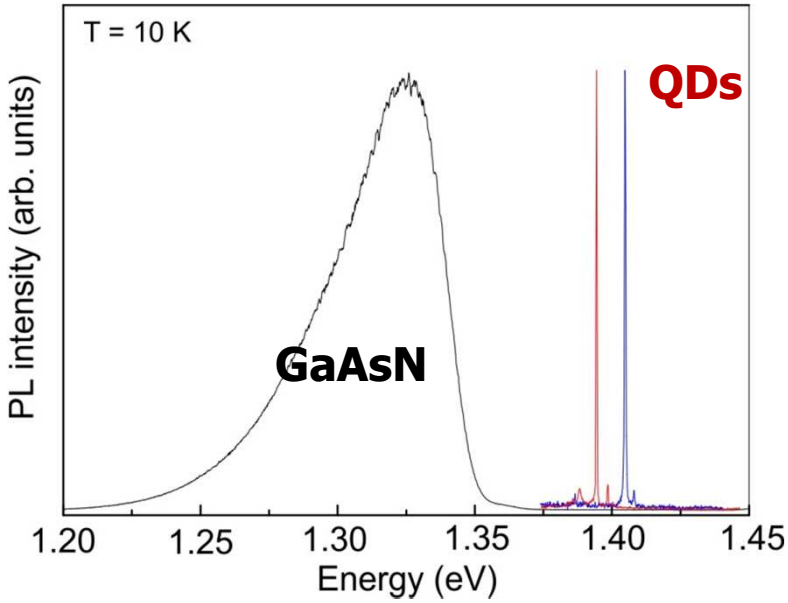

R. Trotta *et al.*, Adv. Mater. 23, 2706 (2011)
S. Birindelli *et al.*, Nano Lett. 14, 1275 (2014)

2.1.e Cleaved edge overgrowth

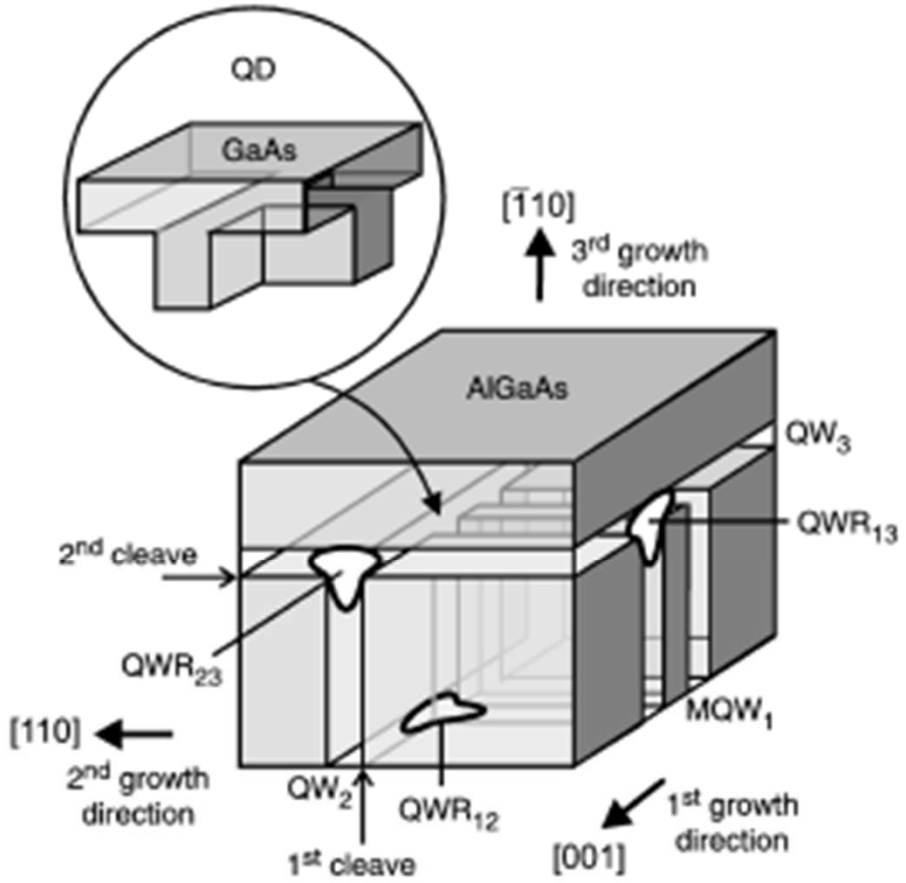

FIG. 1. Schematic illustration of the quantum dot structure (not to scale) obtained after three growth steps separated by two *in situ* cleaves. The junction of three quantum wells and wires, at which a quantum dot forms, is shown in the magnified part of the figure. The T-shaped contours are lines of constant probability for electrons confined in the quantum wires.

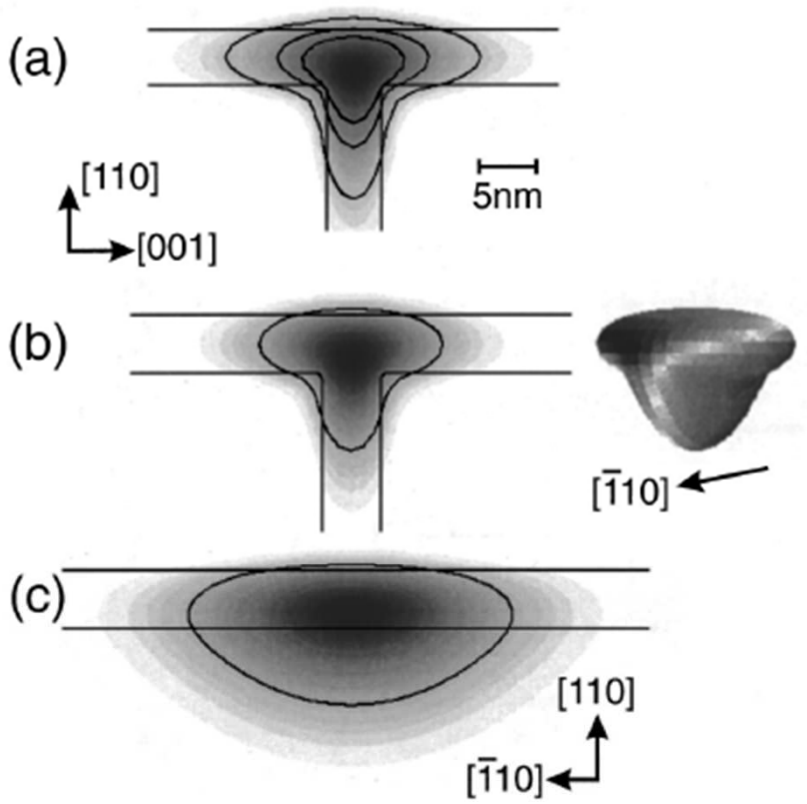

FIG. 2. (a) Single-particle electron wave-function probability (Ψ^2) in a L_{QW}=5 nm *T*-shaped GaAs/$Al_{0.35}Ga_{0.65}As$ quantum wire. Contour lines are for 90%, 70%, and 50% probability inside the line. (b) and (c) show the electron wave function (after convergence of the variational procedure, n=5) in the excitonic case. (c) depicts the extension along the wire, (b) shows the (110) cross-section plane through the center of the exciton. The perspective view (70% orbital) in (b) is rotated by 20° around the [110] axis.

From W. Wegscheider, et al. Phys. Rev. Lett. 79, 1917 (1997)
M. Grundmann et al., Phys. Rev. B 55, 4054 (1997)

2.1.e Electrical gating or local depletion of a 2DEG

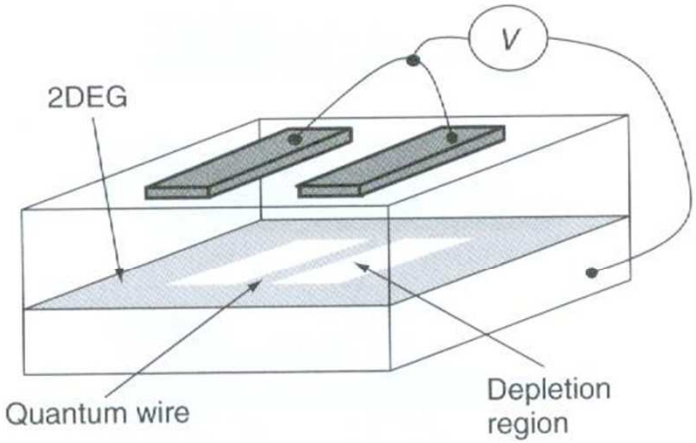

Figure 3.17 A schematic diagram of a split gate quantum wire. The electrons remaining below the gap between the gates form a quantum wire. A 2DEG remains in the regions away from the gates

By applying negative bias on surface electrodes, electron gas is locally depleted

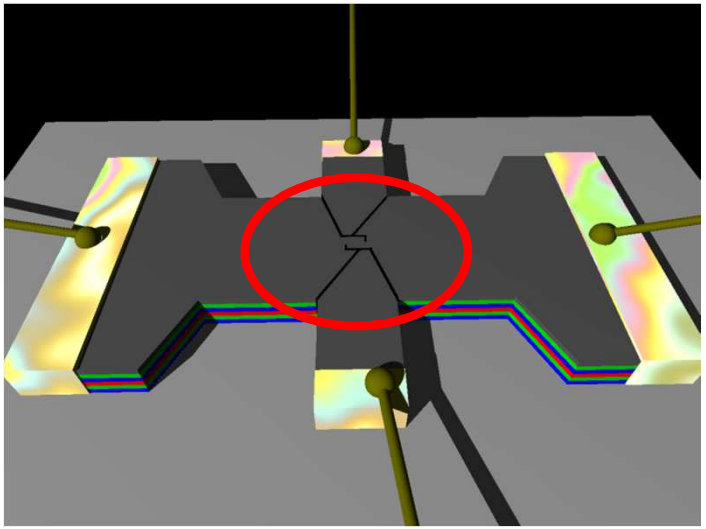

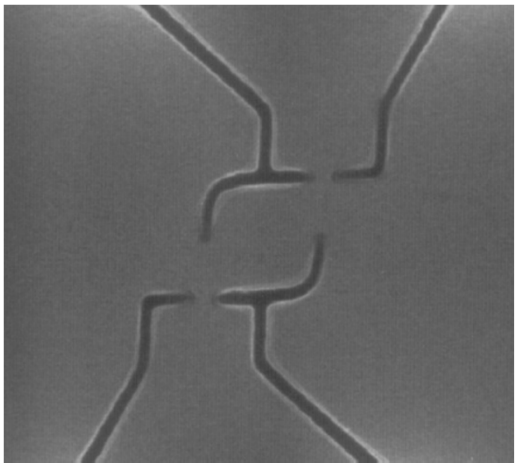

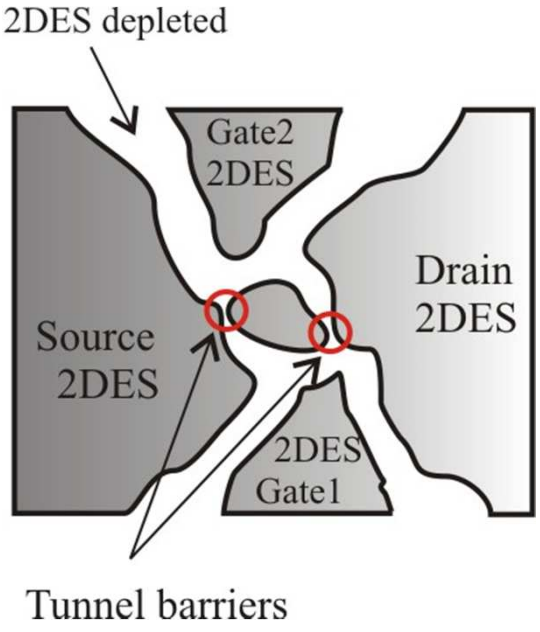

2.2.a Bottom-up + top-down: location of a QD → "device"

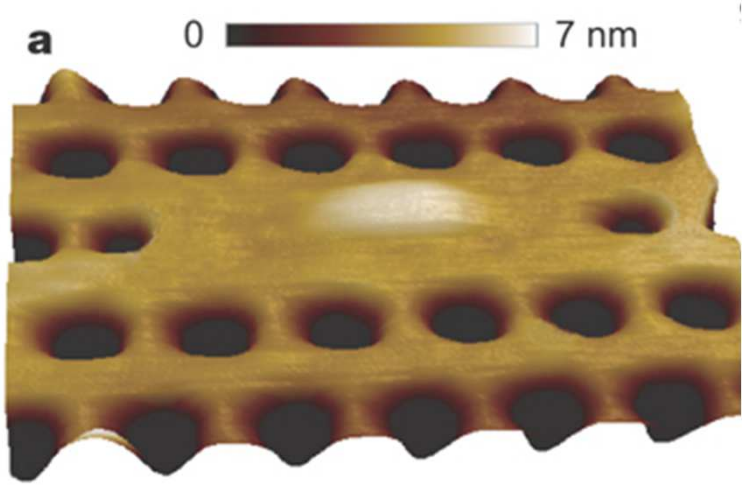

Location of buried InGaAs QD position with respect to markers via AFM → lithographic definition of photonic-crystal microcavity around QD (via e-beam)

***K. Hennessy et al, Nature* 445, 896-899 (2007)**

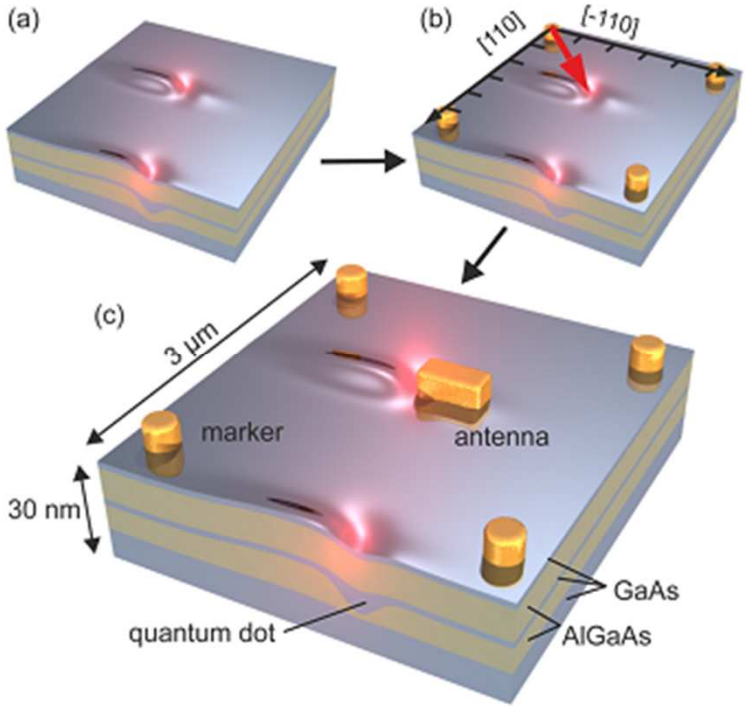

Location of buried GaAs QD position with respect to markers via SEM → lithographic definition of plasmonic antenna over QD

***M. Pfeiffer et al, Nano Lett.* 14, 197-201 (2014)**

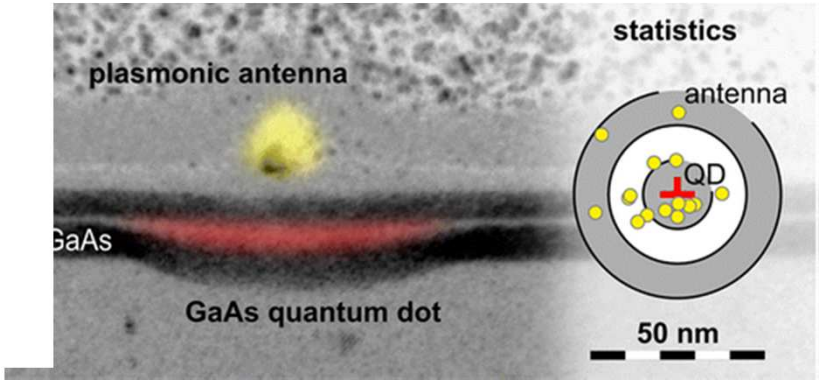

2.2.a Bottom-up + top-down: location of a QD → "device"

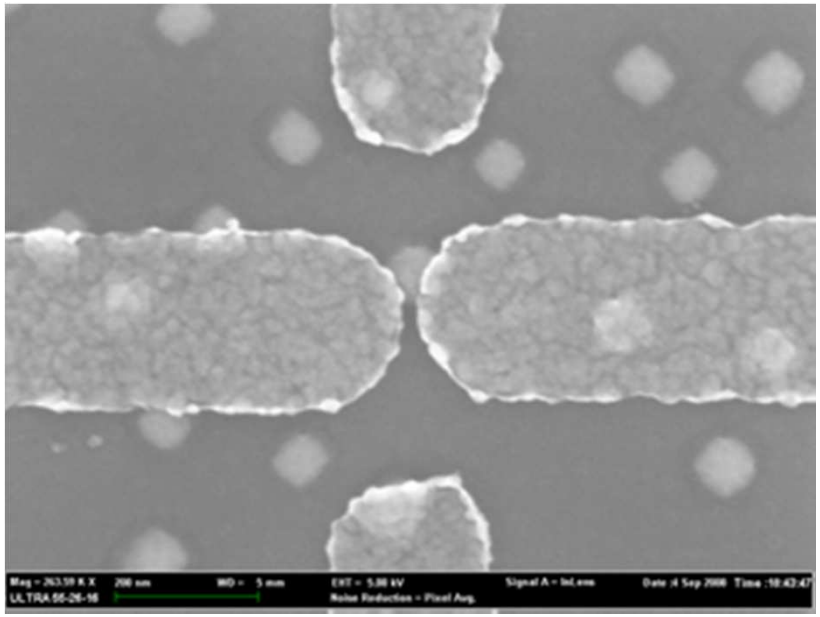

Location of a Ge QD position with respect to predefined markers via SEM → lithographic definition of electric contacts on QD (via e-beam)

G. Katsaros et al. Nature Nanotech. 5, 458-464 (2010)

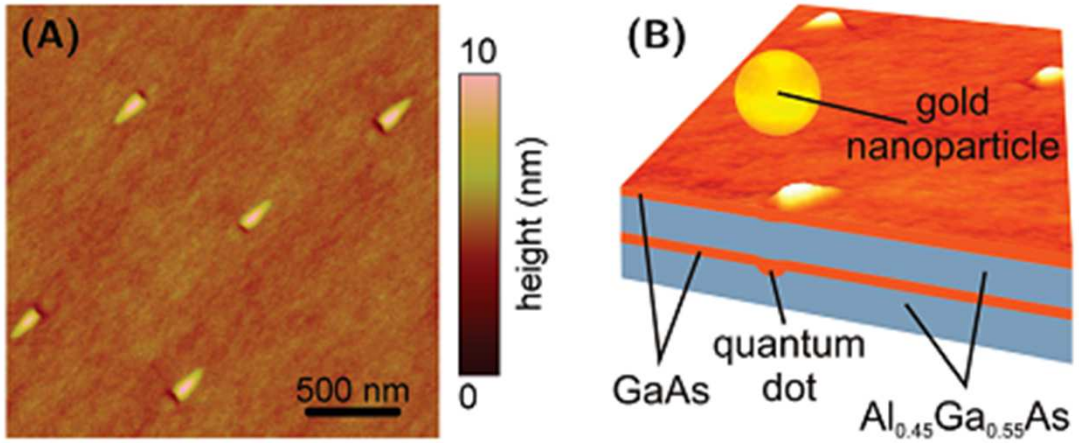

Location of a buried GaAs/AlGaAs QD position via AFM followed by nanomanipulation with AFM tip

M. Pfeiffer et al. Nano Lett. 10, 4566 (2010)

2.2.a Bottom-up + top-down: location of a QD → "device"

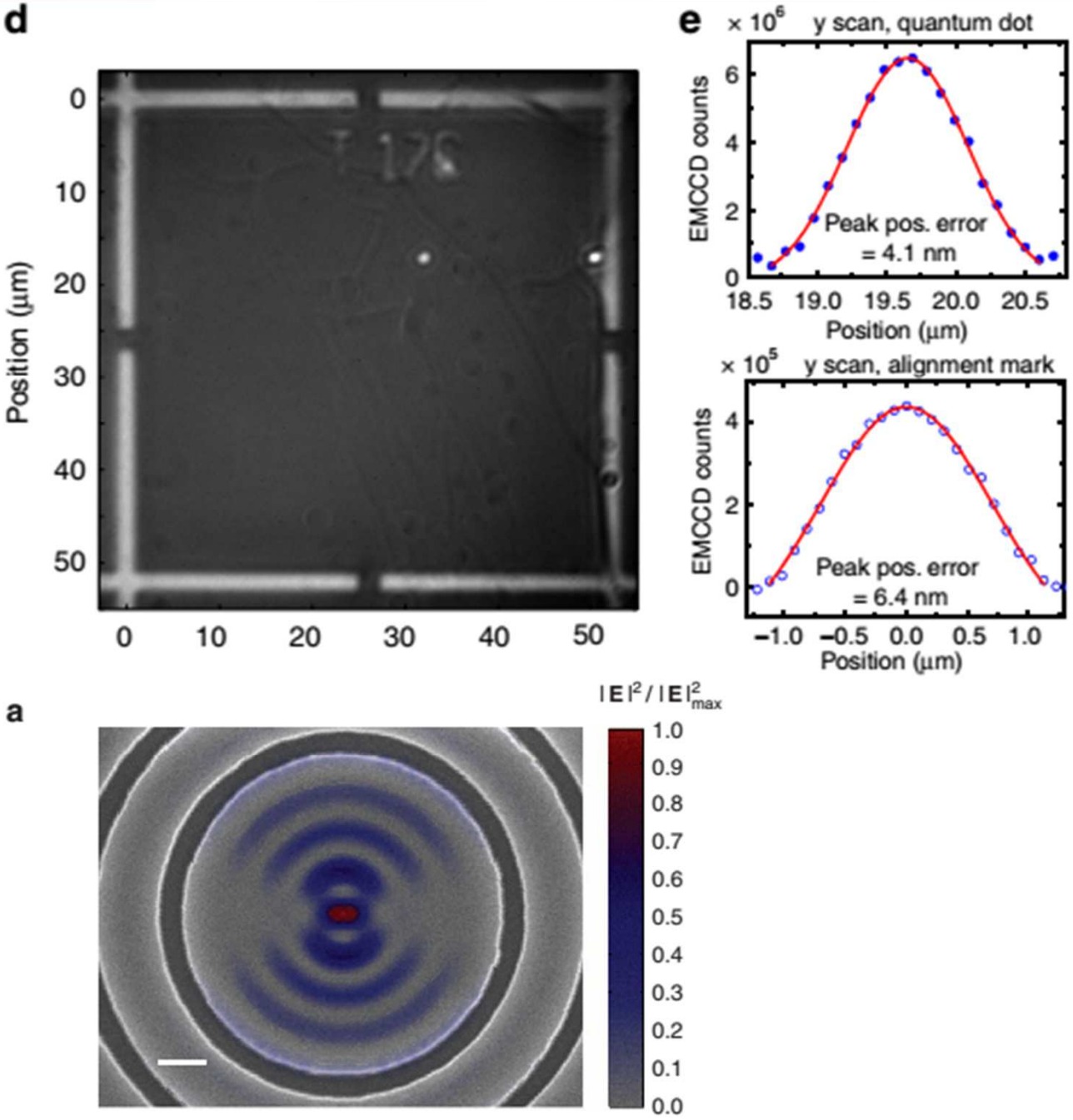

Location of an InGaAs QD with respect to predefined markers by optical imaging and fitting (~10 nm resolution achievable) followed by e-beam → QD surrounded by circular Bragg grating

L. Sapienza et al., Nature Comm. **DOI: 10.1038/ncomms8833 (2015)**

See also T. Kojima et al. Appl. Phys. Lett. 102, 011110 (2013)

2.2.b Bottom-up + top-down: In-situ lithography

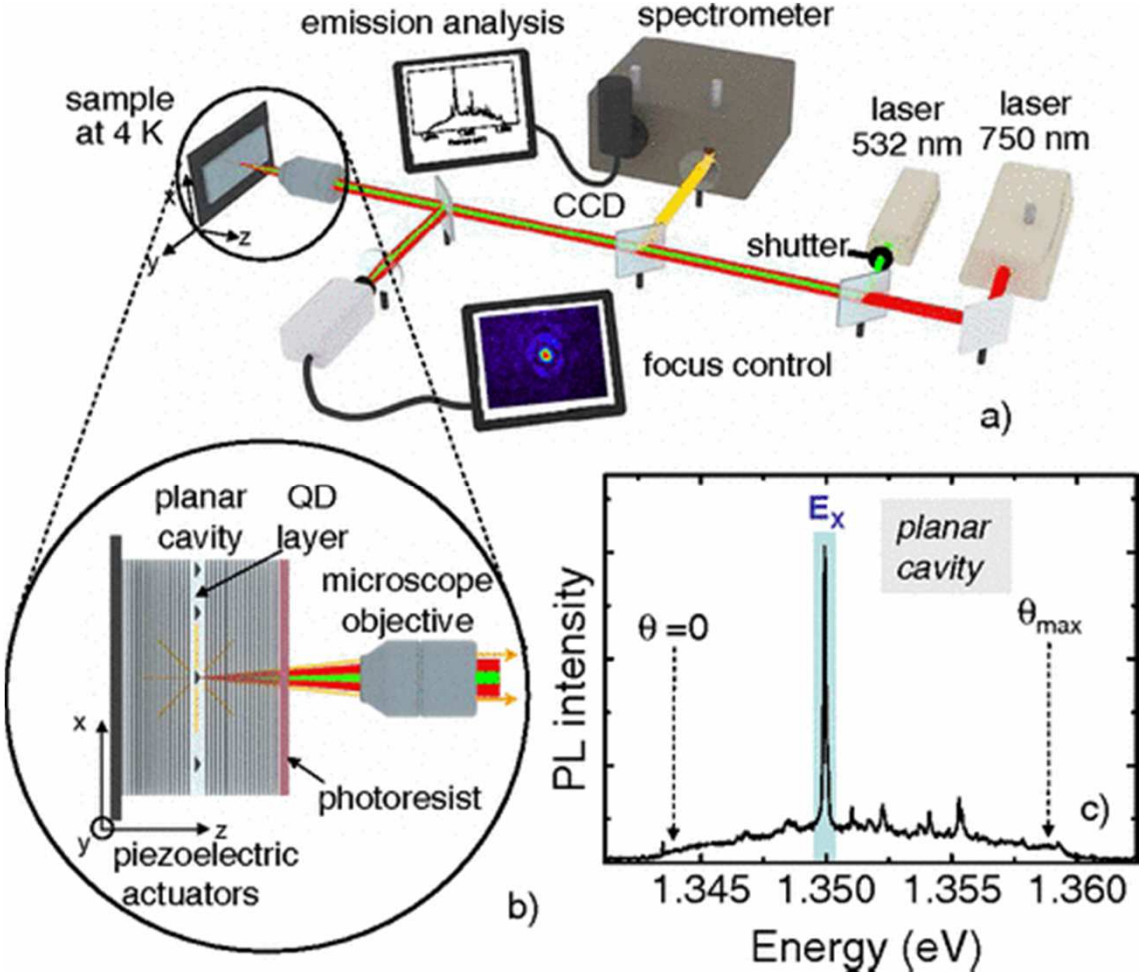

μ-PL setup used to measure QD properties, select suitable QDs, and expose (via a second laser) photoresist.

Subsequent etching results in pillar microcavities with proper characteristics around selected QDs.

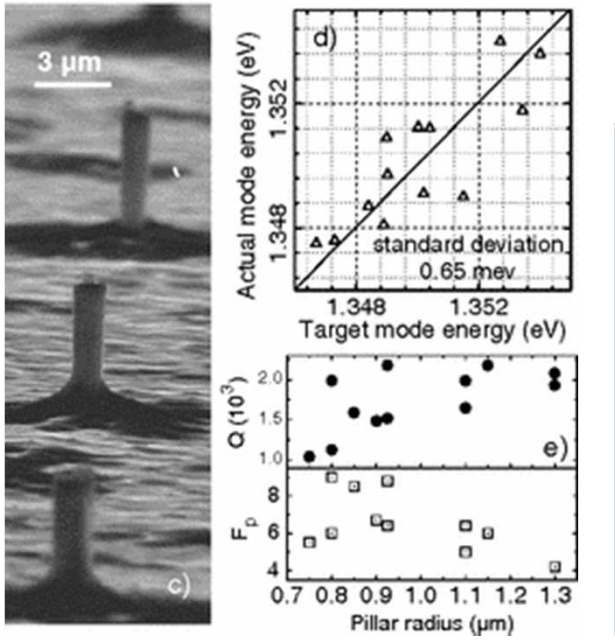

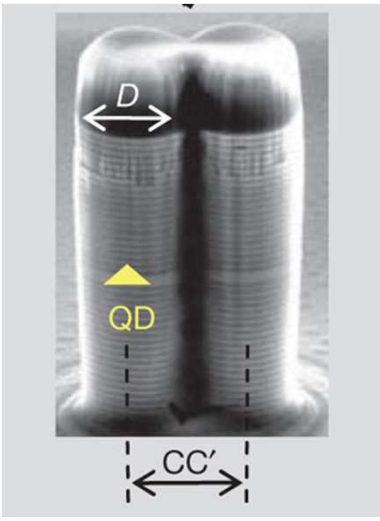

Dousse et al. PRL 101, 267404 (2008)
Dousse et al. Nature 466, 217 (2010)

2.2.b Bottom-up + top-down: In-situ lithography

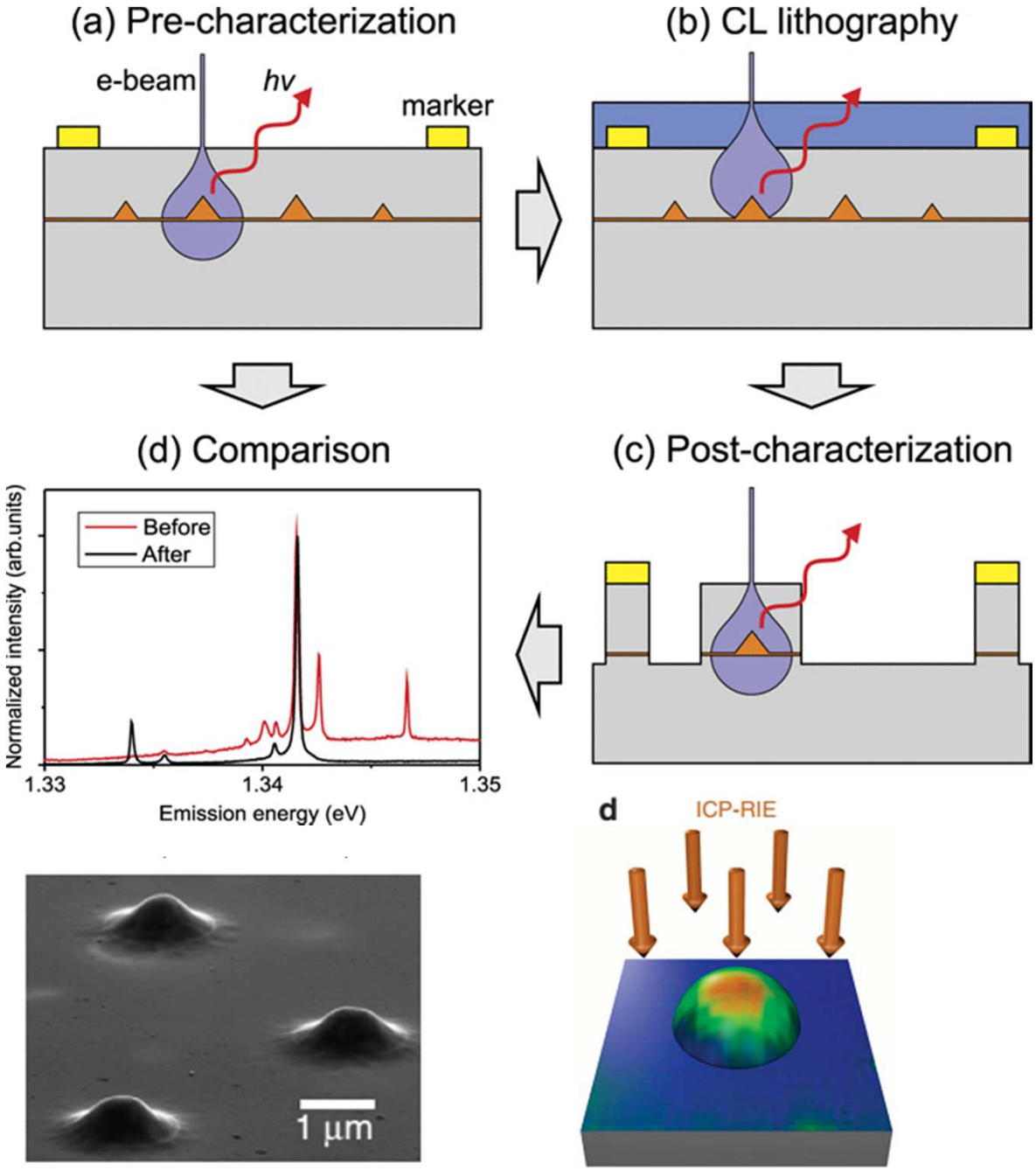

In-situ electron-beam lithography via cathodoluminescence in an SEM

→ lithographic definition of microlenses on top of QD
***R. Kaganskyi et al, Rev. Sci. Instr.* 86, 073903 (2015)**

M. Gschrey et al. Nature Comm. DOI: 10.1038/ncomms8662 (2015)

Bottom-up + top-down vs Top-down + bottom-up

ments[3,4] to be realized. However, the construction of such elaborate QD–PCNC coupled systems requires a technique to detect the positions and wavelengths of individual QDs for precise alignment. This is because high-quality QDs are normally realized using self-assembled S–K mode growth methods with random positions and emission wavelengths. There has been a research about positioning of QDs;[5] however, the emission linewidths of the positioned QDs tend to be broader than typical QDs grown in S–K mode, which means that the quality of positioned QDs was slightly degraded. There have been another kinds of researches about

vs

K. Hennessy et al, Nature 445, 896-899 (2007)

controlled within the device for optimal interaction. While site-controlled growth of QDs presents one attractive option[3], the properties of such QDs (in terms of homogeneous linewidth, for example) have not yet matched those of QDs grown by strain-mediated self-assembly (Stranski–Krastanow growth)[4].

L. Sapienza et al., Nature Comm. **DOI: 10.1038/ncomms8833 (2015)**

2.3 Top-down + bottom-up

Basic idea (continuous view):
Lithographic definition of the position of QDs on the substrate, i.e. modification of the surface so as to have a lateral modulation of the chemical potential for adatoms (or of the decomposition of precursors, in MOVPE) → epitaxial growth

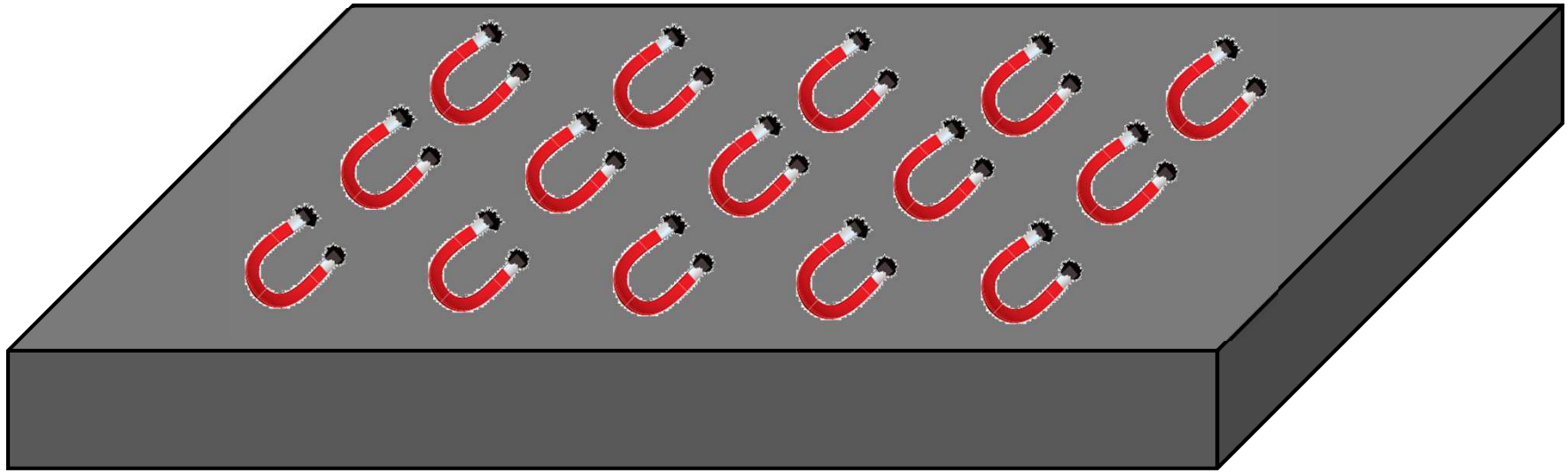

Regions of low chemical potential act as sinks for adatoms → increase dot formation rate.

2.3 Top-down + bottom-up

How to obtain a lateral modulation of the chemical potential for adatoms?

$$\mu(x,y,z) = \mu_0 + \Omega[\gamma(x,y,z)\kappa(x,y,z) + E_S(x,y,z)]$$

μ: chemical potential (Free energy per atom)
μ_0: chemical potential of flat, unstrained surface
Ω: atomic volume [nm^3]
γ: surface energy per unit area [eV nm^{-2}]
κ: surface curvature [nm^{-1}], positive for convex and negative for concave areas
E_S: strain energy [eV]

By:
- Surface energy modulation
- Curvature modulation
- Strain modulation

See B. Yang et al. Phys. Rev. Lett. 92, 025502 (2004)

2.3.a SK growth on mesa structures

$$\mu = \mu_0 + \Omega[\gamma\kappa + E_S]$$

Surface curvature favors concave regions (the larger the curvature, the stronger the μ reduction) → Capillarity. Microscopic view: an „atom" in a pit has many neighbors and so strongly bound.

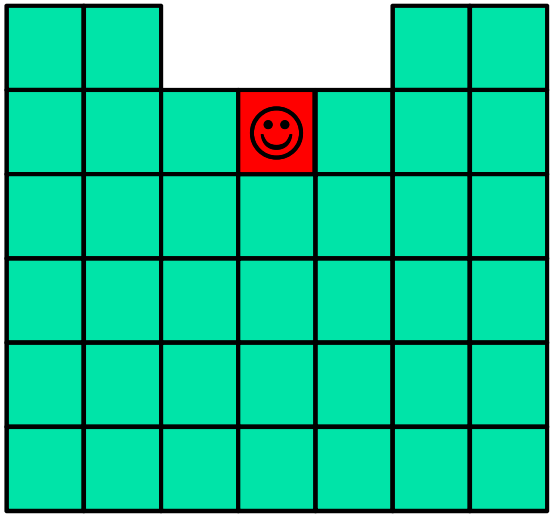

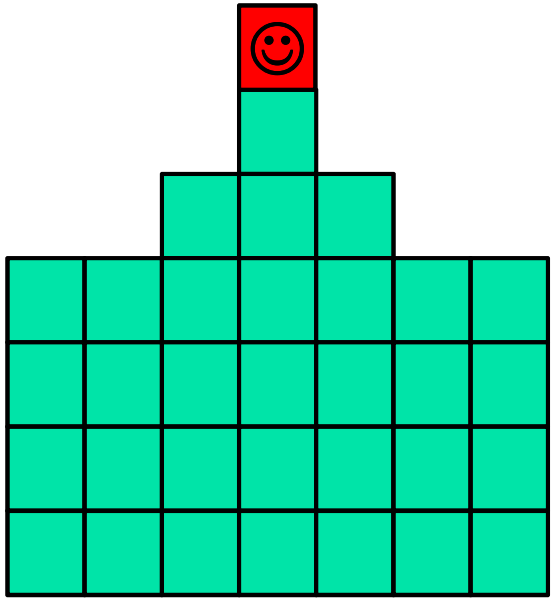

Strain relaxation favors convex regions (at least over flat regions).

2.3.a SK growth on mesa structures

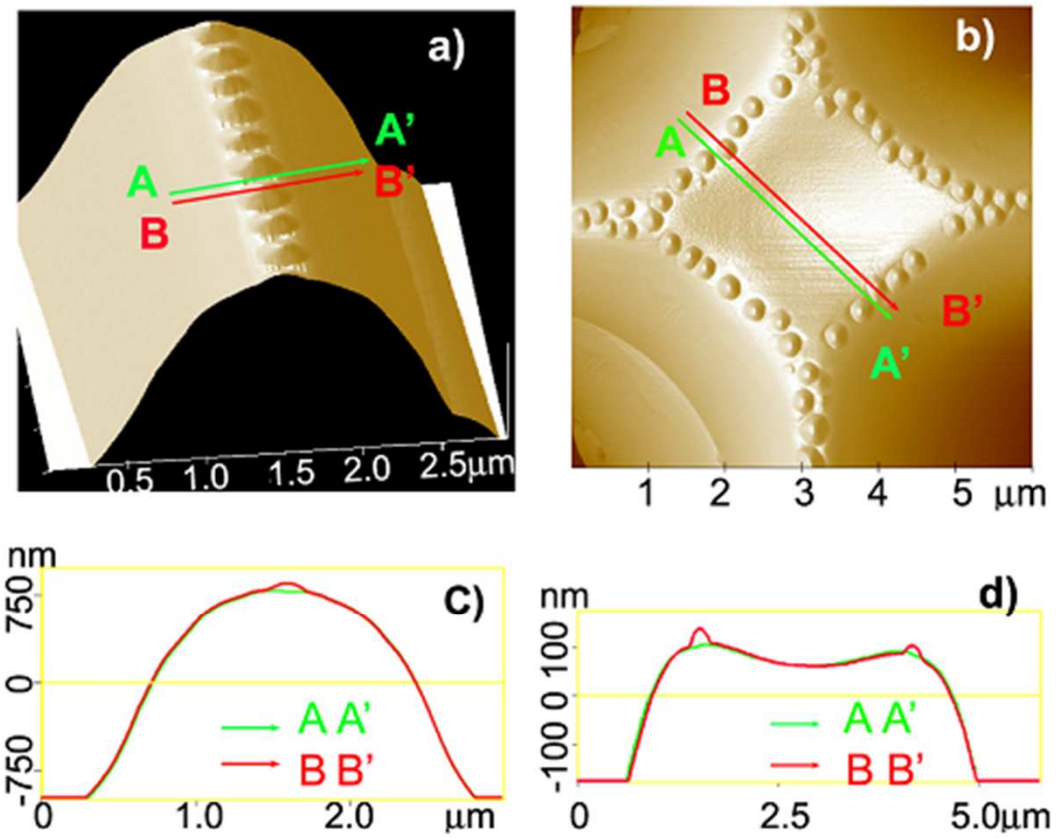

FIG. 2 (color online). AFM images of Ge 3D island ordering on patterned Si(001) structures: (a) a stripe ridge; (b) a diamond-shaped stripe cross. (c) and (d) are the cross sections through (a) and (b), respectively, with AA' and BB' between dots and over dots, respectively. The z-scale difference in (c) and (d) is due to different plane-flatten processing. The nominal coverage is 60 ML.

$$\mu = \mu_0 + \Omega[\gamma\kappa + E_S]$$

Convex regions are not favored by capillarity effects, but if E_S is lower than in the surrounding regions → nucelation at edges

← Example for Ge grown on Si mesa structures

See B. Yang et al. Phys. Rev. Lett. 92, 025502 (2004)

Chains of QDs on lithographically defined stripes

Growth of Ge/Si on SiO_2 apertures

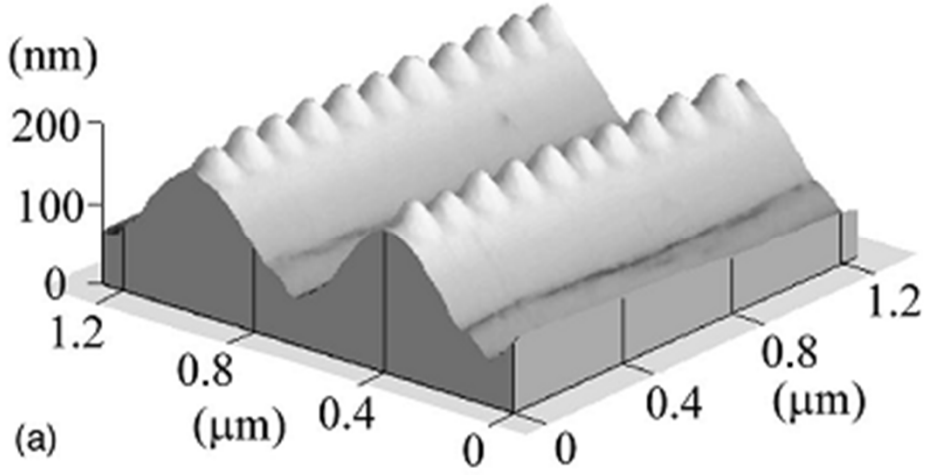

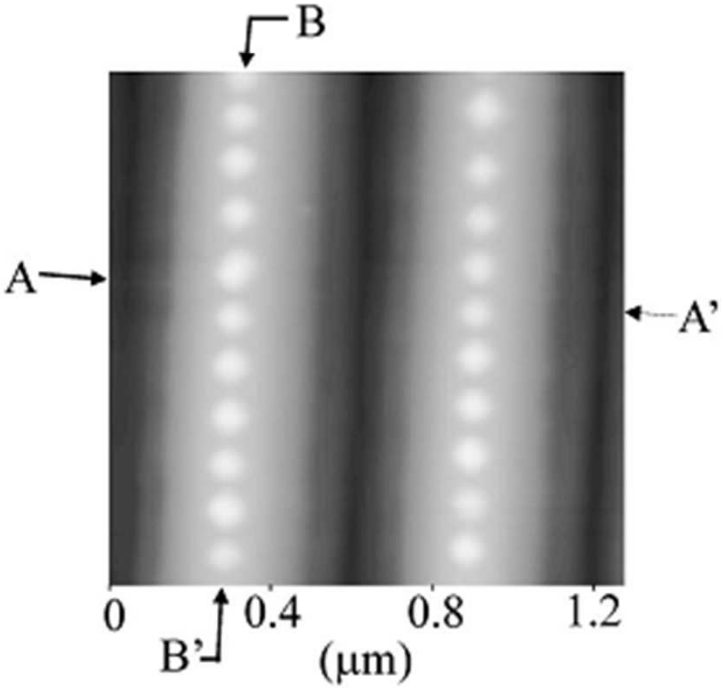

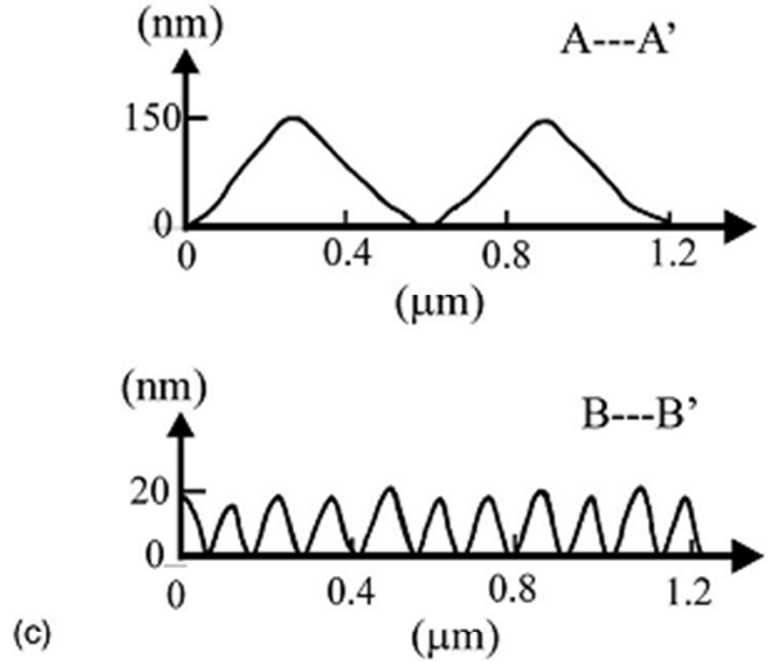

FIG. 1. (a) A 3D AFM image of the self-organized Ge islands on the ⟨110⟩-oriented Si stripe mesas with a window width of 0.6 μm. Self-aligned and well-spaced 1D arrays of the Ge islands are formed on the ridges of the Si mesas after the deposition of 10 ML Ge. (b) The 2D image of the island arrays in (a), along with the cross sections of the mesas (line AA′) and one array of the islands (line BB′), respectively. The sidewall facets are {113} facets.

Shape is monomodal → regular arrangement improves also size homogeneity

B. Jin et al. Appl. Phys. Lett. 75, 2752 (1999)

T. Kamins et al. Appl. Phys. Lett. 72, 1202 (1997)

InAs/GaAs chains in photonic structures

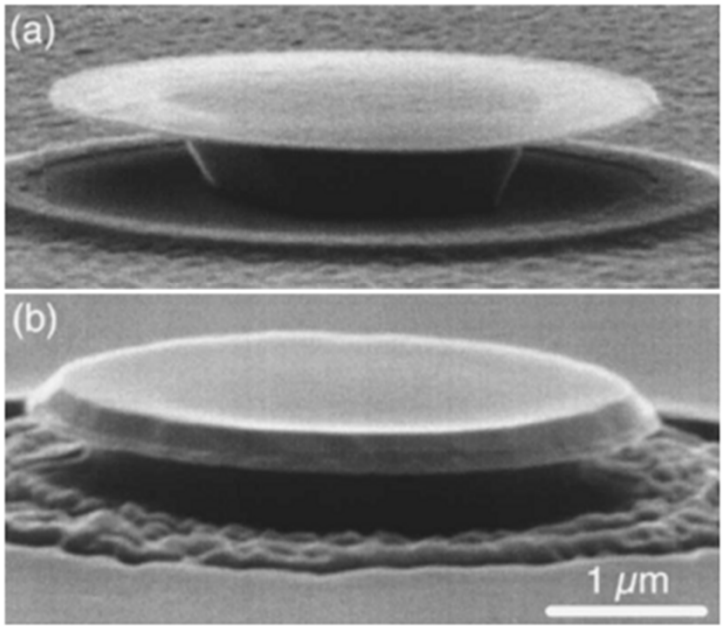

FIG. 1. (a) SEM of the microdisk sample before regrowth. It is ≈50 nm thick and 4 μm in diameter. (b) The microdisk sample after regrowth; the thickness is ≈250 nm.

Disk edges allow for larger strain relaxation than middle → QDs chains form there. These are the regions where optical modes („whispering gallery modes") are located → QDs form where needed.

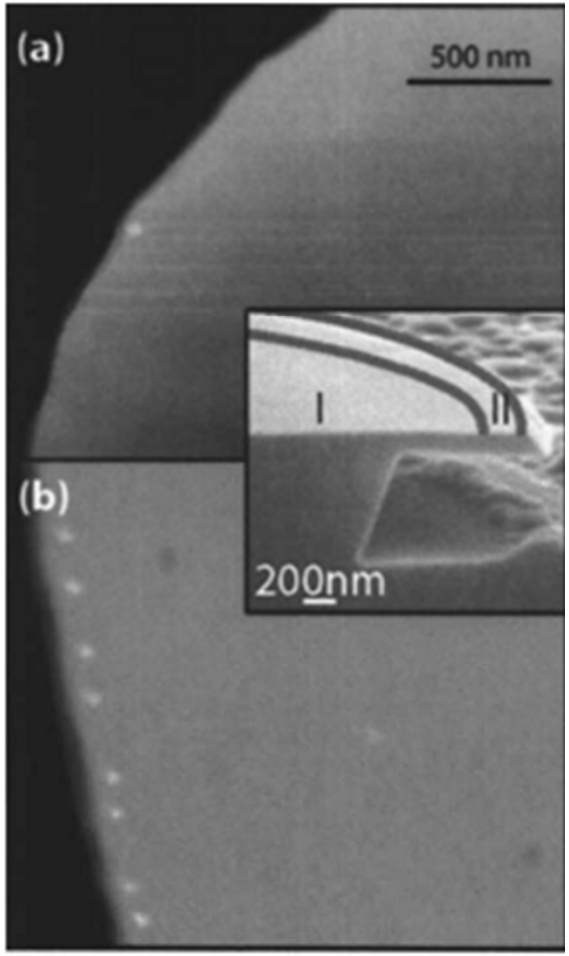

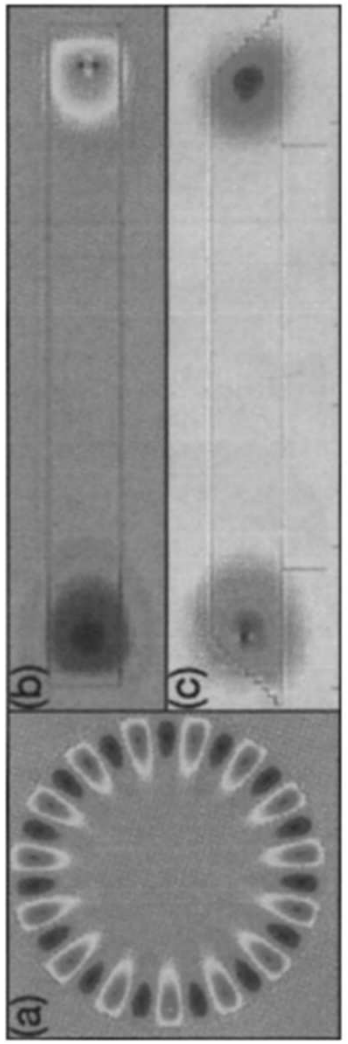

FIG. 3. Electromagnetic field amplitude distribution of $TE_{15,1}$ mode in a 1.8 μm microdisk, made with 3D FDTD simulations. (a) Top-view of the disk; (b) Side-view cross section through the center of the microdisk with vertical sidewalls indicating positive (right) and negative (left) nodes; (c) Corresponding side-view with 45° sidewalls.

Z. G. Xie et al. Appl. Phys. Lett.87, 093106 (2005)

Similar behavior for InAs/GaAs

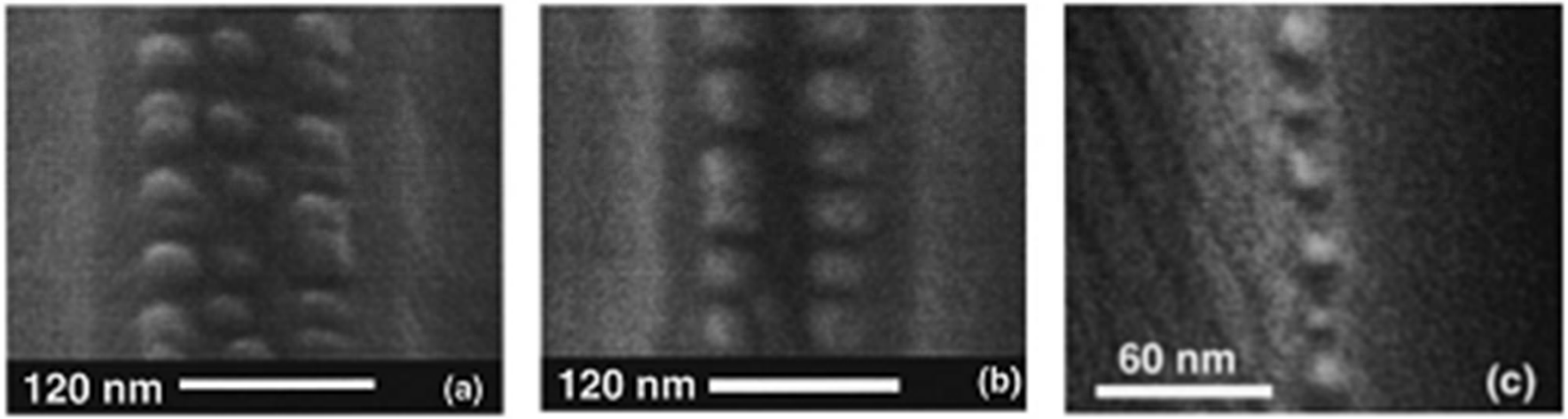

R. Zhang et al. Appl. Phys. Lett. 73, 507 (1998)

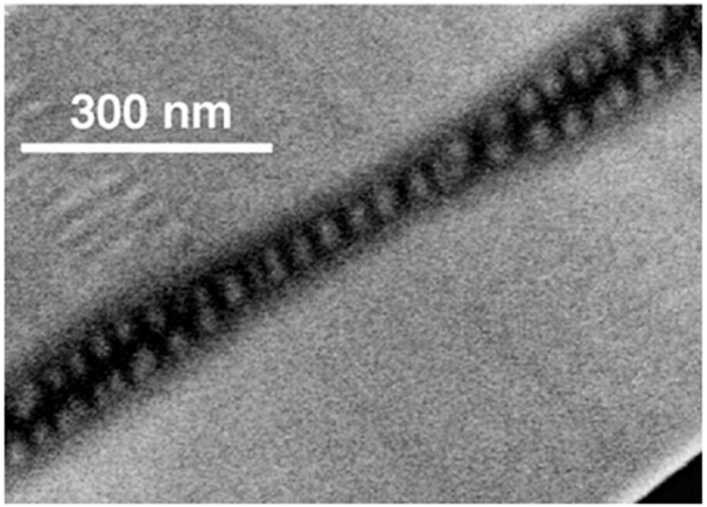

Fig. 2. Top-view SEM image showing InAs SOQDs on mesa tops (regions of dark contrast), going from two to three and back to two rows (top), and from two to one and back to two rows (bottom). No SOQDs are formed on the mesa sidewalls.

GaAs mesas obtained by selective-area growth on oxide windows on GaAs (001).
Subsequent InAs deposition results in chains of QDs.
Depending on ridge width chain of single dots or multiple chains.

K. Shiralagi et al. J. Cryst. Growth 201, 1209 (1999)

2D arrays on small mesas

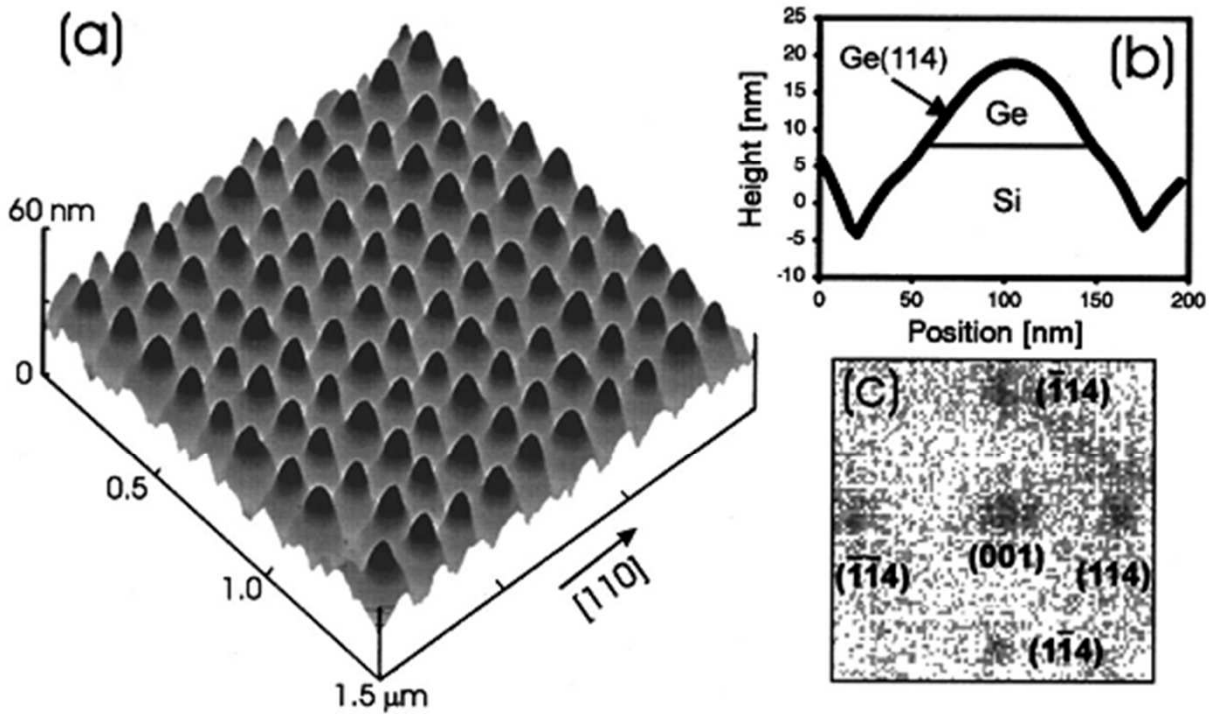

FIG. 1. (a) AFM image of an array of Ge islands (dark-colored dots) on prepatterned Si(001) surfaces. (b) Cross-sectional measurement of a typical Ge island. (c) Normal view of a histogram of the statistics of the island surface normal vectors that are measured vertically with respect to the [001] direction and horizontally with respect to the [110] direction. Peaks of {114} and (001) planes are evident.

Si mesas obtained by e-beam and RIE (20 nm deep). When mesa width and spacing compable to dot size, dots form only on mesa top → 1 QD per mesa with homogeneous size

Single InGaAs/GaAs QDs at pyramid tips

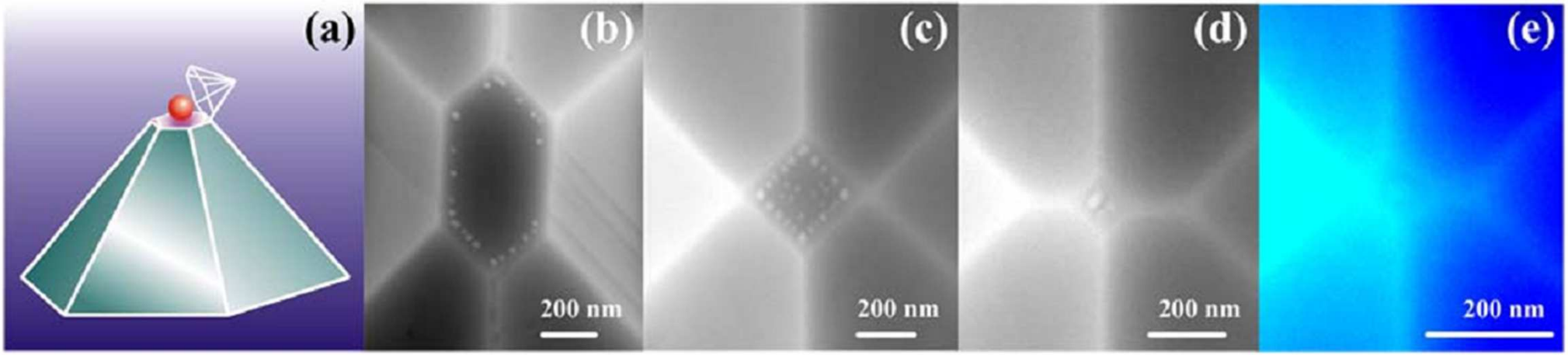

- GaAs pyramids develop during MOVPE growth of GaAs on mesa-patterned GaAs(001).
- InAs growth leads to dot formation at apex (again because of strain relaxation at convex edges).
- Growth of side facets and edges not bounding (001) facets is suppressed because of larger critical thickness for dot formation. Specific facets (γ) also plays a role!
- Geometry also enhances ligth extraction.

$$\mu = \mu_0 + \Omega[\gamma\kappa + E_S]$$

Tung-Po Hsieh et al. Applied Physics Letters 90, 073105 (2007)

Single GaN/AlGaN QDs at pyramid tips

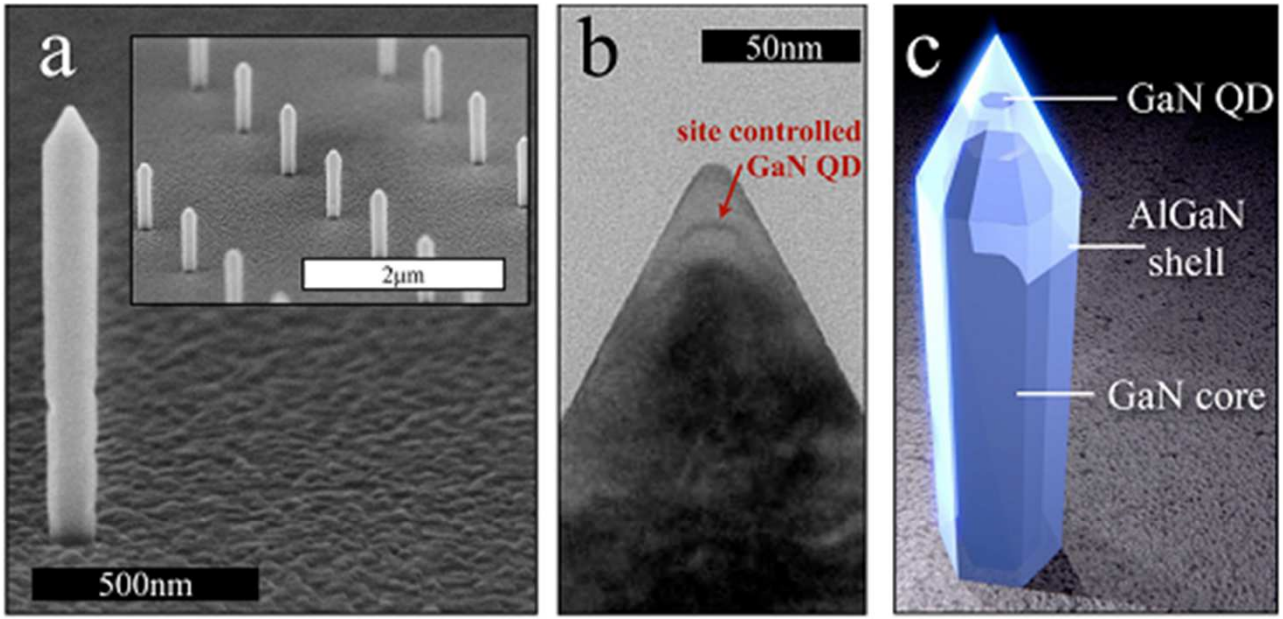

Figure 1. Images of site-controlled nanowire-QDs. (a) SEM image showing a single nanowire grown on a patterned SiO_2 substrate by selective area MOCVD. The inset shows an array of nanowires separated by 2 μm (a spacing of 20 μm was used for the optical experiments). (b) TEM image clearly showing the formation of a single QD near the tip of a single nanowire. (c) Schematic of a nanowire containing a single QD.

GaN nanowires with pyramidal top develop during MOVPE growth of GaN on AlN on sapphire with SiO2 apertures.
Wire is coated with AlGaN (higher bandgap) followed by GaN and AlGaN → GaN QD at apex.

Room temperature emission possible because of strong exciton binding energy in III-Ns

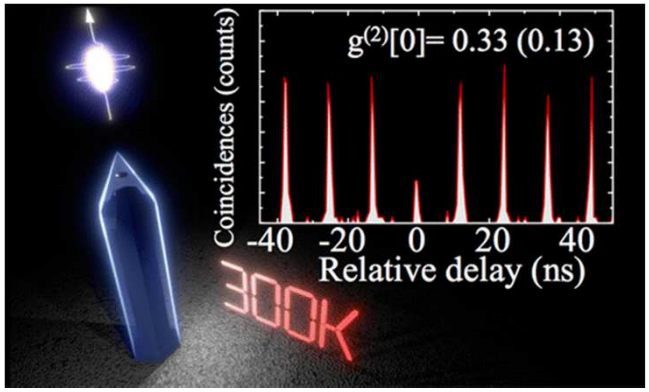

M. J. Holmes et al. Nano Lett., 14, 982−986 (2014)

2.3.b SK growth on buried stressors

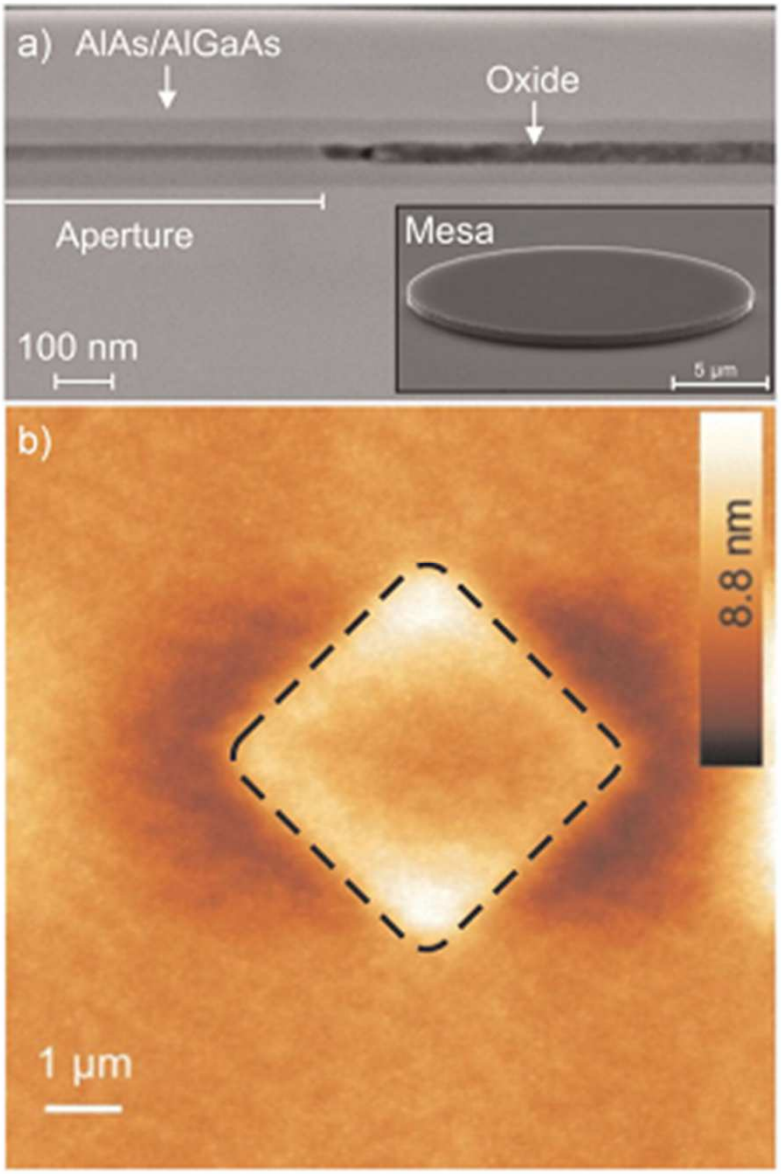

- Growth of layer sequence including an Al-rich AlGaAs layer capped with GaAs
- Mesa etching and controlled lateral oxidation of AlAs layer
- → Formation of a tensile-strained region in the center of the mesa
- GaAs overgrowth and QD growth
- Dot is self-aligned with current channel!

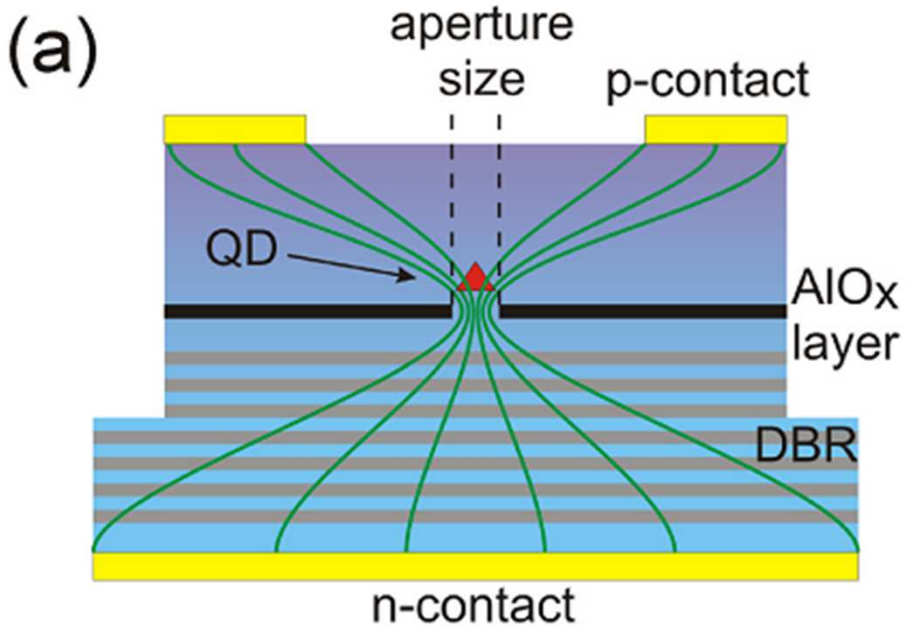

A. Strittmatter et al. Phys. Status Solidi A 209, 2411 (2012); W. Umrau et al. APL 101, 211119 (2012)

2.3.b SK growth on buried stressors

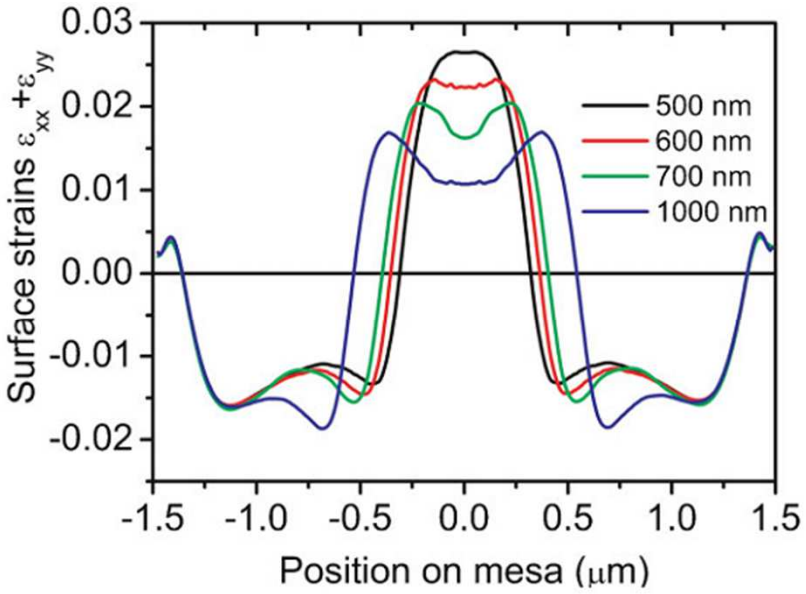

Figure 2 (online colour at: www.pss-a.com) Line scans of surface strains $\varepsilon_{xx} + \varepsilon_{yy}$ across a circular mesa of 3 μm diameter exhibiting different aperture sizes. The horizontal line marks unstrained GaAs.

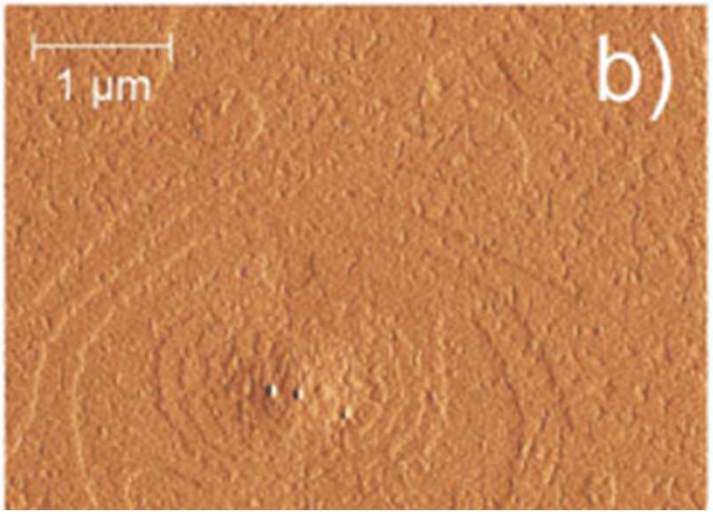

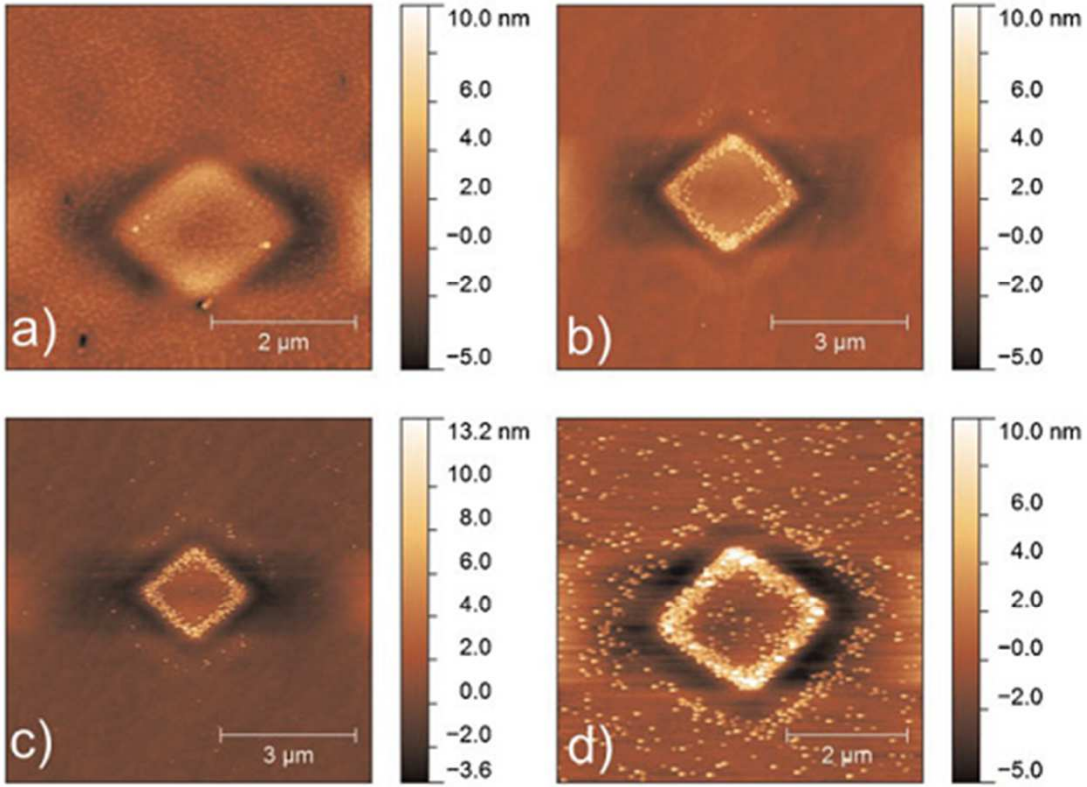

Figure 8 (online colour at: www.pss-a.com) Evolution of the QD distribution during growth interruptions of (a) 5 s; (b) 30 s; (c) 60 s; (d) 120 s. AFM height profiles.

Lateral modulation of strain (+ mesa structure) affects adatom migration and QD nucleation

A. Strittmatter et al. Phys. Status Solidi A 209, 2411 (2012)

2.3.c SK growth in concave regions

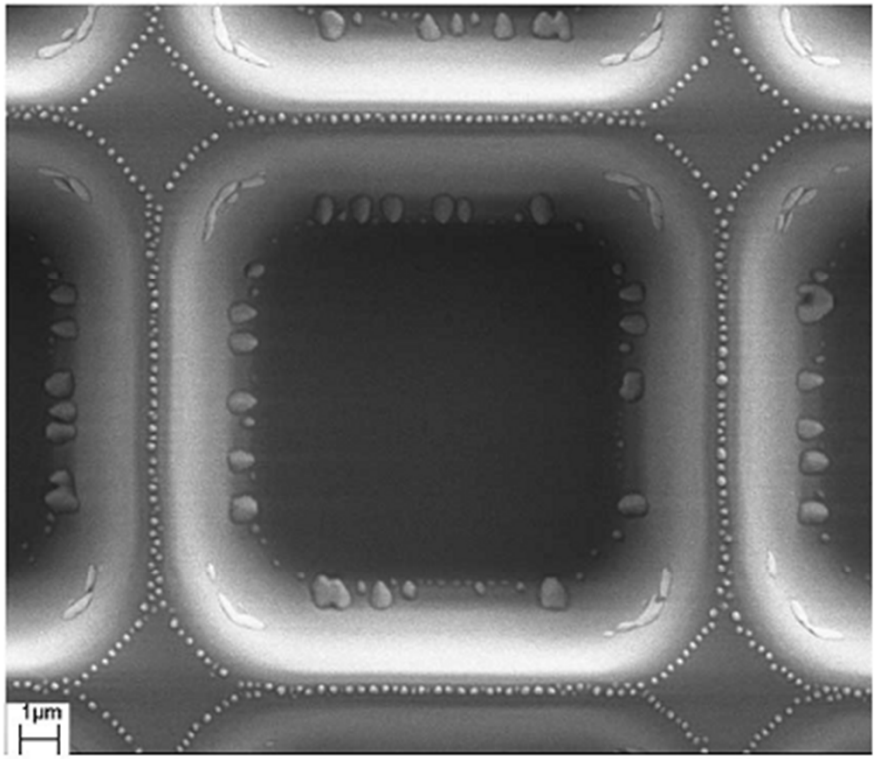

FIG. 3. Scanning electron microscope image of Ge 3D island ordering on patterned stripes on Si(001). $\theta_{Ge} = 60$ ML. The stripes are oriented in ⟨110⟩ directions, but ordering of Ge QDs is independent of direction. Other features (large islands at about half of the height in the upper corners, small islands at the bottom corners, etc.) can also be explained with the model [22].

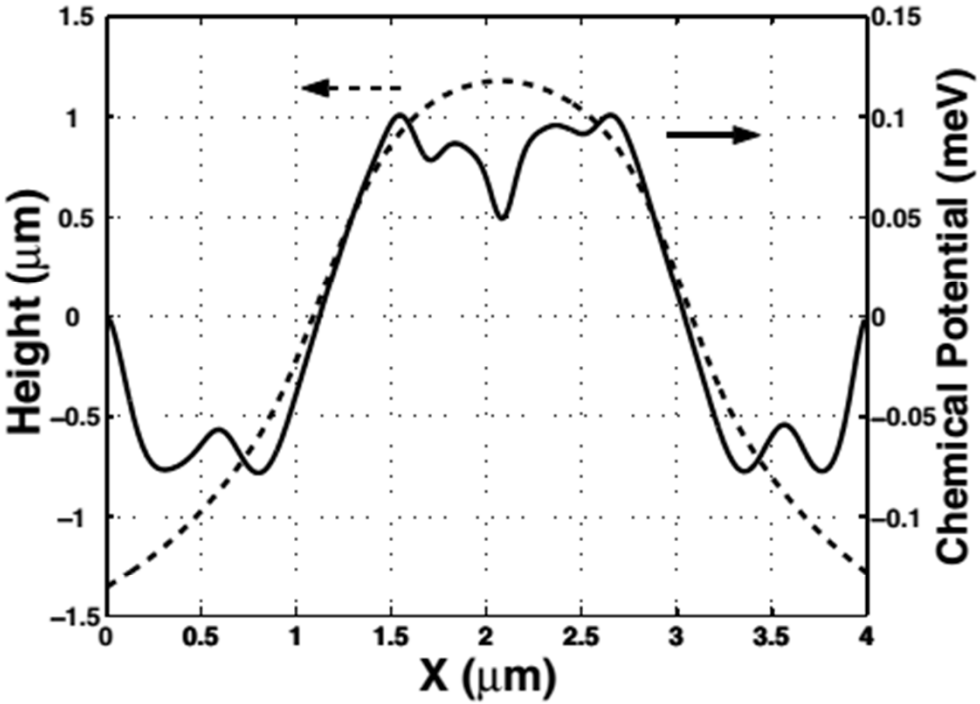

$$\mu = \mu_0 + \Omega[\gamma\kappa + E_S]$$

Surface curvature favors concave regions → formation of clusters at concave regions

See B. Yang et al. Phys. Rev. Lett. 92, 025502 (2004)

1D chains in grooves

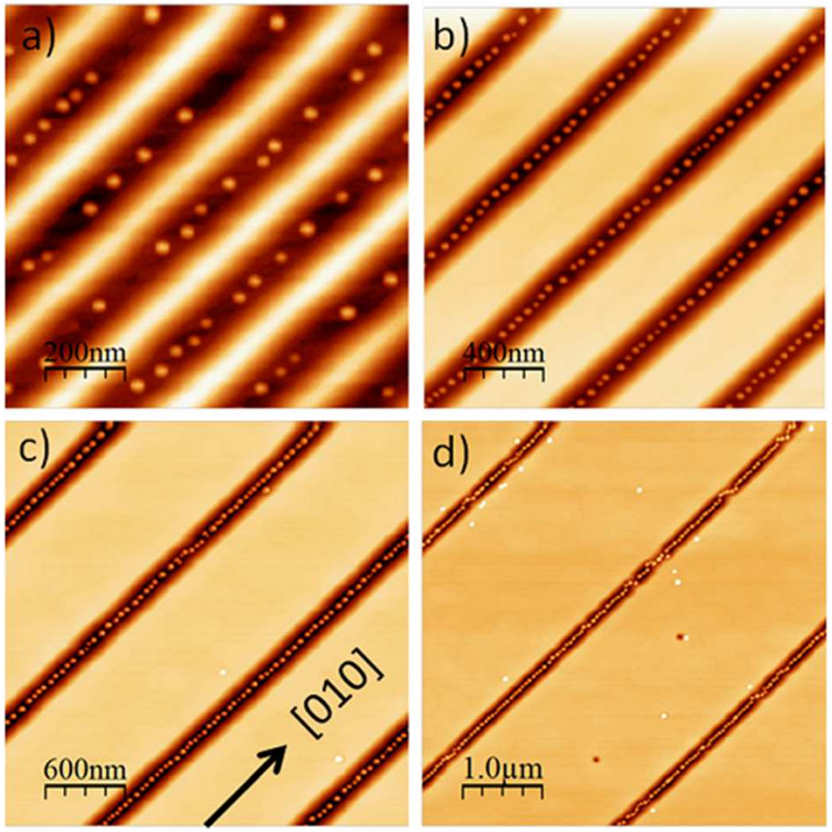

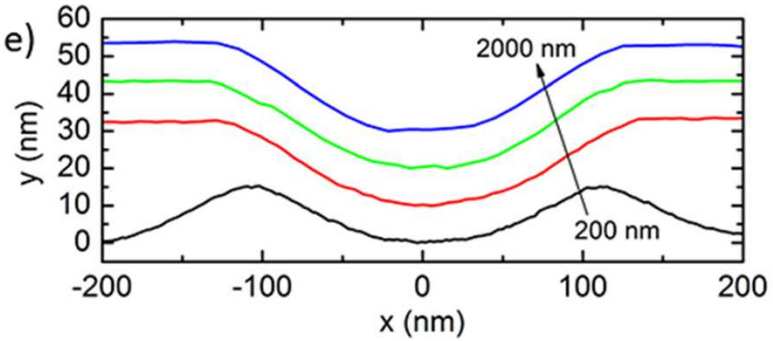

1 a 1, **b** 2, **c** 3, and **d** 5 μm^2 AFM images of surface QDs with groove periods of 200, 500, 1000, and 2000 nm, respectively. **e** The sponding line scans across the grooves

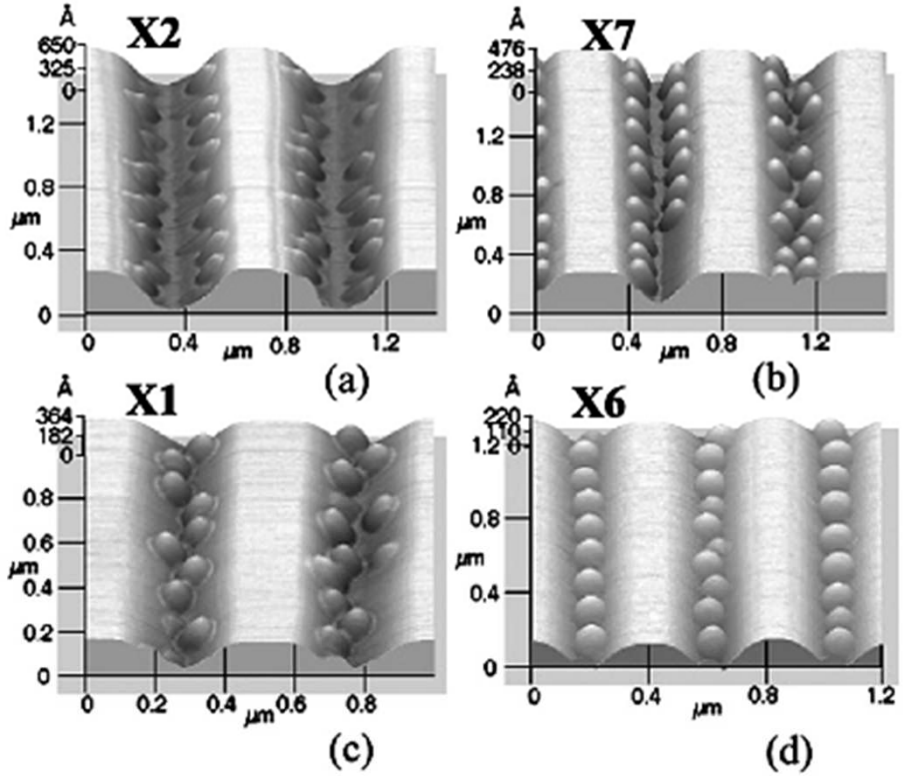

FIG. 1. AFM micrographs of Ge islands formed on stripe-patterned Si substrates of (a) sample X2, (b) sample X7, (c) sample X1, and (d) sample X6.

↑ Ge/Si(001) Z. Zhong et al. J. Appl. Phys., 93, 6259, (2003)

← InAs/GaAs, A. Schramm et al. Nanoscale Research Letters (2015) 10:242

QDs in grooves and pits

What determines whether dots form inside grooves or at edges?

$$\mu = \mu_0 + \Omega[\gamma\kappa + E_S]$$

In grooves or pits $\kappa<0$ → capillarity is always there. Its strength depends on the energy of the surface (low-energy facets may be not as attractive as a stepped surface)

What about strain energy E_S ?
We are talking about deposition of materials with larger lattice constant than substrate. Do they like being placed in a pit? In other words, is E_S larger in a filled pit or on a flat area?

Answer: it depends...

SK growth on pit-patterned substrates

Subcritical amount of Ge deposited on Si pits with different slopes (different curvature of bottom): dots form in pits only in a certain range of slopes

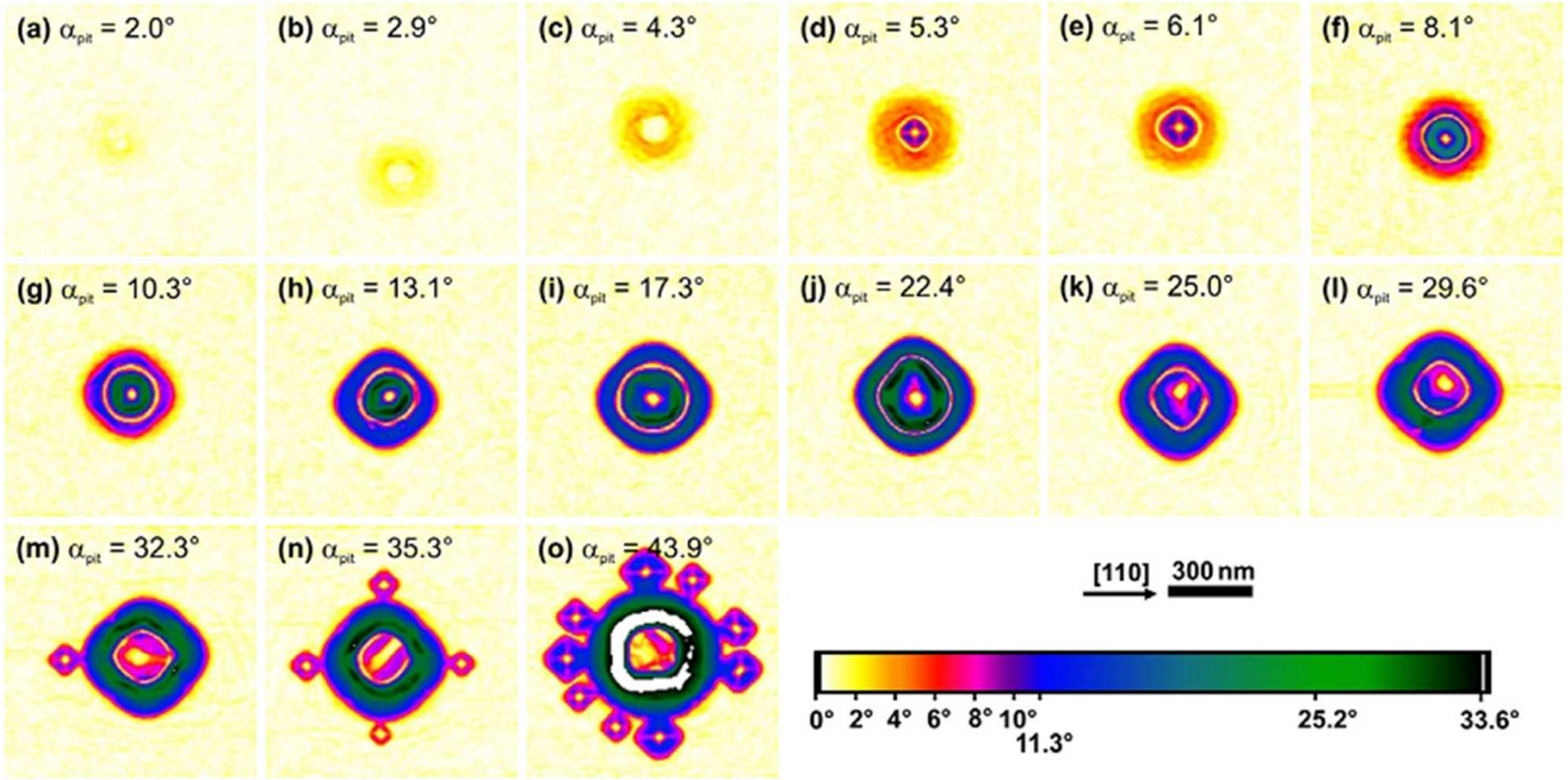

Figure 4. Influence of pit sidewall angle on Ge island growth I. AFM–SAI images of sample S_E. (a)–(o) Originally {111}-pits with $d_{pit} = 1\ \mu m$ and varying opening size (150 nm for (a) and 295 nm for (o)) after Si buffer layer growth and deposition of 3.8 ML of Ge at 700 °C. For none of the pits with $\alpha_{pit} < \sim 5°$ island formation is observed in the pit. (See also figures 2(a) and (b), panels iii), while for $\alpha_{pit} > \sim 30°$, in (m)–(o), islands nucleate at the rim of the pit. Only for $\sim 5° < \alpha_{pit} < \sim 18°$ highly symmetric islands grow in the middle of the pits.

M. Grydlik et al. Nanotechnology 24 (2013) 105601

SK growth on pit-patterned substrates

Elastic energy density of a Ge (or SiGe) dome islands in a pyramidal pit

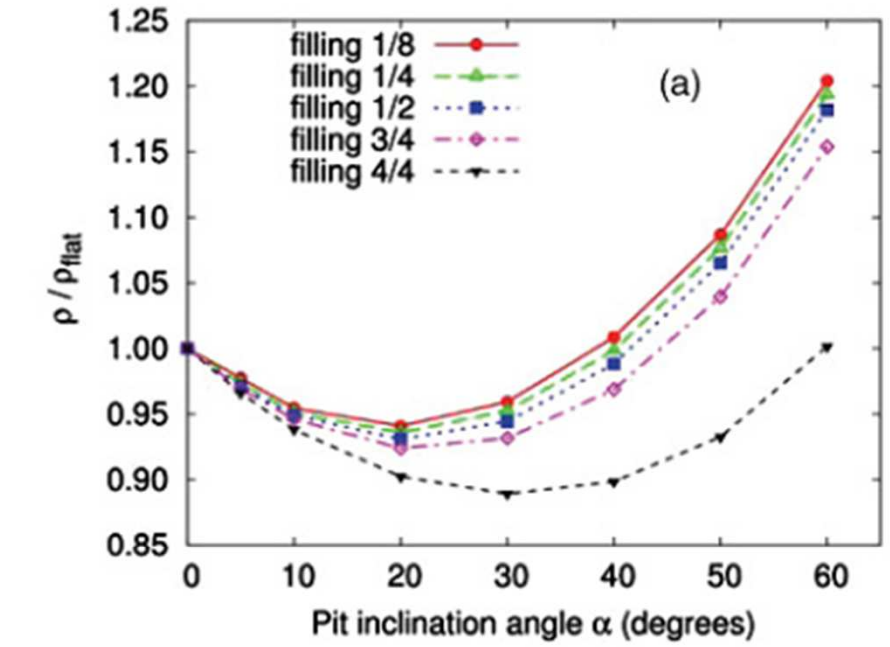

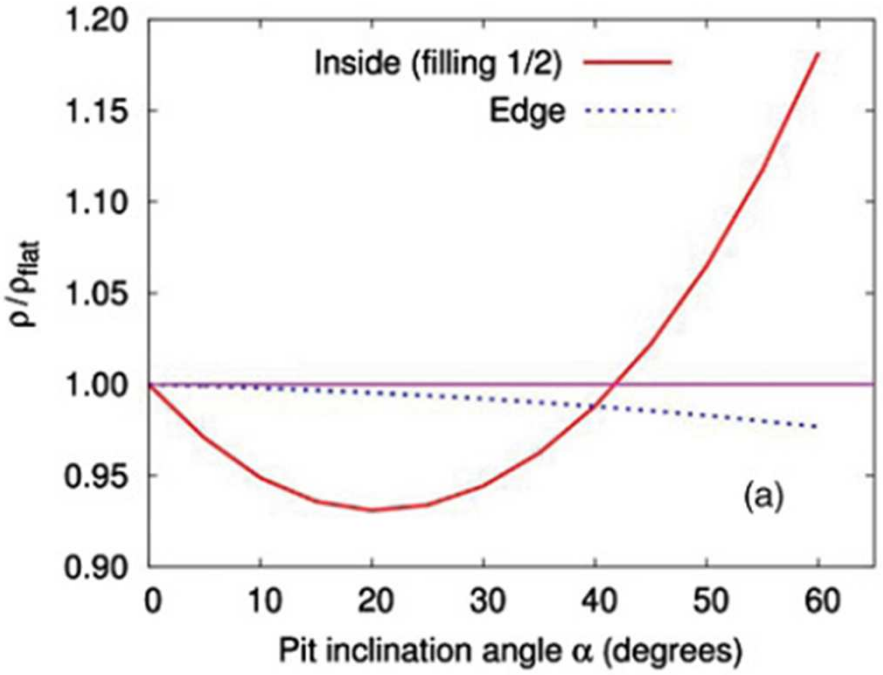

- If pit curvature is not too large, strain favors dot formation in pit!
- 2 driving forces: capillarity + strain relaxation

Note: strain relaxation requires first capillarity → if a pit is too shallow it may be „not attractive enough“ (nucleation may occur outside pit first/also)

G. Vastola et al. Phys Rev. B 84, 155415 (2011)

Pit attraction from a self-assembled trench

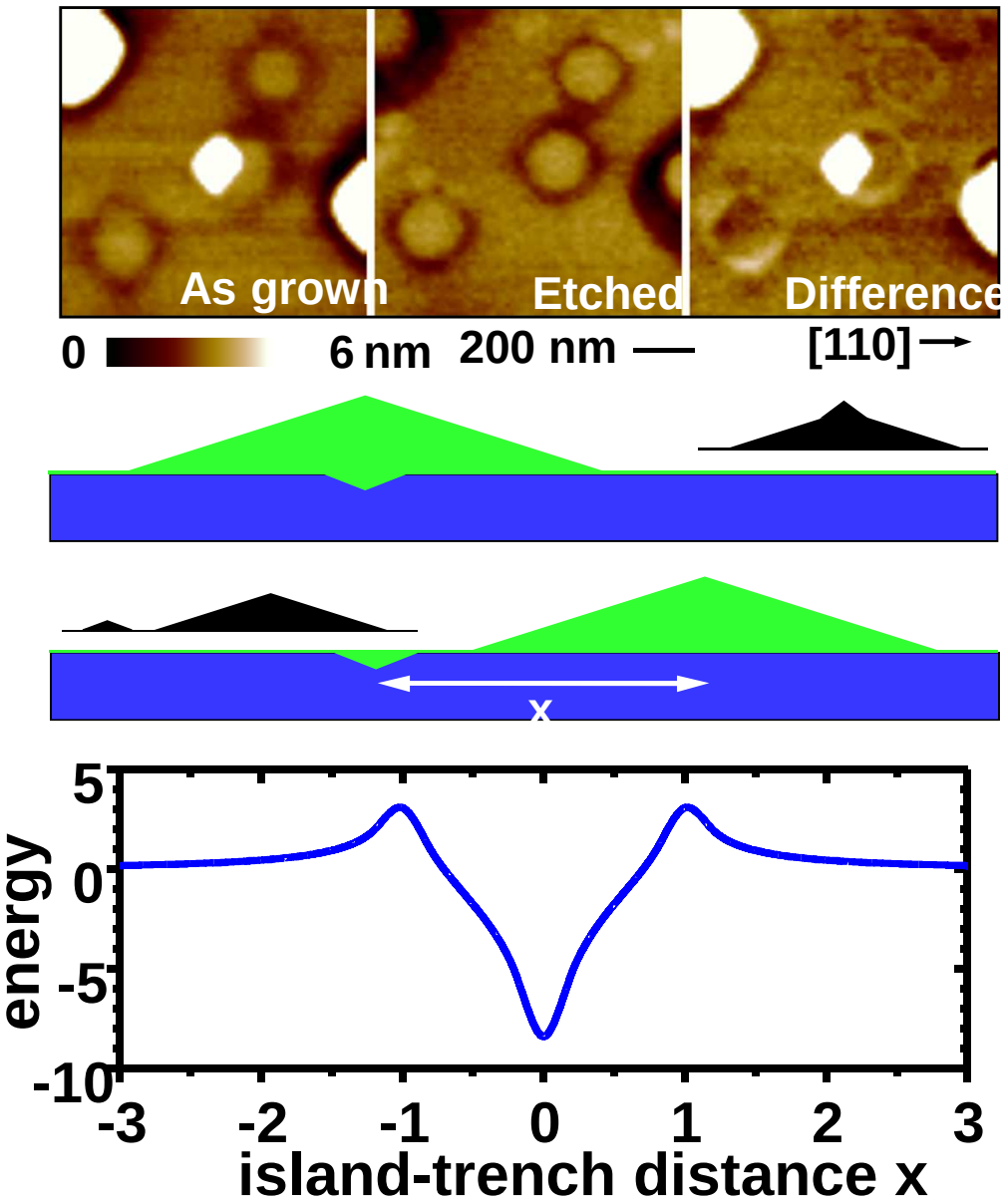

← Ge/Si
Trenches are self-assembled during island growth: they form because Si is expelled from highly compressed regions at QD edge and are partially filled with SiGe

During coarsening, some islands disappear and leave behind empty trench

Islands which have not completely dissolved move on top of shallow trench because of strain relaxation

G. Katsaros et al. Phys. Rev. Lett. 101, 096103 (2008)

Pit attraction from a self-assembled trench

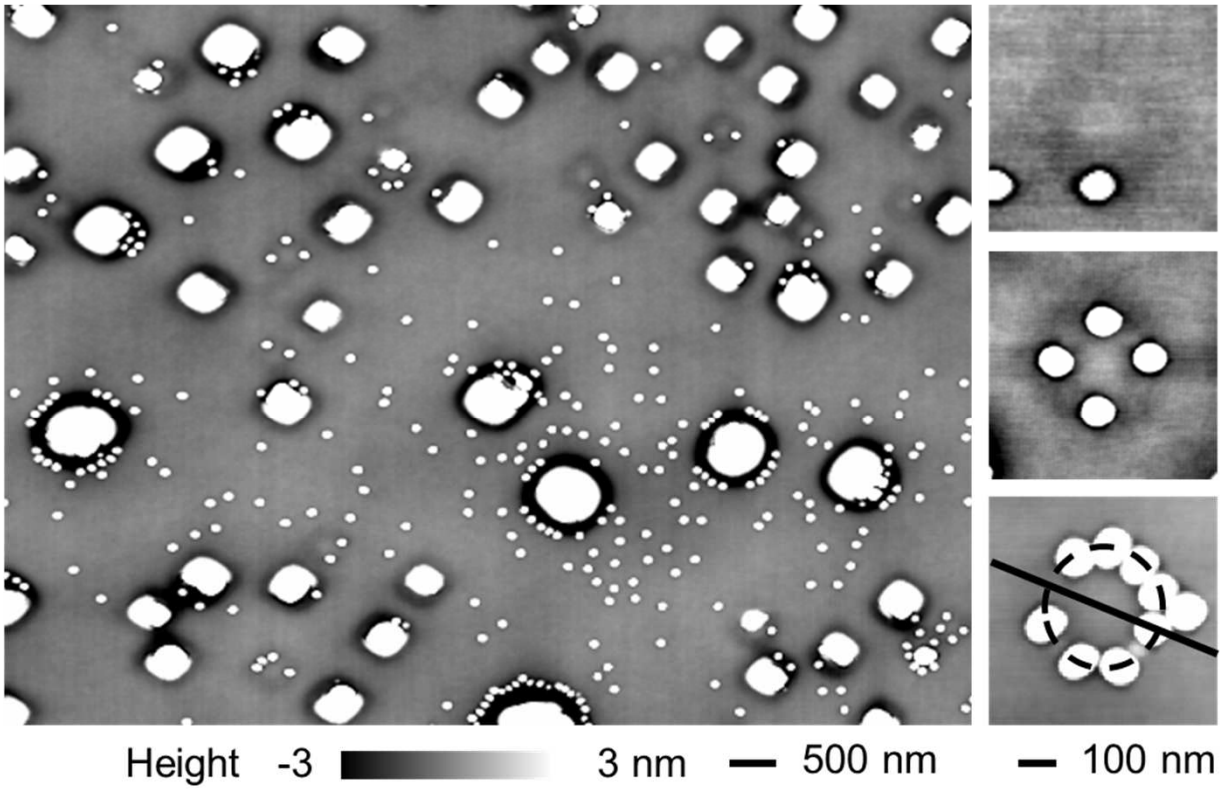

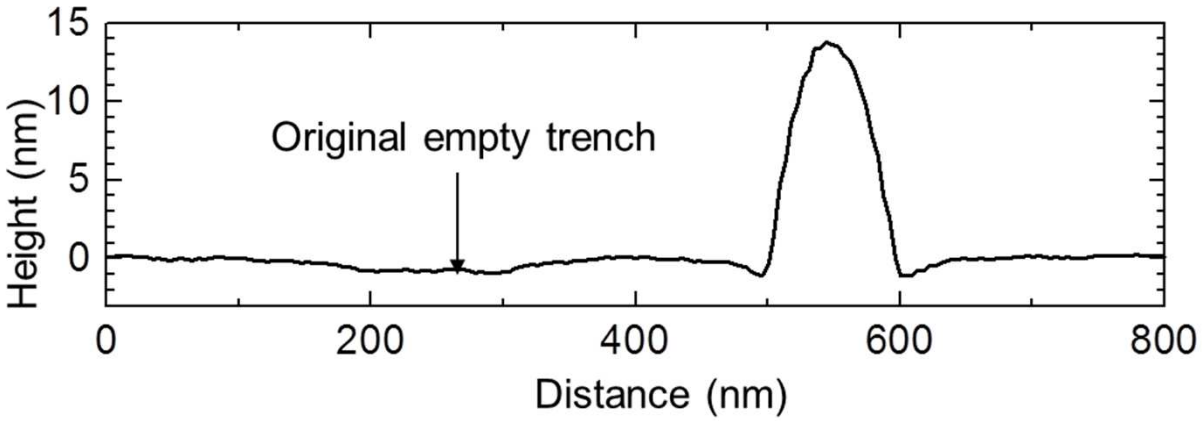

By depositing Ge on trench-decorated surface QDs grow inside shallow trenches and at the edges of deep trenches

G. Katsaros et al. Phys. Rev. Lett. 101, 096103 (2008)

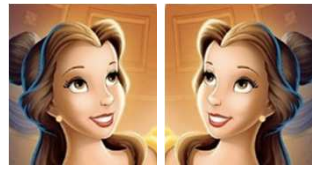

Growth on pit-patterned substrates

Patterned surface **+32 nm Si buffer**

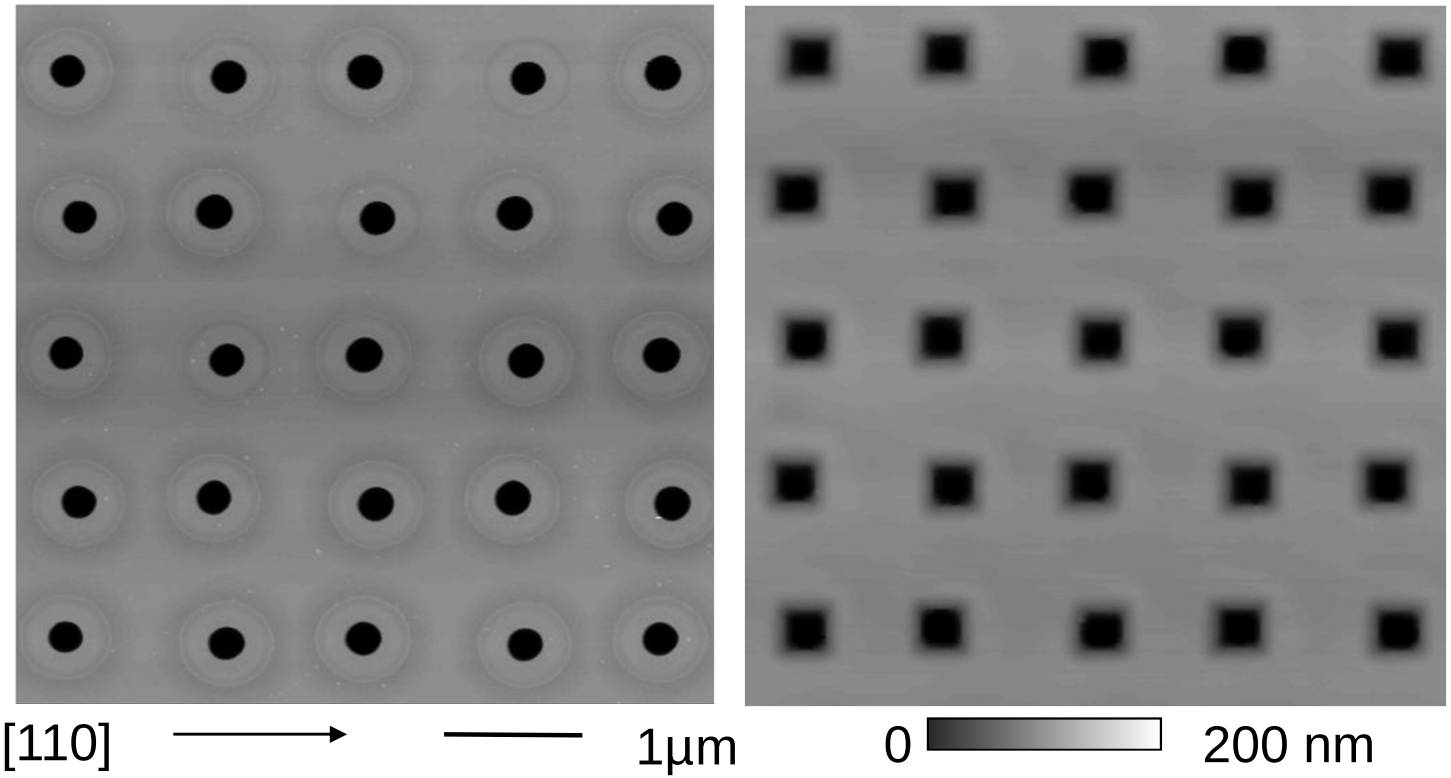

General behavior during buffer growth (necessary to recover clean surface):

- Holes' depth decreases, holes' width increases $\mu = \mu_0 + \Omega\gamma\kappa$
- Faceting may occur
- Pits are not thermodynamically stable → careful growth optimization needed to obtain desired shape and size

J. Zhang et al, Appl. Phys. Lett. 91, 173115 (2007)

Shapes of QDs grown on patterned pits

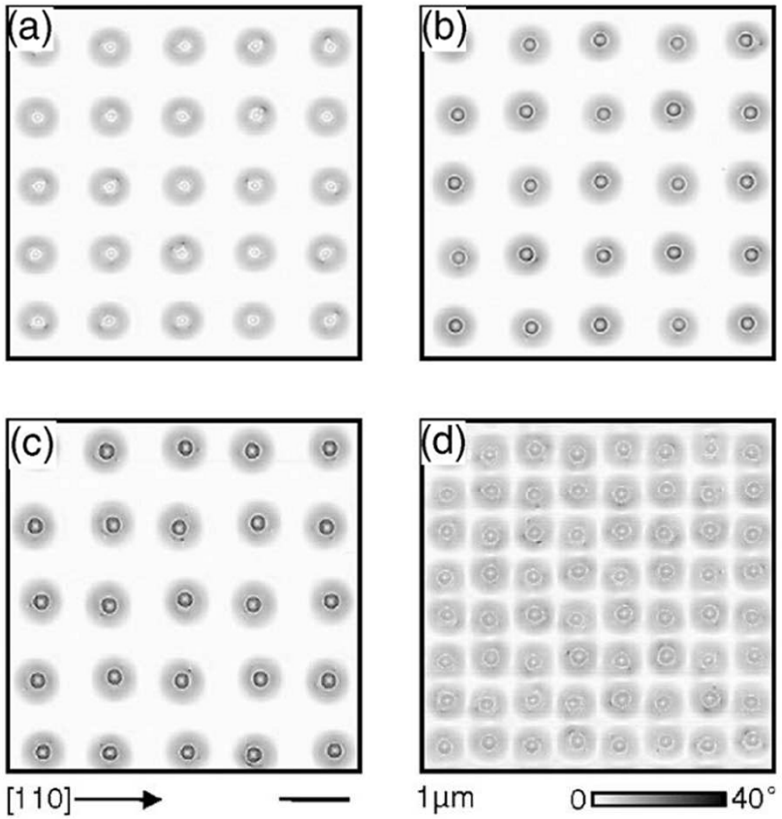

Ge/Si(001)

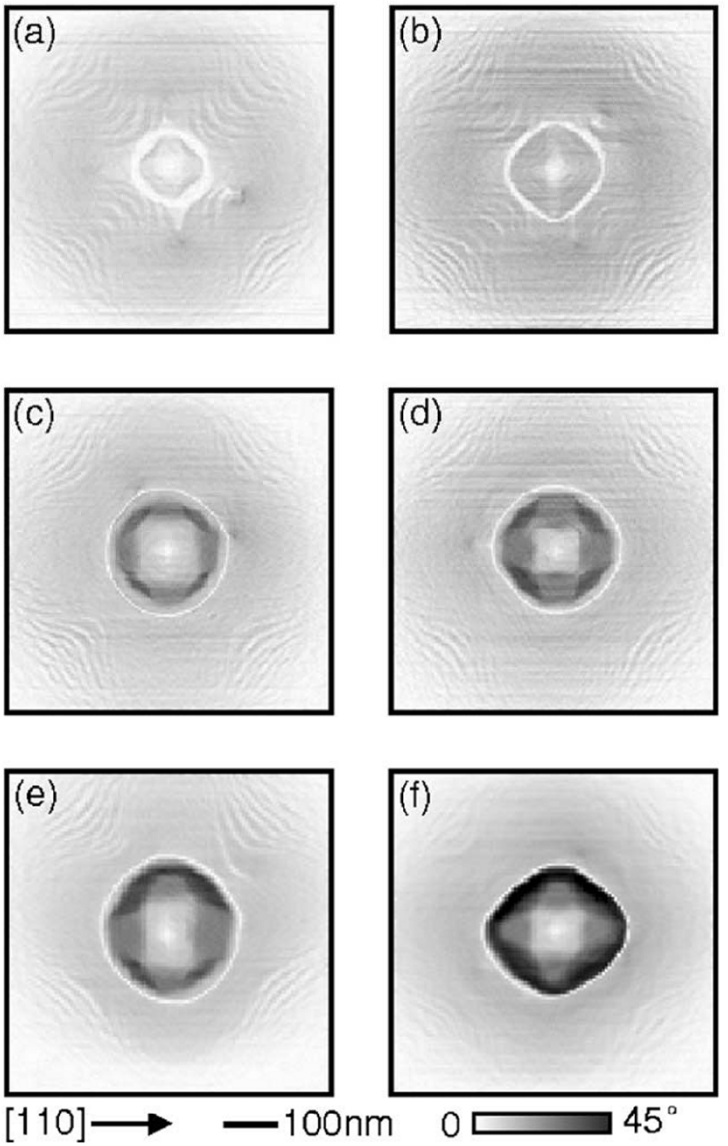

FIG. 2. AFM scans obtained upon deposition of 36 nm Si and subsequent deposition of 3.75 ML Ge (a), 5.0 ML Ge (b), and 6 ML Ge, period 1000 nm (c), and 6 ML Ge, period 600 nm (d) at 700 °C.

Depending on amount of material available per QD, different shapes are obtained (but they are the same as on flat surfaces). Size/shape distribution is monomodal.

→ Spatial ordering improves size homogeneity

J. Zhang et al, Appl. Phys. Lett. 91, 173115 (2007)

Shapes of QDs grown on patterned pits

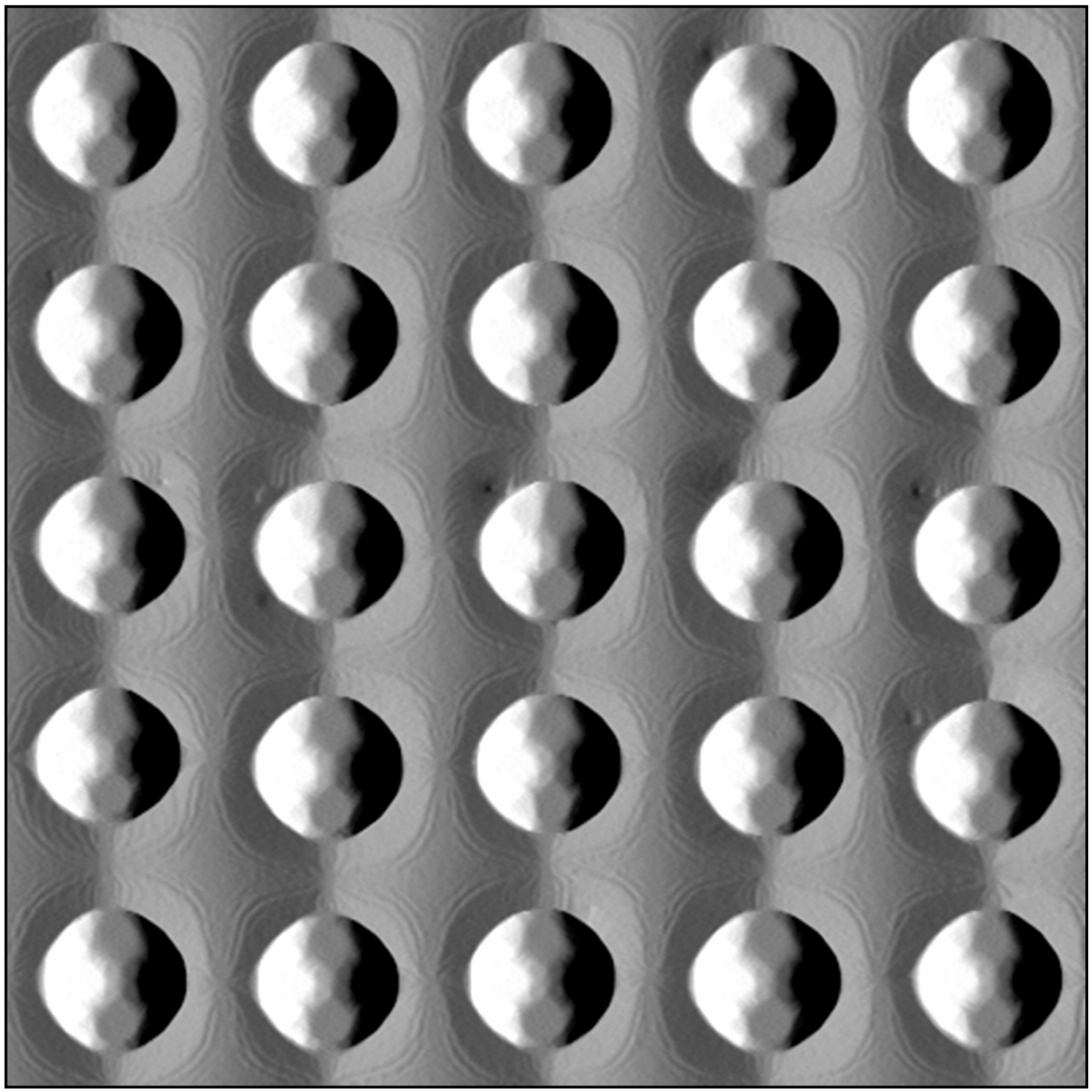

Depending on amount of material available per QD, different shapes are obtained (but they are the same as on flat surfaces). Size/shape distribution is monomodal.

→ Spatial ordering improves size homogeneity

J. Zhang et al, Appl. Phys. Lett. 91, 173115 (2007)

InAs/GaAs(001) – similar behavior as Ge/Si

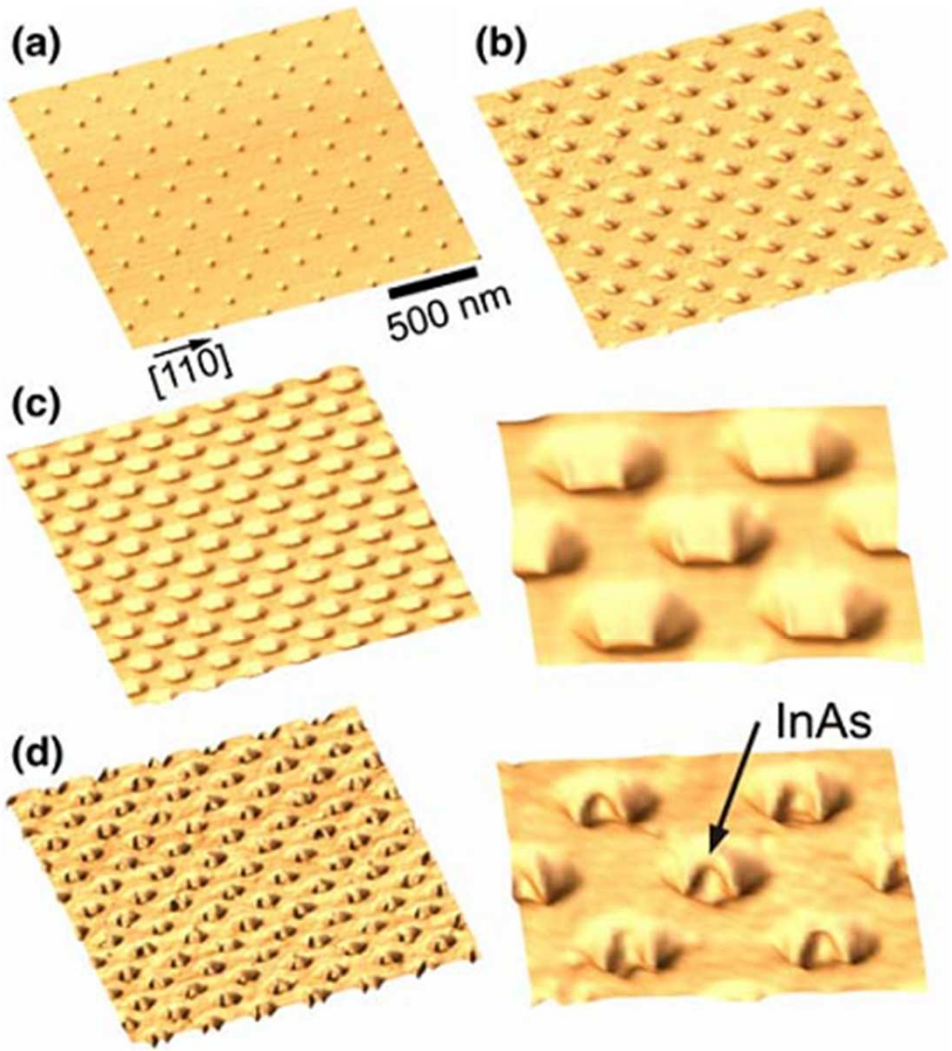

Fig. 11 3D view AFM images of (**a**) initial patterned hole surface, patterned hole surface overgrown with (**b**) 18 ML and (**c**) 36 ML GaAs buffer layer and (**d**) patterned hole surface after 18 ML GaAs buffer layer growth and 2 ML InAs. On the right side of (**c**) and (**d**) magnified images are shown

Flat surface with nanoholes:

- Convex curvature lowers locally μ
- Buffer growth alters in general pit shape
- Nucleation in pit depends critically on pit properties

S. Kiravittaya, Nanoscale Res Lett 1, 1–10 (2006)
See also Lateral alignment of epitaxial QDs, Ed. O.G. Schmidt, Springer , 2007

Shapes of InAs/GaAs site-controlled QDs

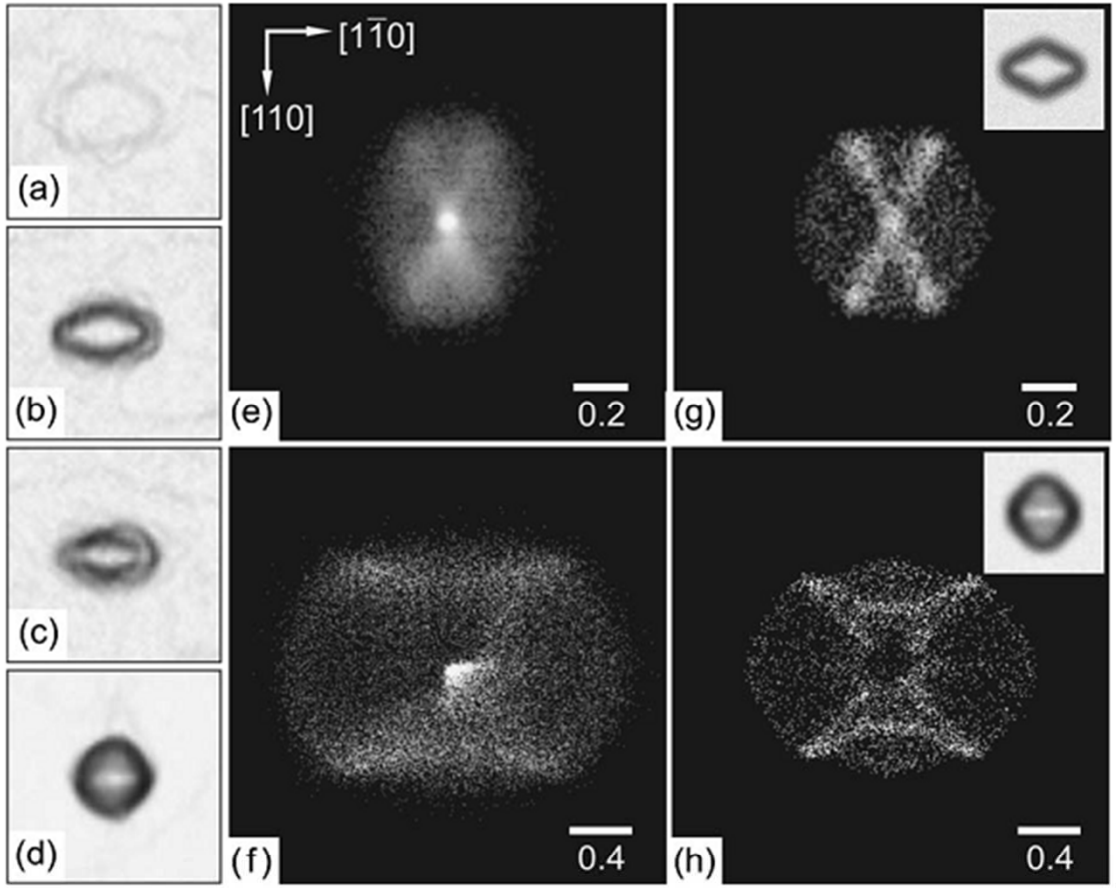

FIG. 4. Zoomed AFM images (160×160 nm^2) of the QDs observed in the samples with 1.6 ML [(a)–(c)] and 1.8 ML (d) InAs. The grayscale corresponds to the local surface slope [(a)–(c) 0–27° and (d) 0–45°]. Facet plots obtained from the samples with 1.6 ML(e) and 1.8 ML (f) and from model QD shapes of a truncated pyramid (g) and a dome (h). The corresponding model shapes, including the effect of finite AFM tip size and noise, are shown in the insets.

Also in this case the shapes are the same as those observed on planar surfaces

S. Kiravittaya et al. Appl. Phys. Lett. 87, 243112 (2005)

Composition profiles of site-controlled QDs

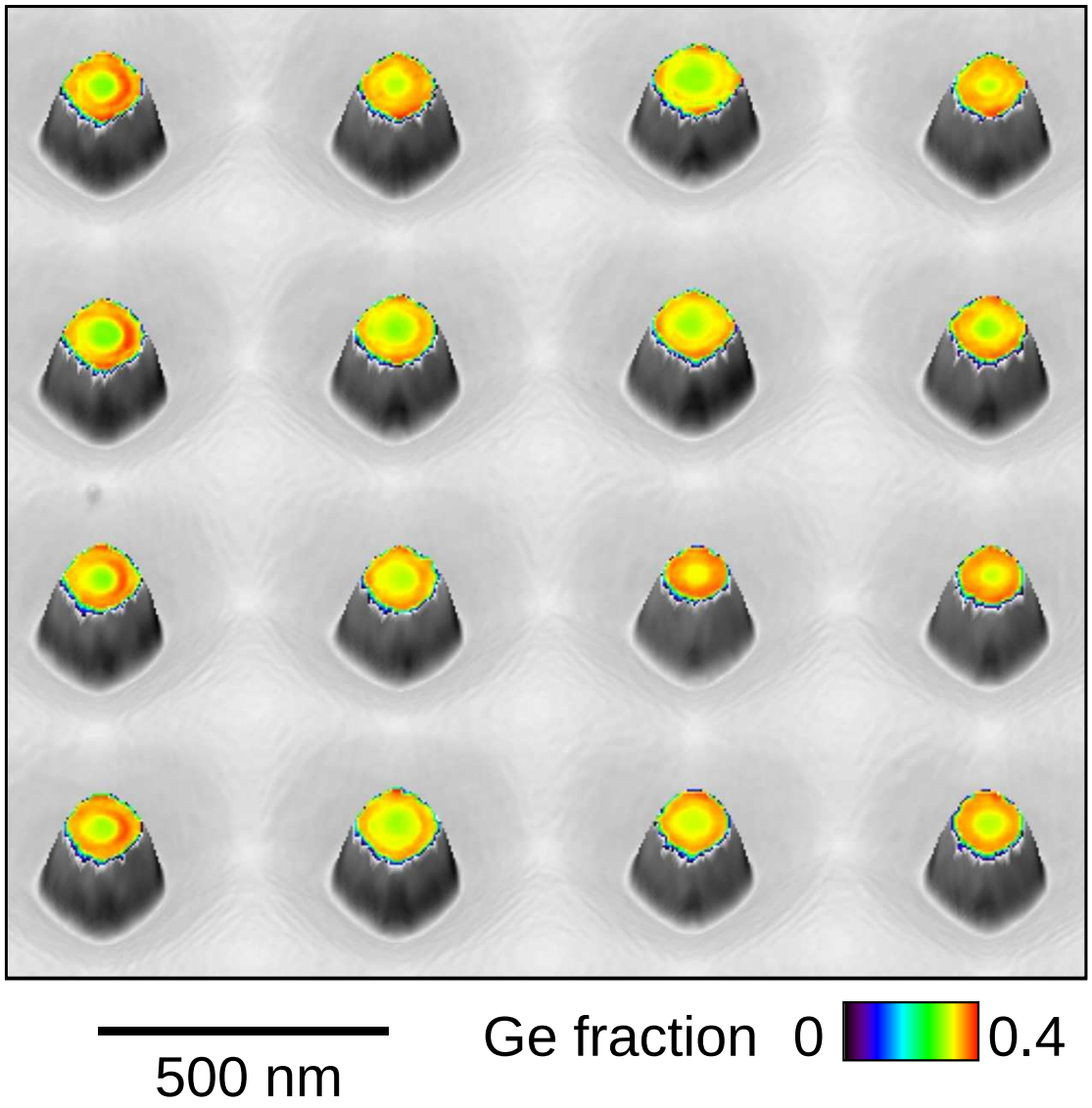

AR *et al*. Nano Lett. 8, 1404 (2008)

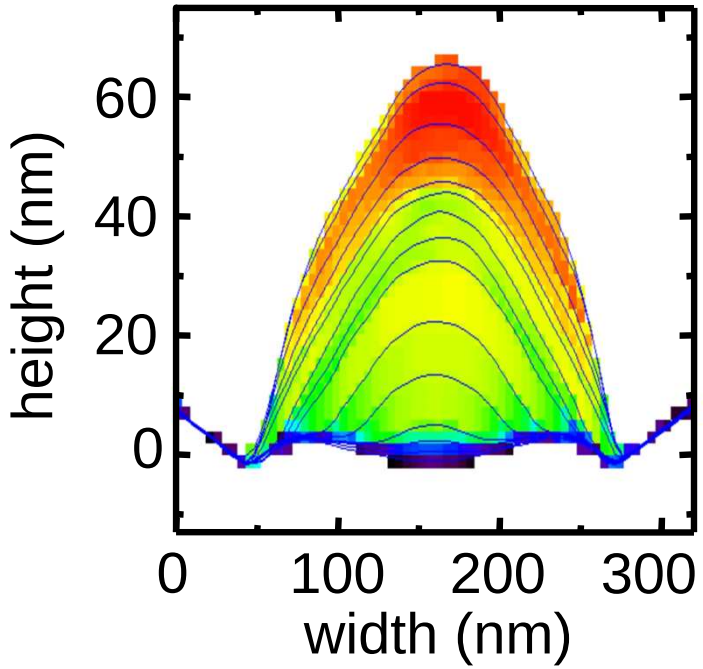

Improved composition homogeneity and symmetry

J. Zhang et al. Appl. Phys. Lett. 97, 203103 (2010)

F. Pezzoli et al. Nano Res. Lett. (2009)

Composition profiles of site-controlled QDs

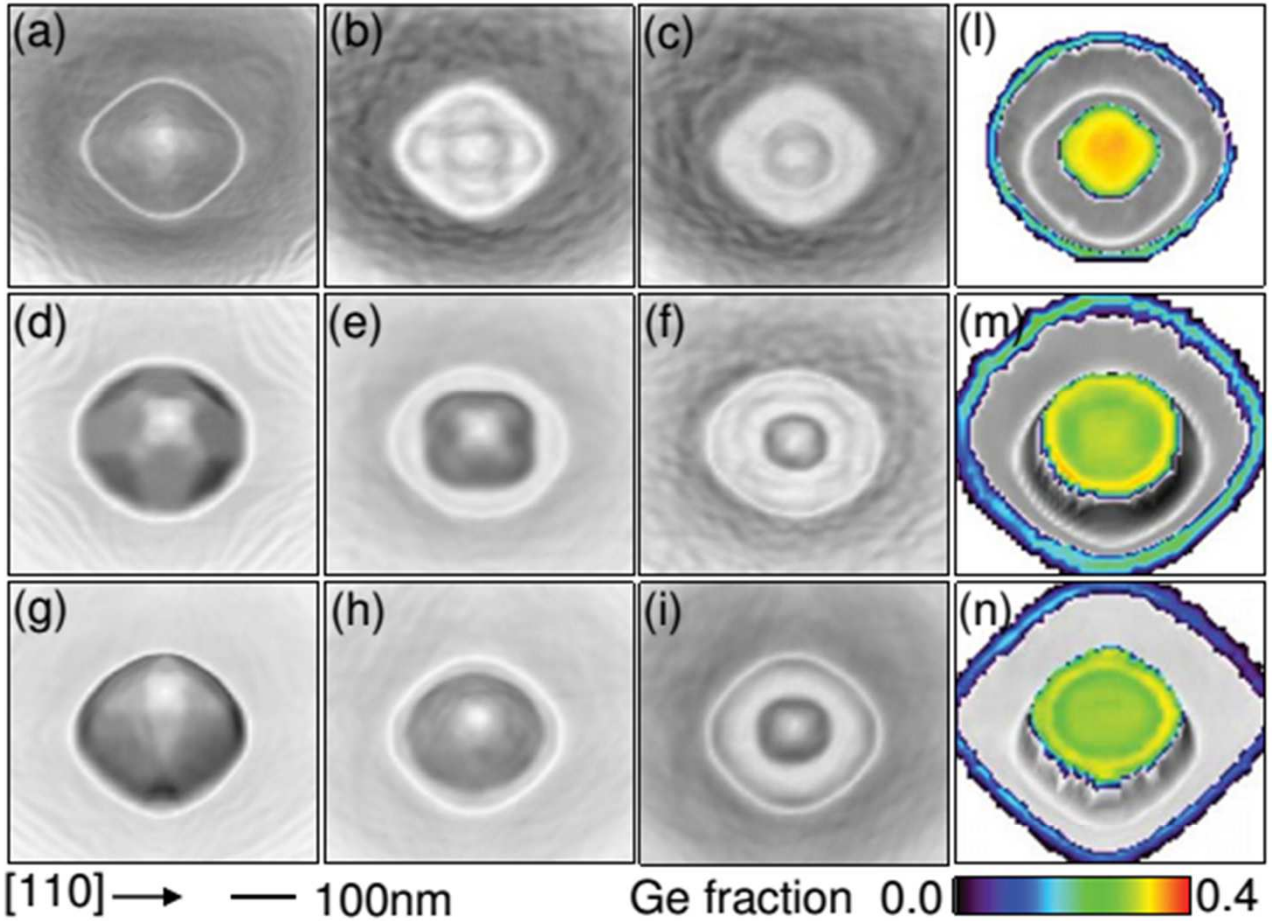

FIG. 3. (Color online) Sequences of 3D AFM images of individual islands prior to etching and after different etching times in NHH solution for pyramid [(a)–(c)], dome [(d)–(f)], and barn [(g)–(i)], respectively. [(l)–(m)] Horizontal cross-cuts of the pyramid, dome, and barn with in-plane compositions at a height of 10 nm with respect to the level of island bases.

Result independent of shape (pyramid, dome, barn)

J. Zhang et al. Appl. Phys. Lett. 97, 203103 (2010)

Comparison with self-assembled QDs

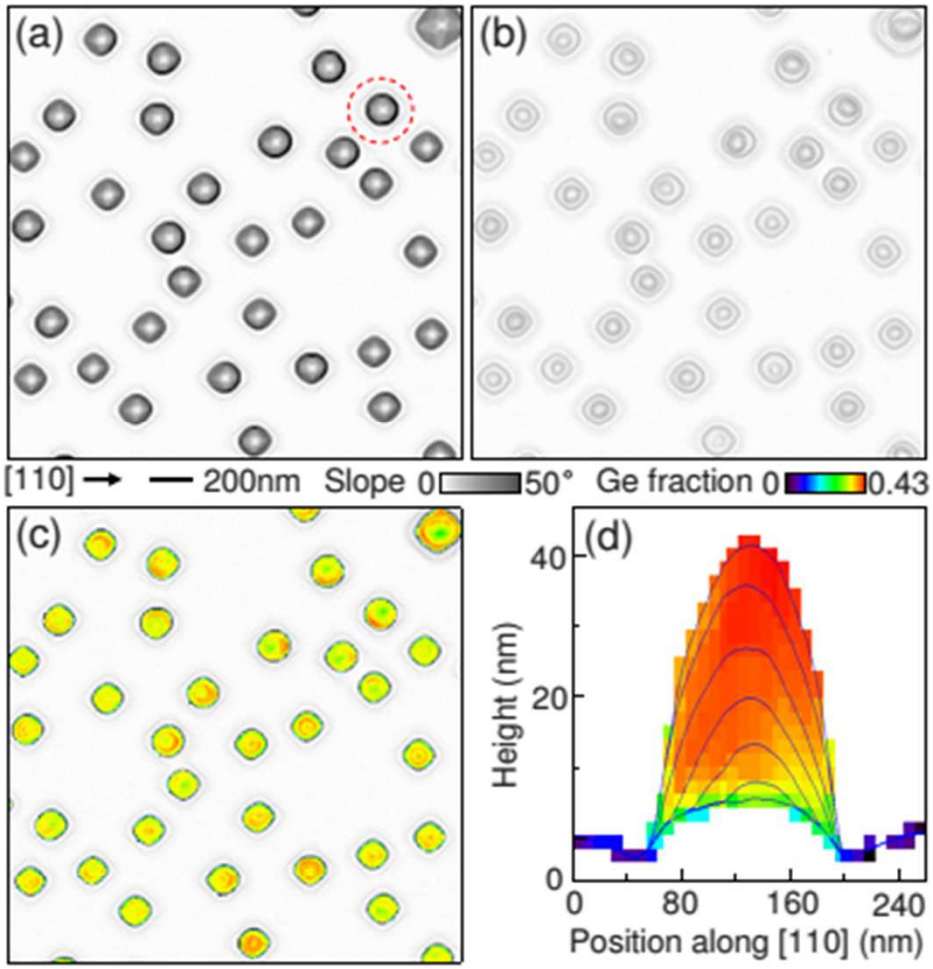

FIG. 2. (Color online) AFM images of a sample obtained after deposition of 8 ML Ge on planar Si(001) at 720 °C (a) and after selective etching in NHH solution for 55 min (b). The dashed circle in (a) marks a barn-shaped island. (c) Horizontal cross-cut of the islands shown in (a) with in-plane Ge composition at a height of 4 nm with respect to the level of the substrate. (d) Vertical cross-cut of the marked island shown in (a) with color-coded Ge distribution, passing through the island center along [110] direction.

On flat surfaces also morphologically symmetric islands may have asymmetric composition profiles.

Growth on periodically patterned substrates favor symmetric shapes and compositions

J. Zhang et al. Appl. Phys. Lett. 97, 203103 (2010)

Considerations to obtain perfect ordering

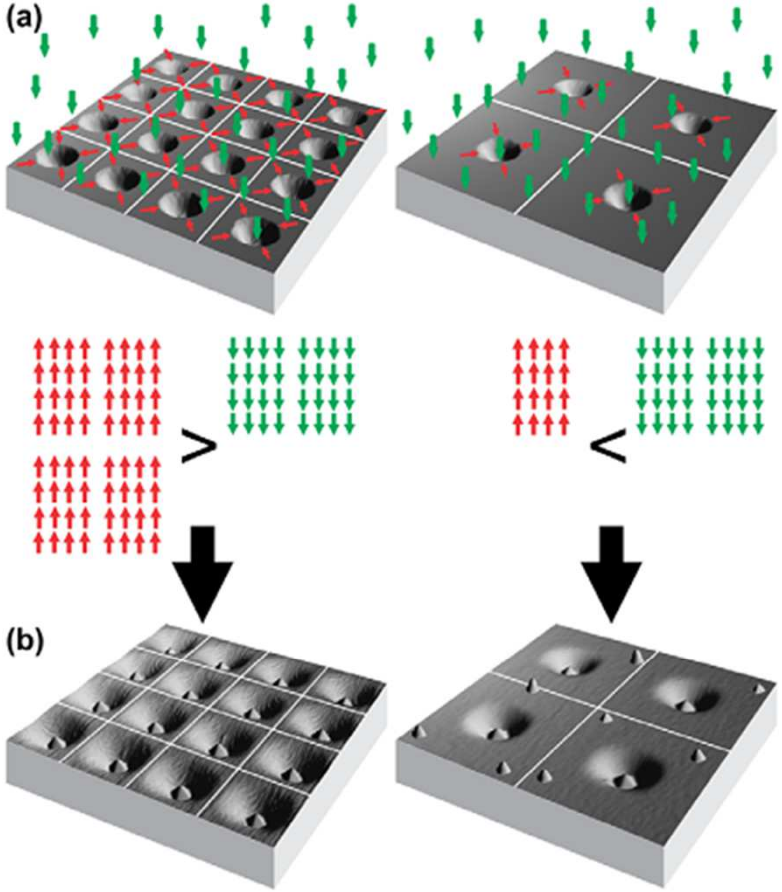

Figure 9. Influence of deposition and incorporation rate on the location of island nucleation. Schematic representation of a pit-patterned substrate with small and large d_{pit} but otherwise identical pit dimensions. Every pit collects randomly Ge atoms from the surroundings with a specific capture rate indicated by red arrows. The deposition rate is indicated by green arrows. If the incorporation rate (number of red arrows) is equal to or higher than the deposition rate (number of green arrows) then islands nucleate only on their favourable position (in the pit for rather flat pits (inclination angles between 5° and 18°)). Otherwise, secondary island nucleation on the flat areas between the pits is unavoidable, once the WL there exceeds its critical thickness of ~4.2 ML.

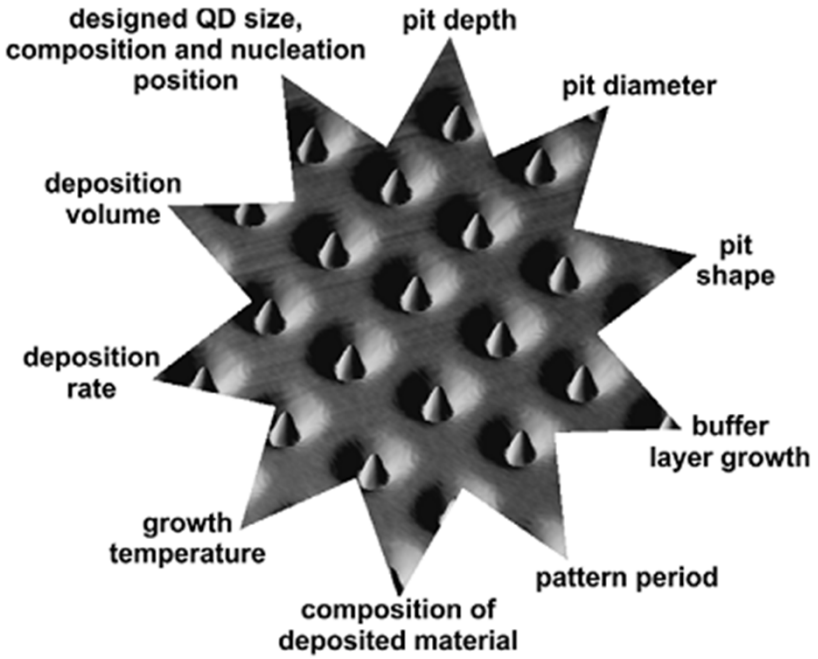

Figure 1. Parameter space for strictly ordered island growth on pit-patterned substrates, linking the most important factors for the growth of strictly ordered Ge/Si quantum dots on pit-patterned Si(001) substrates.

Depending on deposition rate and temperature, nucleation outside pits can be avoided. Result mostly depends on ratio between deposition and incorporation rate

M. Grydlik et al. Nanotechnology 24 (2013) 105601

Considerations to obtain perfect ordering

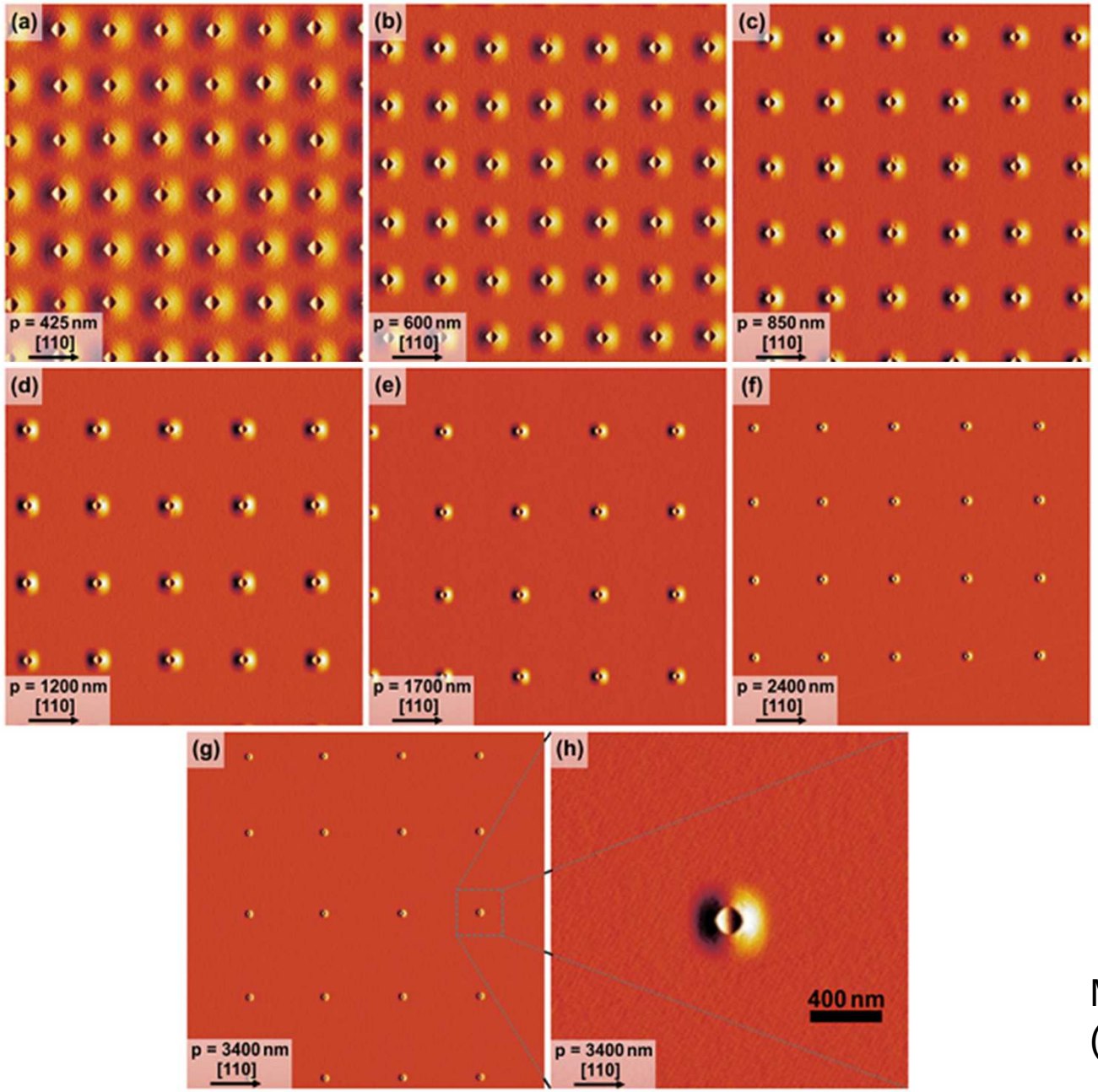

For pits with sufficient slope and using low growth rate and high substrate temperature, perfect ordering can be achieved rather independent on pit spacing.

← 3 ML of Ge at 700°C and Ge growth rate of 0.003 nm/s (0.08 ML/min)

Note: critical thickness is reached in pits earlier than in flat areas. By depositing subcritical Ge amount QD formation outside pits can be completely avoided

M. Grydlik et al. Nanotechnology 24 (2013) 105601

Effects of imperfect pit geometry

Small e-beam lithographically patterned holes in GaAs substrates (~50-100 nm wide, ~20 nm deep obtained by RIE or wet chemical etching)

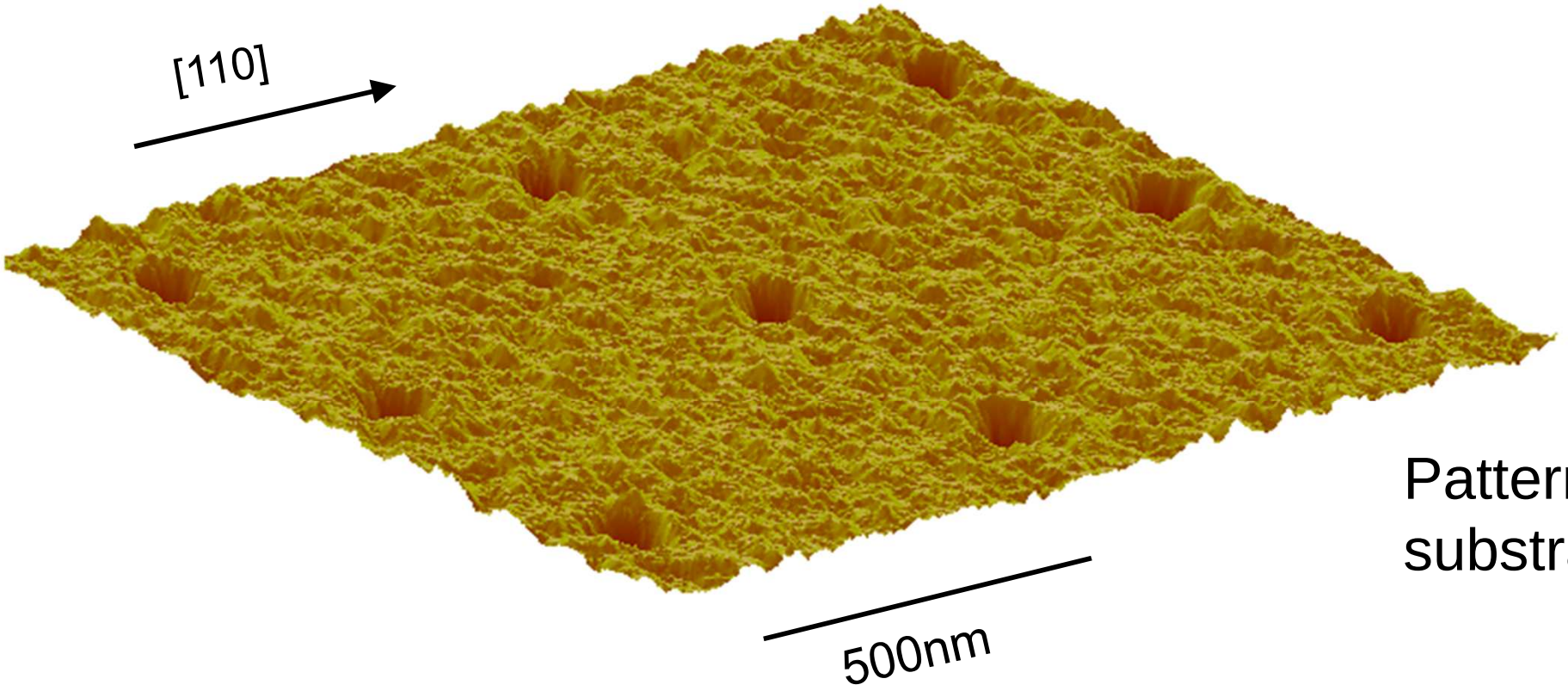

Patterned substrate

Courtesy of Paola Atkinson

Effects of imperfect pit geometry (InAs/GaAs)

In-situ deoxidation at low temperature (H-assisted at 400°C or Ga-assisted at ~450°C) followed by buffer growth

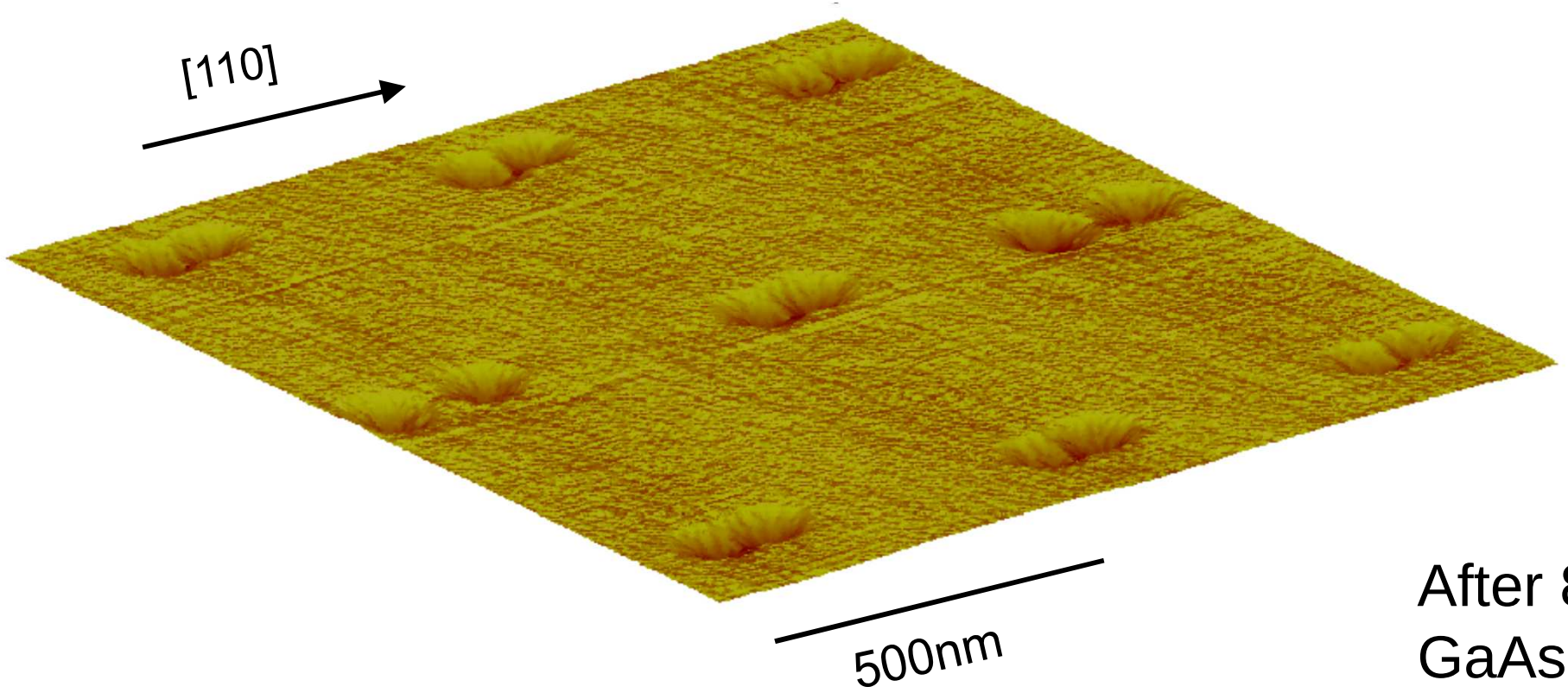

After 8 nm GaAs buffer

Courtesy of Paola Atkinson

Effects of imperfect pit geometry

InAs growth: dots form on pattern before unpatterned regions (local reduction of critical thickness due to hole filling)

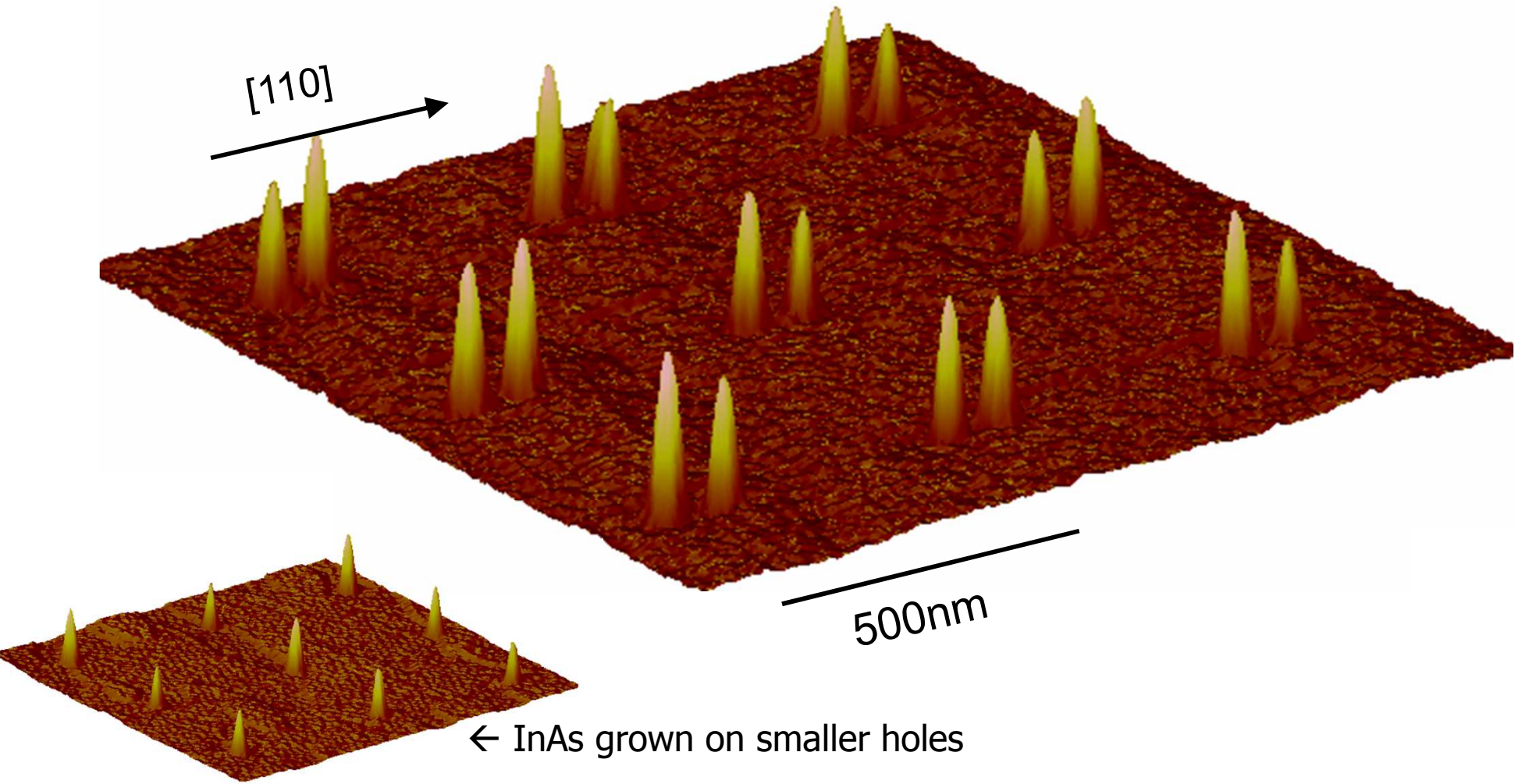

Edge effects

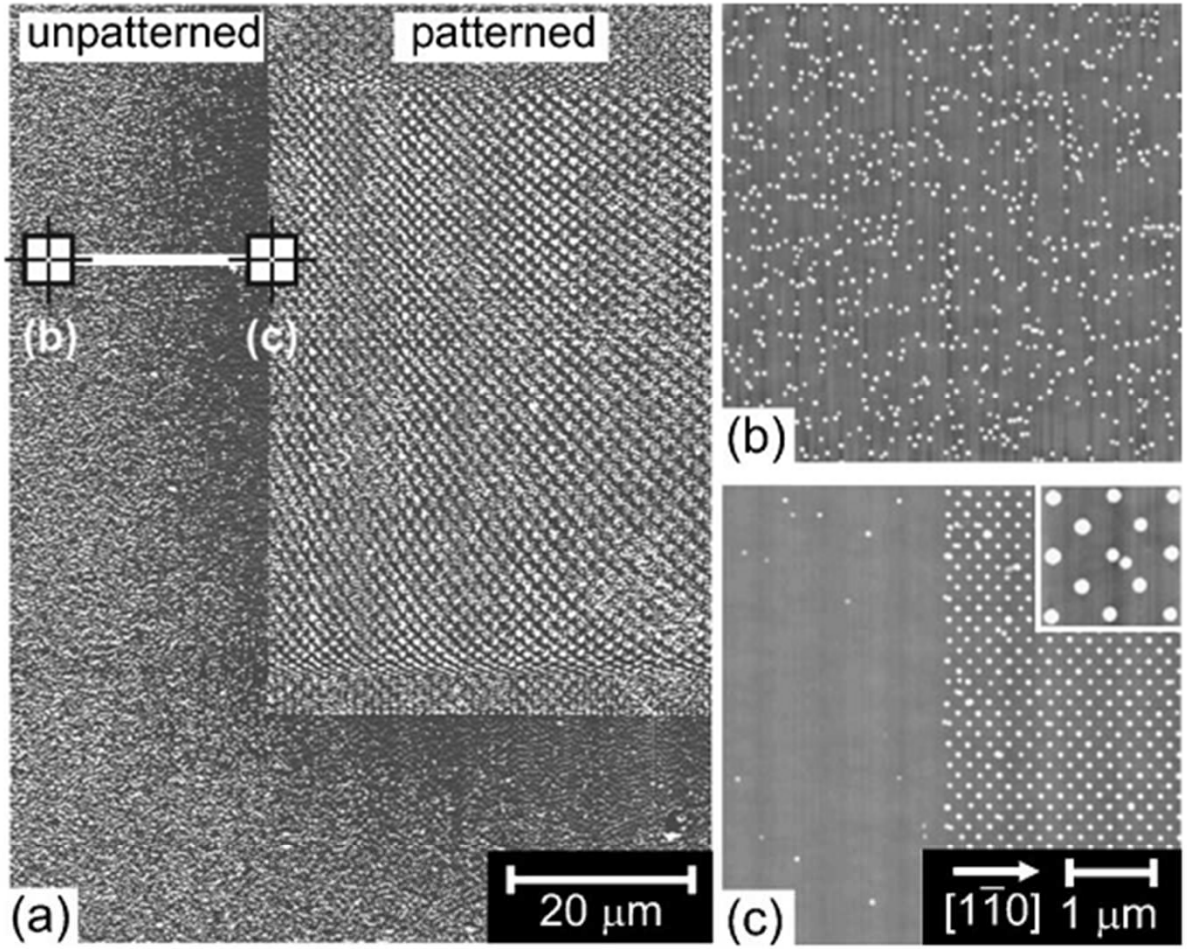

FIG. 1. (a) Large AFM image (75×100 μm^2) of QDs on the patterned and unpatterned surface of a twofold stack of InAs QDs with 1.8 ML InAs in the second layer. (b), (c) AFM images (5×5 μm^2) taken from the corresponding marked areas in (a). Inset of (c) shows a close-up image of a single QD interstitial defect in the patterned area.

← InAs/GaAs QDs

For deposited amount > critical thickness on planar surface, patterned area is surrounded by a denuded zone due to preferential diffusion of material into patterned area.

Note: the incorporation rate at pits changes when island forms: mature islands grow slower than small islands

S. Kiravittaya et al. Appl. Phys. Lett. 87, 243112 (2005)

Edge effects

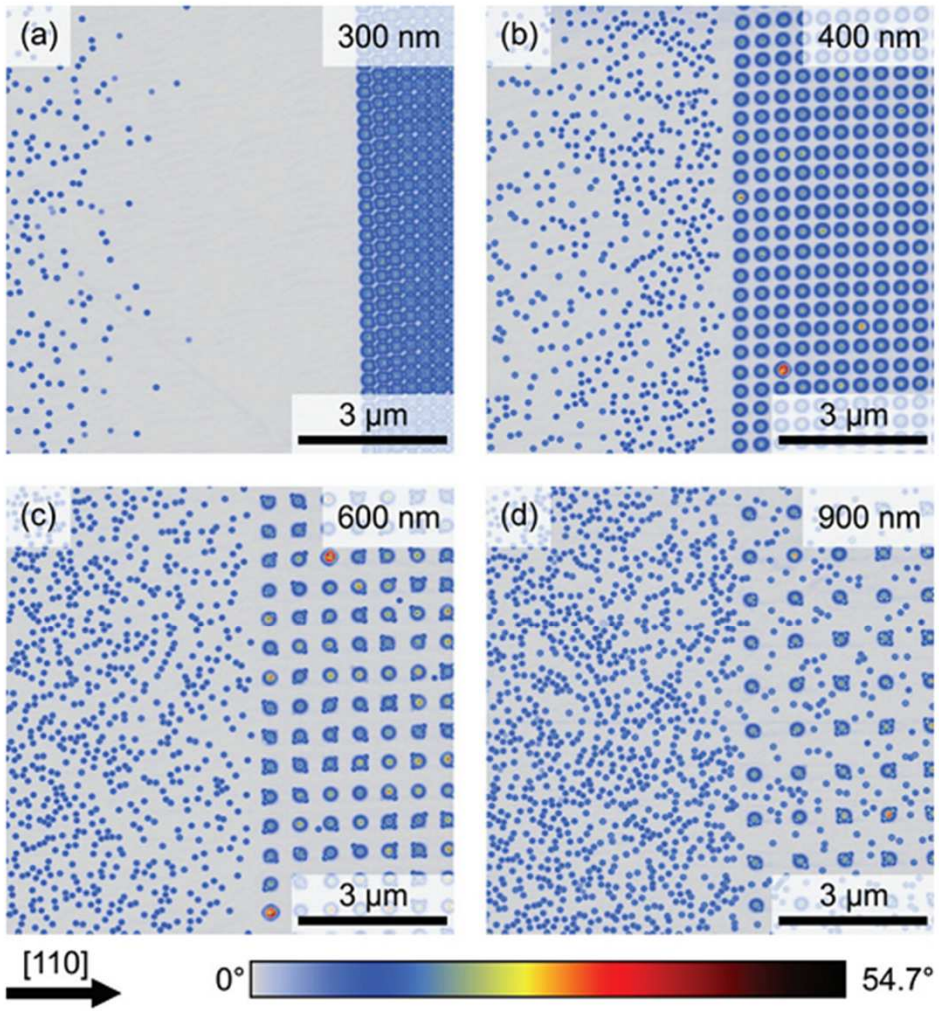

FIG. 2. (Color online) 10×10 μm^2 AFM micrographs taken in the vicinity of the border between unpatterned and patterned substrate regions with (a) $d_{pit} = 300$ nm, (b) 400 nm, (c) 600 nm, and (d) 900 nm. The color coding represents the local surface slope with respect to the (001) surface.

Ge/Si

a) Small pit distance → high density of μ-minima in pattern → high incorportation rate into pattern → large denuded zone
b) Large interpit distance → all sites are rapidly occupied, denuded zone disappears and nucleation starts also between pits

M. Grydlik et al, Phys. Rev B 88, 115311 (2013)

Edge effects

6 ML Ge on pits @ 650°C, R = 0.025 Å/s. Shape island volume integrated over unit cell area

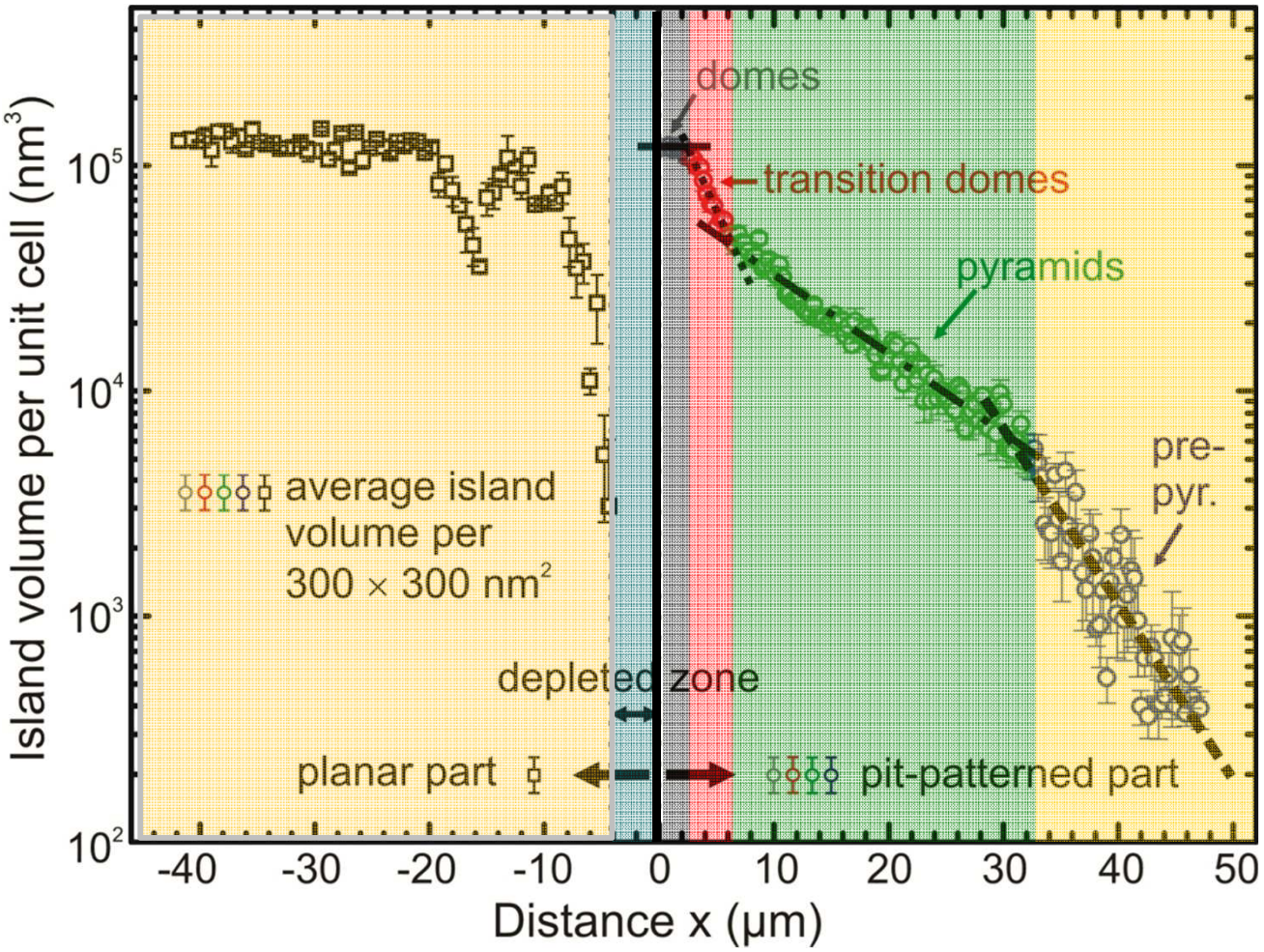

patterned area:

- **pre-pyramids**
- **pyramids**
- **transition domes**
- **domes**

- **Exponential decay of island volume with distance.**
- **Different island types differ in Ge "absorption".**
- **Islands with unfinished facets (t-domes, pre-pyramids) "absorb" Ge stronger (steeper slopes)**

Edge effects

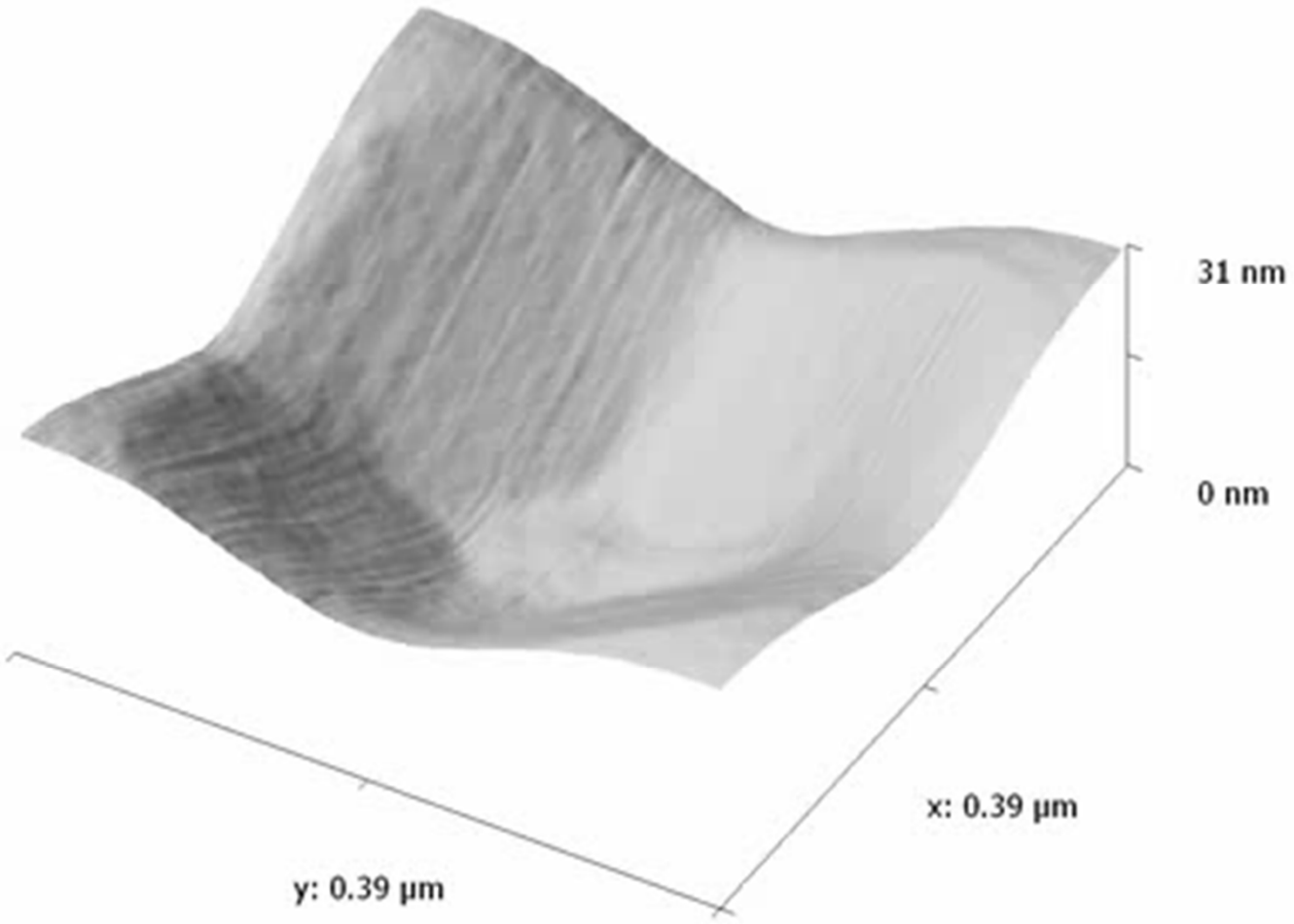

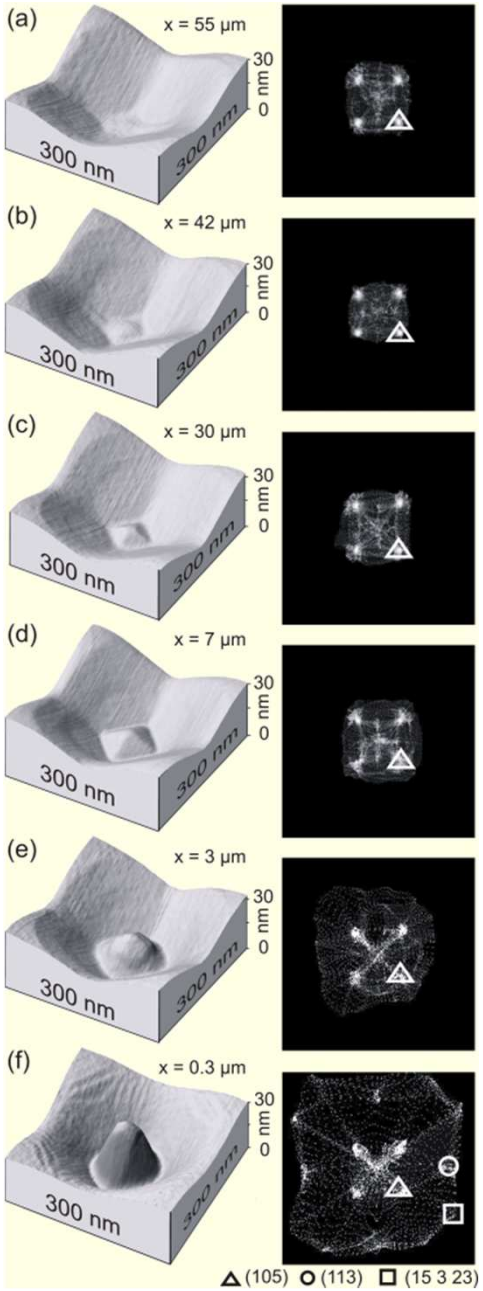

Moving from pattern center towards edge, all island morphologies can be seen on the same pattern.
Courtesy M. Grydlik, M. Brehm, JKU Linz

How are pits done?

- e-beam (or holographic lithography) + RIE or wet chemical etching

- Nanoimprint lithography

- AFM local oxidation

see J. Martin-Sanchez et al. ACS Nano 6, 1513 (2009)

- STM nanoindentation (in situ)

see K. Asakawa et al., in "Lateral alignment of QDs", Springer, 2007

- FIB (in some case in situ)

see I. Berbezier et al., in "Lateral alignment of QDs", Springer, 2007

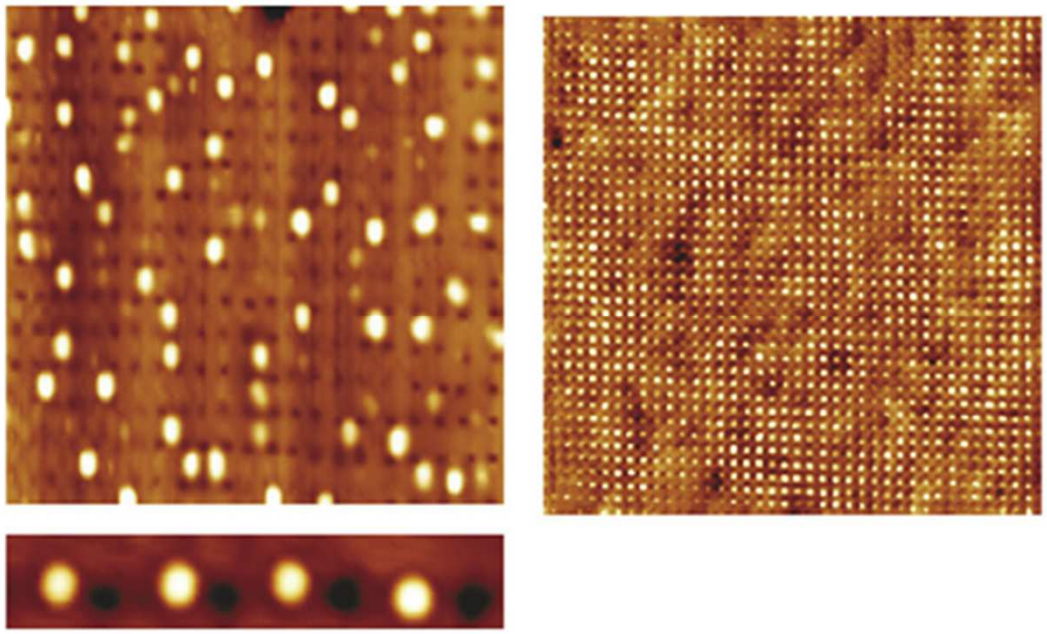

Example: Ge dots on pits with 75 nm interpit distance prepared by focused ion beam

[from J.-N. Aqua, I. Berbezier, et al., Phys. Rep. 522, 59–189 (2013)]

Note on nanohole fabrication

Major problem of top-down: surface contamination combined with limited buffer thickness (thick buffers tend to planarize surface due to capillarity)

→Substrate cleaning is critical!

Even in absence of extended defects and „beautiful“ growth of site-controlled QDs, the grown QDs can well be useless ☹

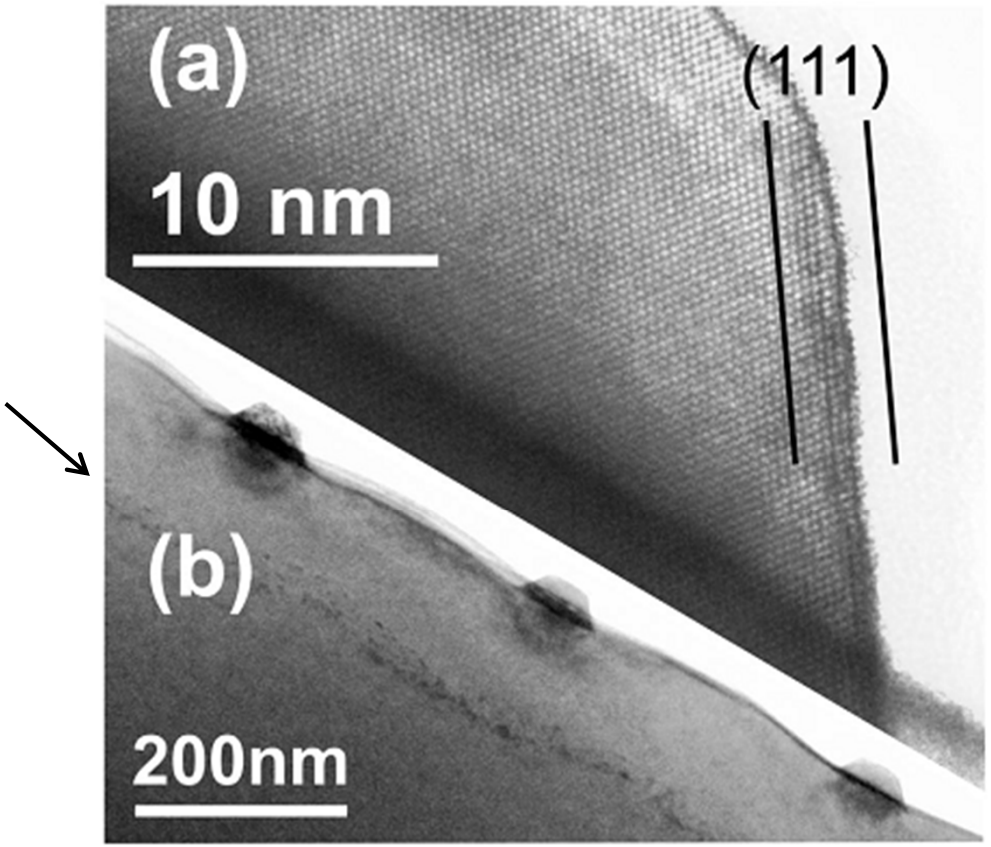

FIG. 3. High-resolution (a) and larger area (b) XTEM image of islands on sample *C*. The resolved {111} lattice planes in (a) are parallel to the terminating facet (black lines).

Z. Zhong et al PRL98,176102 (2007)

State of the art on quality of site-controlled-QDs

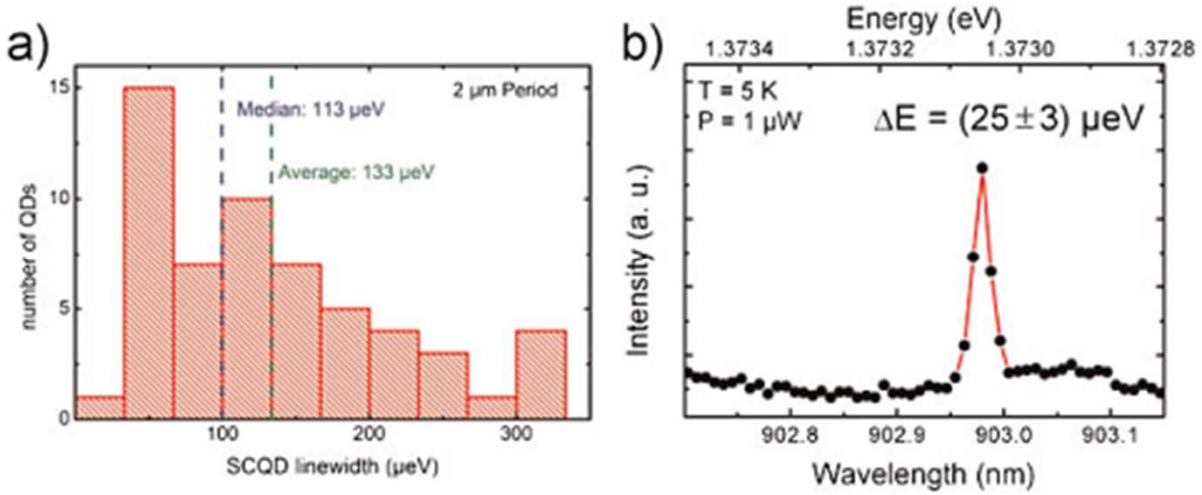

Figure 10 (online colour at: www.pss-a.com) (a) Statistics of emission linewidth in a high purity SCQD sample on the 2 µm period. (b) High-resolution spectrum of single SCQD emission line with a linewidth of 25 µeV.

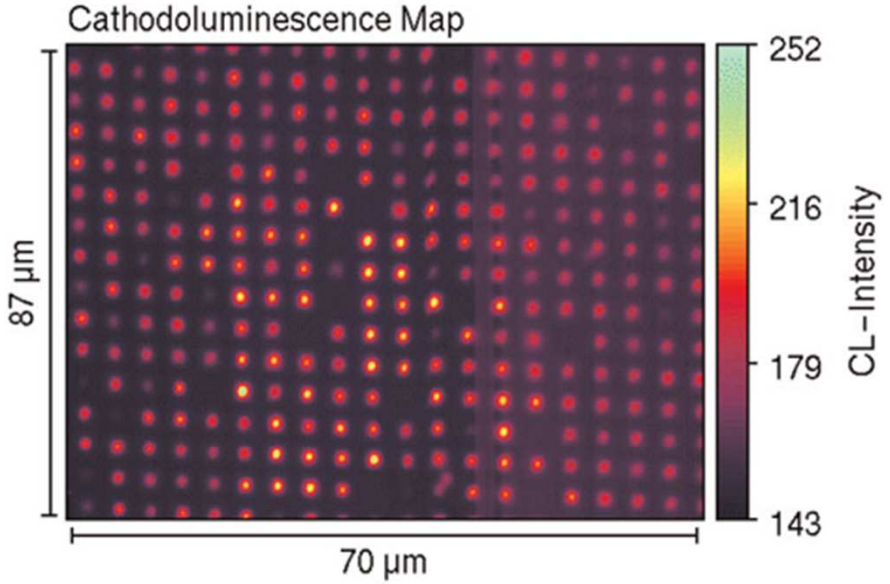

Figure 9 (online colour at: www.pss-a.com) Overview CL map of an array of SCQDs on a 4 µm period.

QDs are „alive“, but the relatively broad linewidth (compared to radiative limit of ~1 µeV) indicates presence of charged impurities in the QD surrounding

C. Schneider et al. Phys. Status Solidi A 209, No. 12 (2012)

State of the art linewidths: K.D. Jöns, P. Atkinson, et al. *Nano Letters* 13, 126 (2013).

Possible solution to alleviate problem: stacking

Lateral ordering of dots located far from the regrowth interface can be achieved by using the strain from a buried layer of site-controlled dots

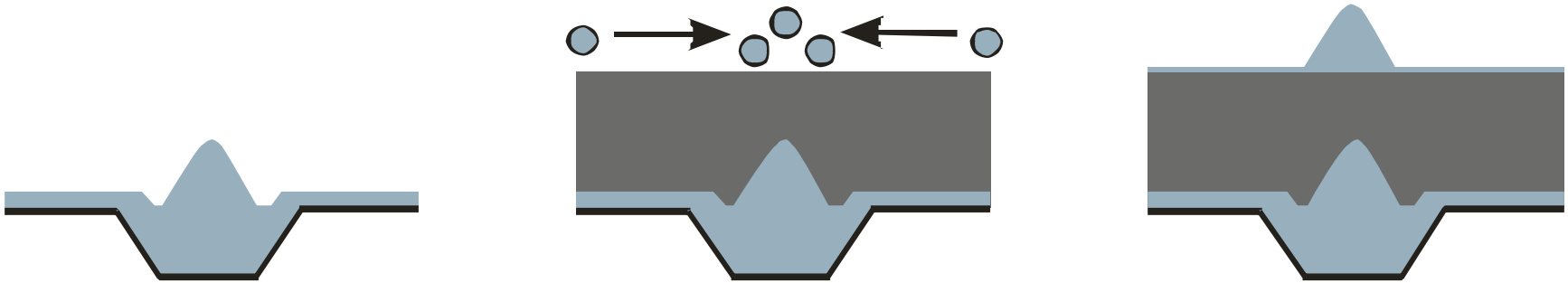

Site controlled dot in close proximity to regrowth interface

Strain driven net migration above capped dot

Vertical ordering of dot bilayer

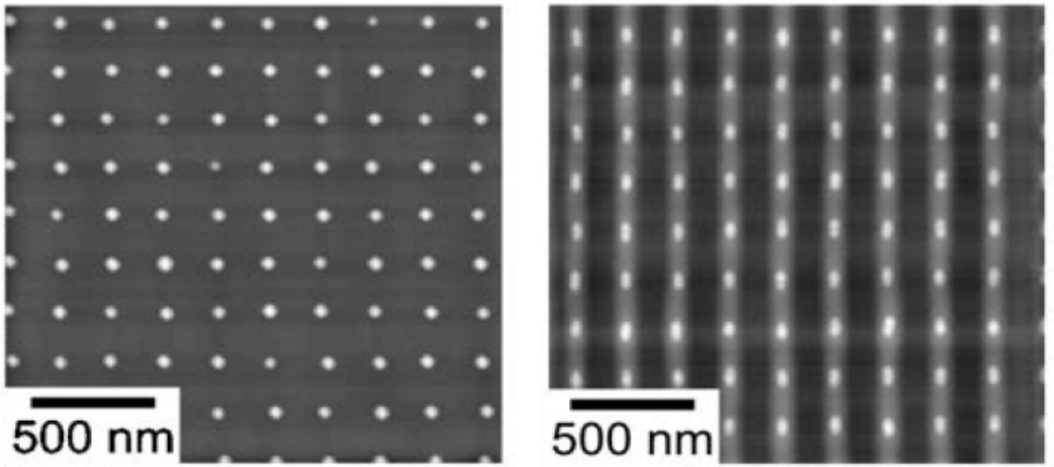

*S. Kiravittaya et al. APL **88** 043112 (2006)*

2.3.d Pit filling without strain

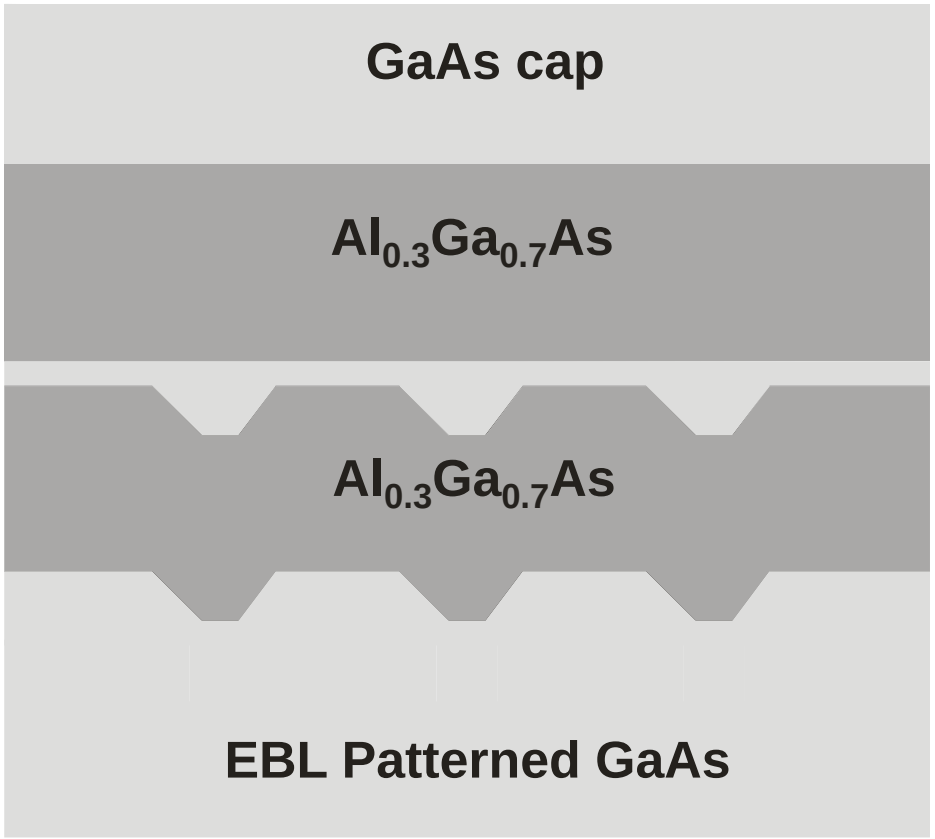

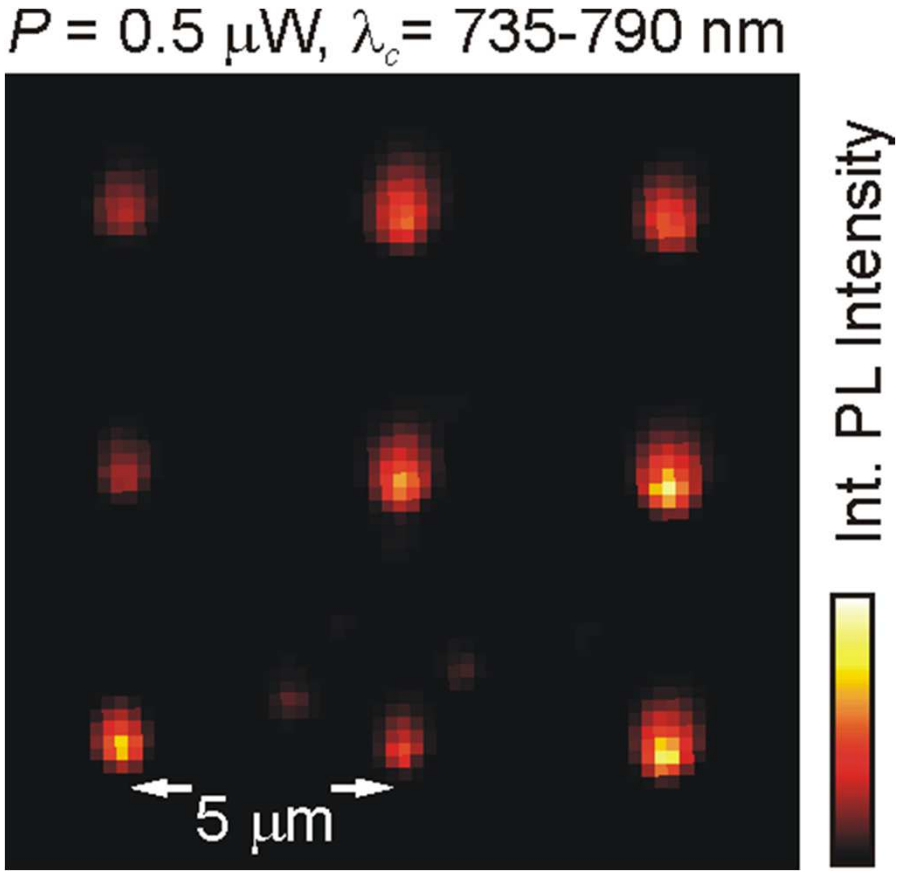

PL map 15×15 μm²

QD position is well controlled but size distribution is broad due to pit irregularities

S. Kiravittaya, M. Benyoucef, R. Zapf-Gottwick, A. Rastelli, O.G. Schmidt, Appl. Phys. Lett. 89, 233102 (2006)

2.3.e Growth on self-limited pits

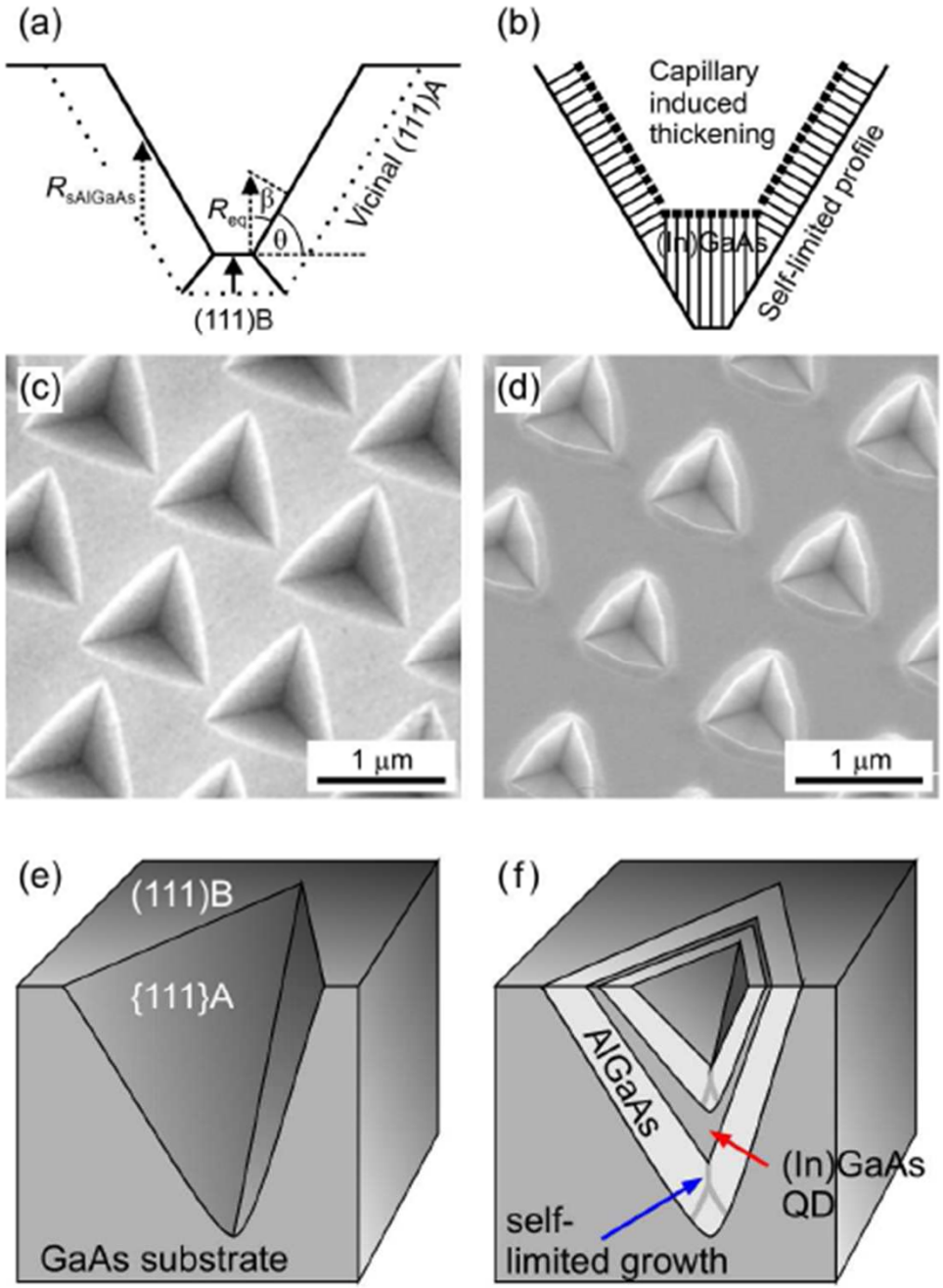

Inverted pyramids are obtained by anysotropic wet-chemical etching of GaAs(111)B substrates.

Strong growth rate anisotropies of AlGaAs on pits → self-limited shape of pits

Growth of (In)GaAs leads to QDs in AlGaAs matrix with record homogeneity (in terms of spread in emission wavelength)

QDs are far from etched surface and associated defects, leading to QDs with good (but not optimal) optical properties

Fig. 1.16. Schematic illustration of the principle of QD growth in inverted pyramids. (a) Growth by MOVPE of an AlGaAs layer, governed by strong growth rate anisotropies. (b) When the system has reached a self-limited profile, the deposition of a (In)GaAs layer results in a strong capillarity contribution which widens the bottom profile, without contributing significantly to the sidewall growth. (c) SEM image of the patterned substrate with arrays of inverted pyramids. (d) SEM image of ordered (In)GaAs QD surface. (e) and (f) are cross-section schematics of the structures shown in (c) and (d), respectively. Adapted from Refs. [99–101].

Example of top-down + bottom-up + top-down

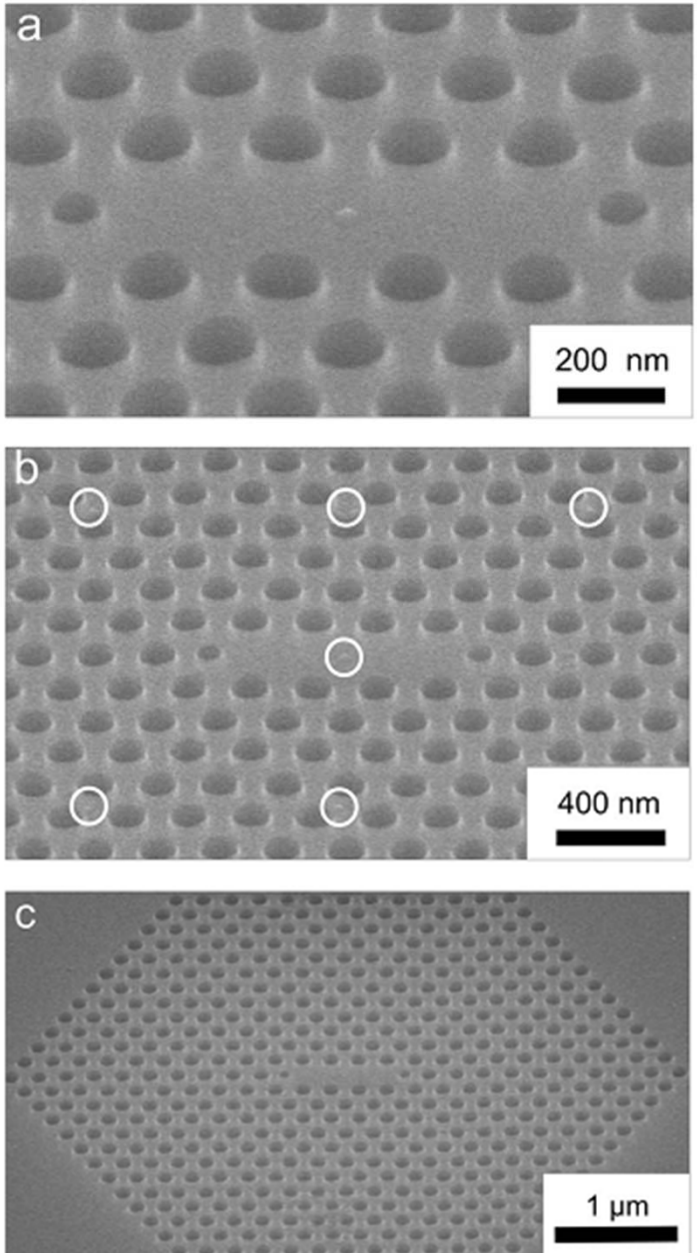

← InGaAs/GaAs QDs in photonic crystal microcavities

Site controlled QDs are grown on pit-patterned substrates

Marker structures allow locating the QDs after growth and fabricate the photonic structures around the QDs

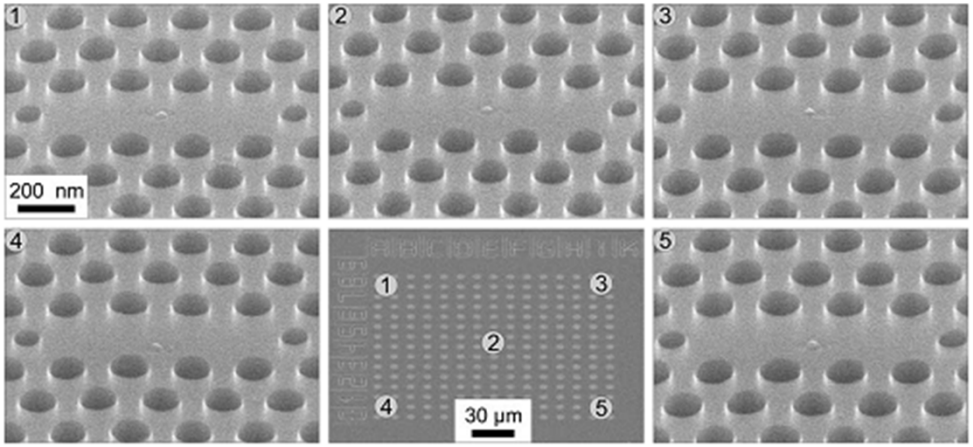

T. Sünner et al., OPTICS LETTERS 33, 1759 (2008)

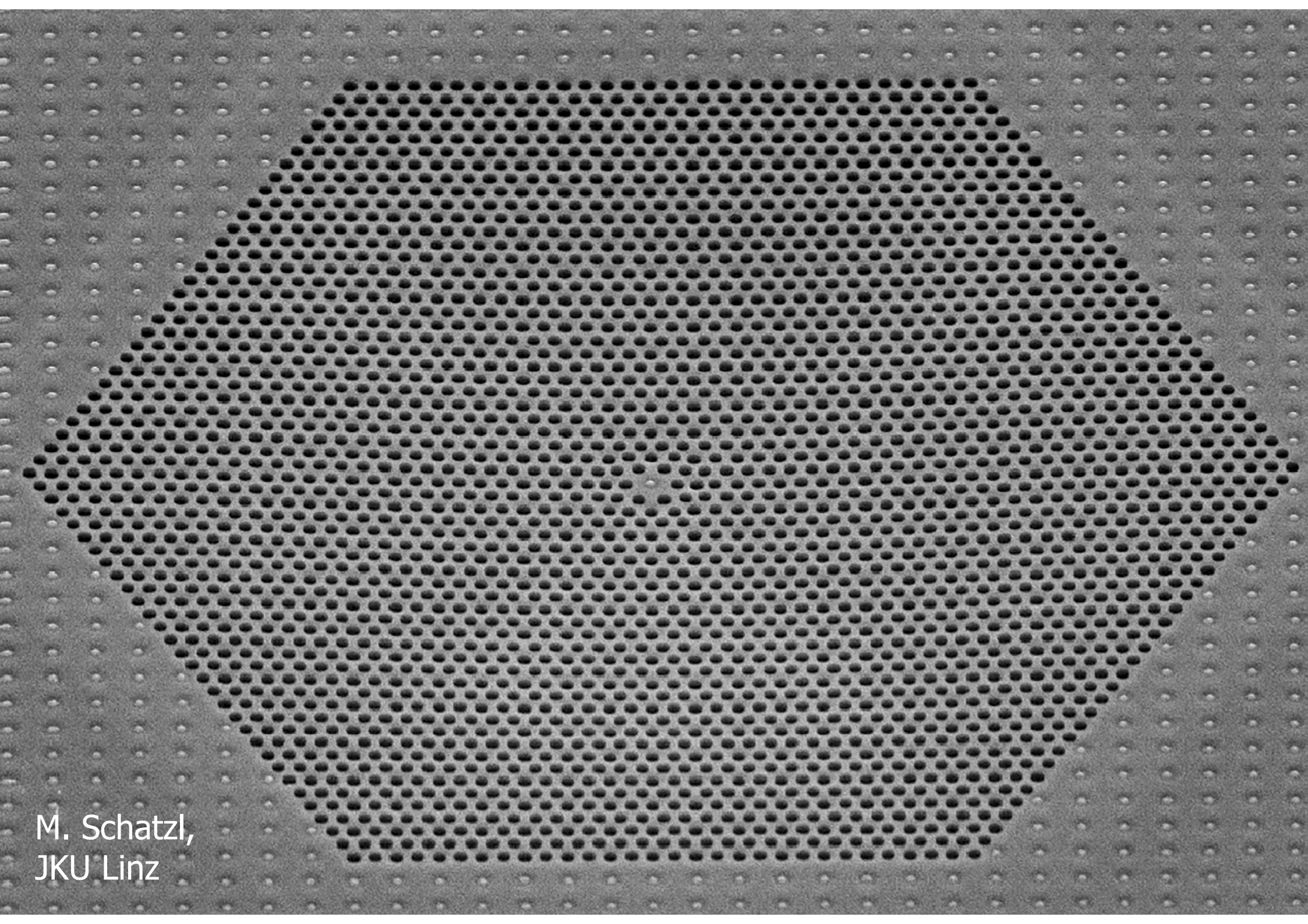
M. Schatzl,
JKU Linz

3. Control of electronic structure of QDs

Scalability requires not only position to be known, but also the QDs to be "reasonably" identical to each other within certain specifications.

Even the most homogeneous QDs realized so far have a spread in emission energy of about ~5 meV

QDs are very attractive for some envisioned applications in quantum communication, but their emission energy should be controlled at the ~μeV level!

… and not only emission energy needs to be controlled!

→ Degree of control achievable with epitaxy is too limited
→ Control after growth

3.1 Post-growth thermal treatment

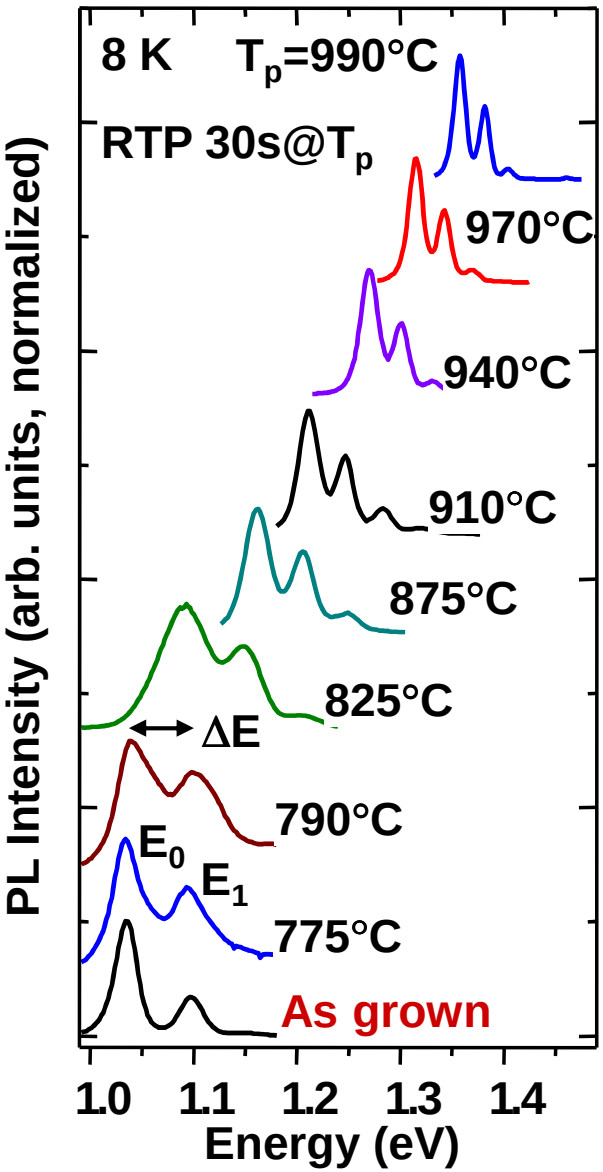

Rapid thermal processing (RTP) of InAs/GaAs QDs. RTP promotes In-Ga intermixing and blue-shift of emission

- **Controllable shift**
- **Reduction of FWHM of PL signal (but not to zero!)**

A.Rastelli et al. Microst. Superlattices, 36, 181 (2004) and Refs. therein

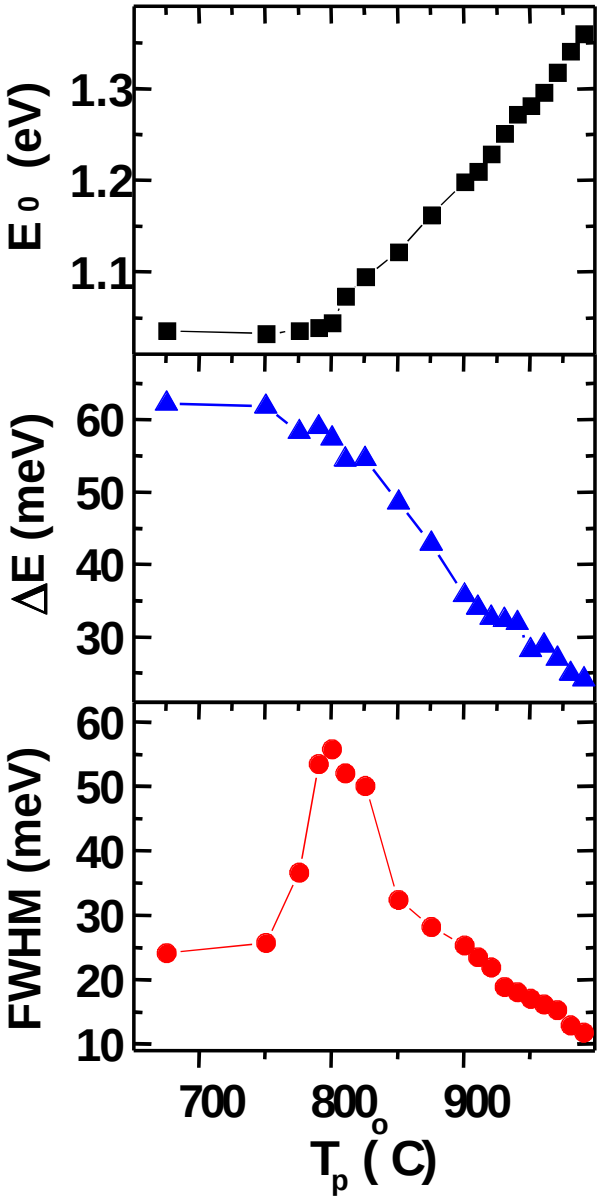

3.1 Post-growth thermal treatment in a cryostat

20 μm **λ>680 nm**

PL movie during local heating with laser (λ_{exc}=532 nm) power up to 2.7 mW (~200 kW cm^{-2})

PL saturation and quenching indicates heating up of the mesa

Tuning of single QD emission

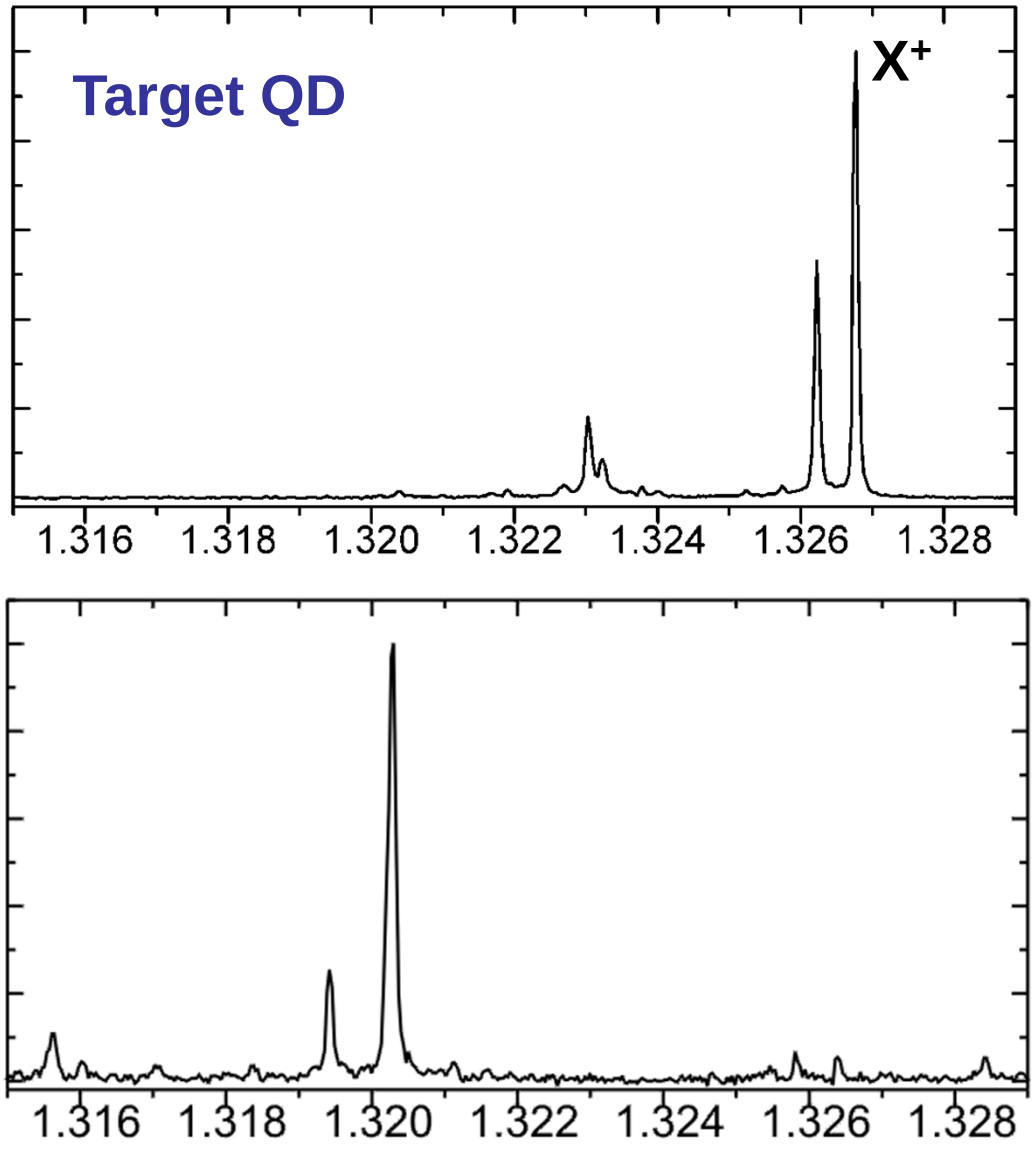

✓ Large shifts (>10 meV) possible (comparable to inhomogeneous broadening)

✓ Absolute accuracy determined by spectral resolution (here 70 μeV)

Problems: possible occurrence of defects due to thermal stress; not reversible

← *In-situ* tuning of QD emission into resonance by laser processing (20 steps) – Laser heating produces intermixing with barrier and consequent blue-shift

A. Rastelli *et al.* Appl. Phys. Lett. 90, 073120 (2007)

3.2 QD tuning via quantum-confined Stark effect

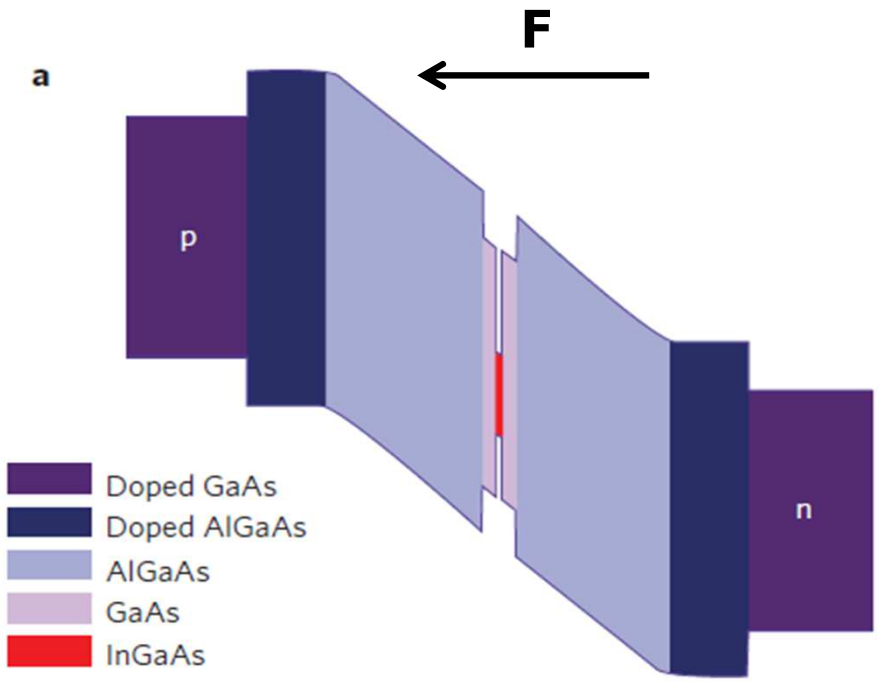

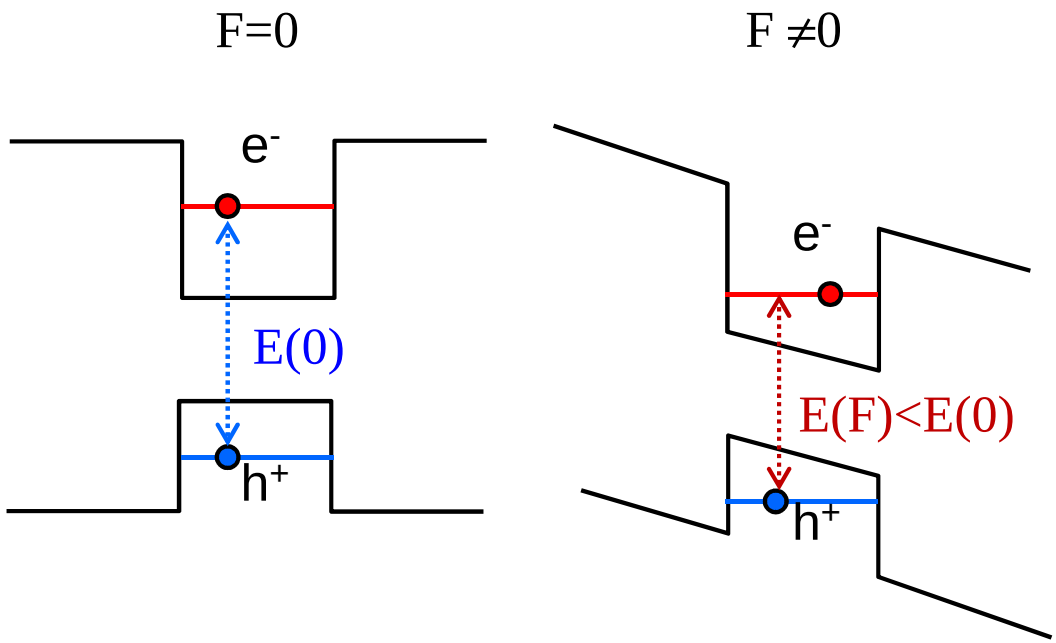

R.B. Patel et al. Nature Photon. **4,** 632 (2010)

- Quantum confined Stark effect (QCSE)
  → Excitonic species shift according to: $E(F) = E_0 - p_z F - \beta F^2$

QD tuning via quantum-confined Stark effect

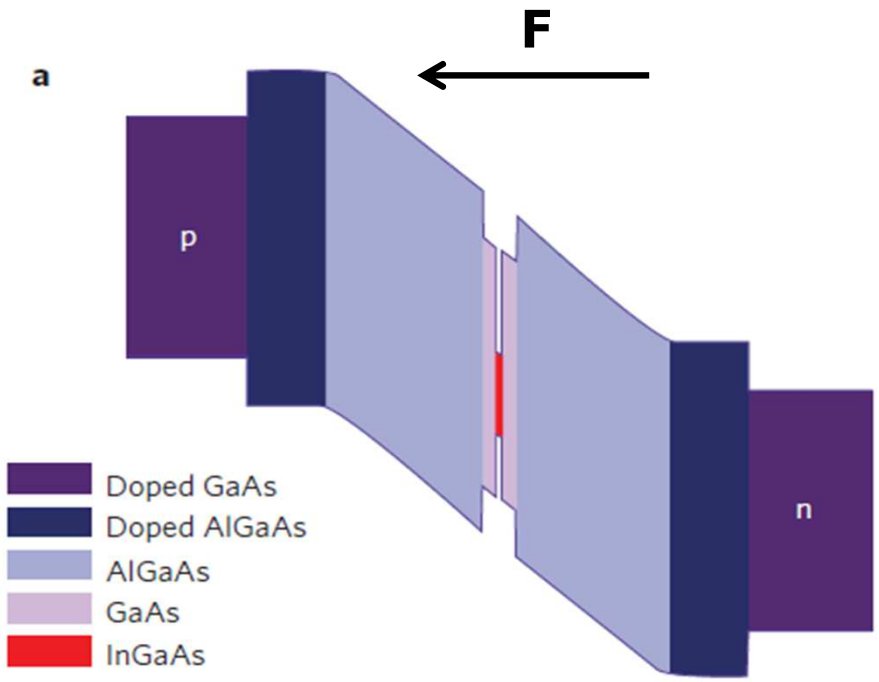

R.B. Patel et al. Nature Photon. **4,** 632 (2010)

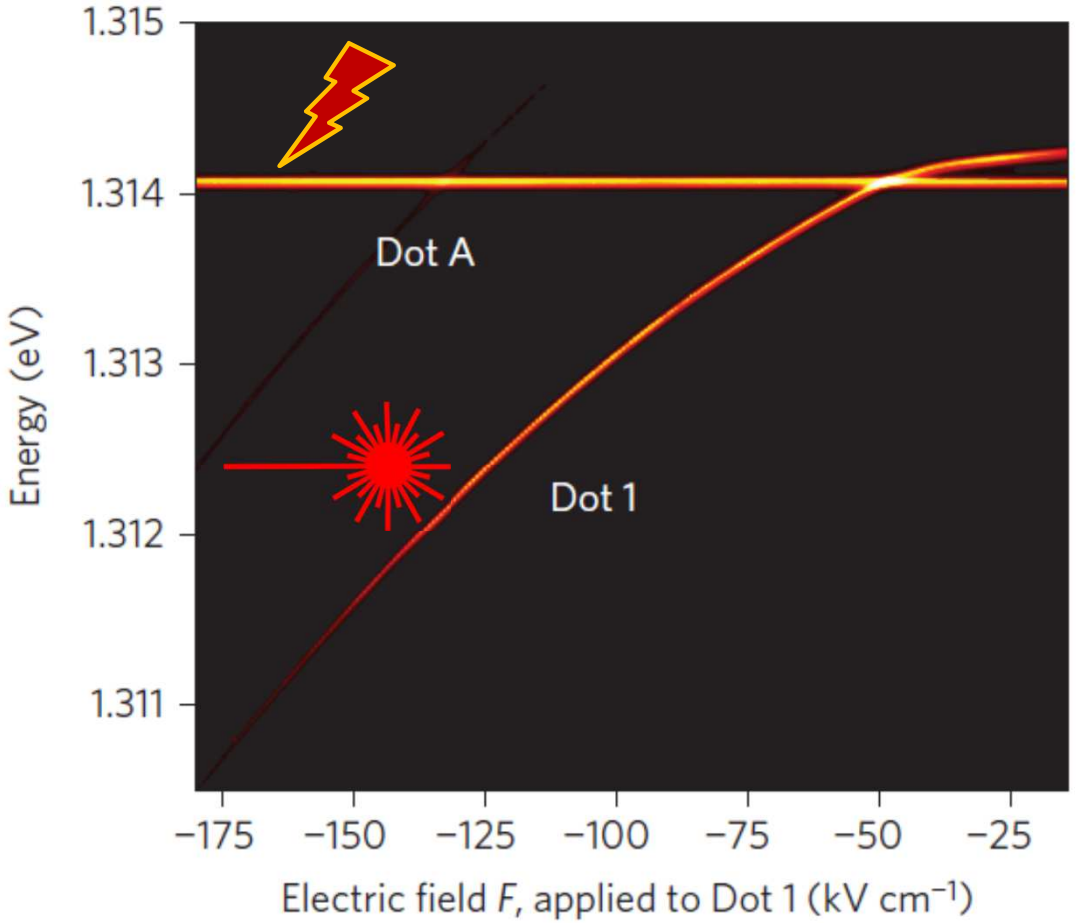

- Quantum confined Stark effect (QCSE)
  → Excitonic species shift according to: $E(F) = E_0 - p_z F - \beta F^2$
- Tuning range >20 meV → ~any two QDs can be brought into resonance
- Can be made local → scalable
- Problem: electrical injection not possible in reverse bias

3.3 Strain-engineering after growth

Besides electric- and magnetic fields, also **elastic strain** can be used to modify semiconductor properties!

MRS Bulletin, Feb. 2014

Classical strain engineering

Example: $In_{0.25}Ga_{0.75}As$

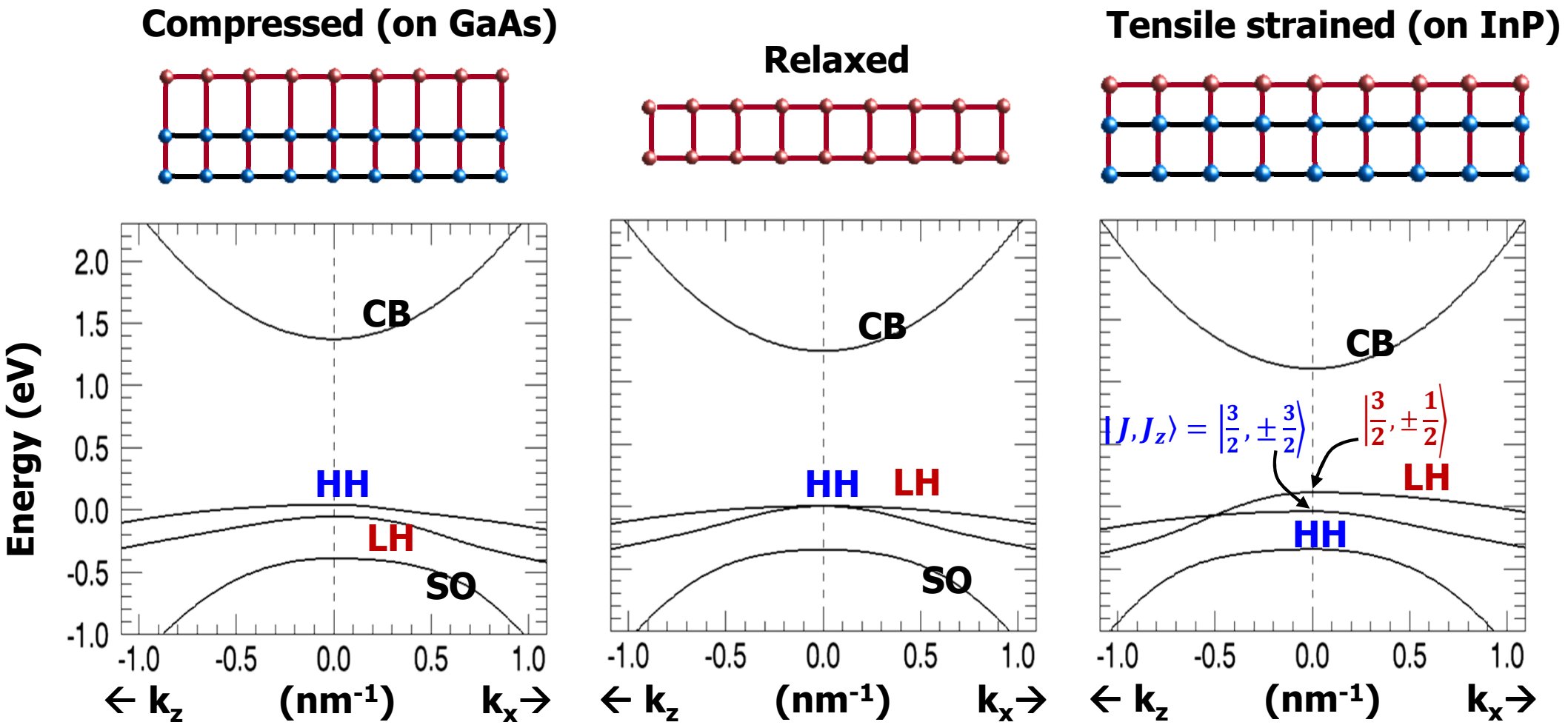

Calculation based on k.p method (see, e.g. S.L. Chuang, *Physics of photonic devices*, Wiley, 2009)

Classical strain engineering and its limitations

Example: $In_{0.25}Ga_{0.75}As$

Strain effects:

- Changes in bond-lengths → Change of energy bandgap → change in emission energy
- Changes in crystal symmetry → Lifting of band degeneracies → Changes in emission and polarization properties
- …

Limitations of classical strain engineering:

- Limited choice of substrates
- Strain affects growth
- Fine tuning?

Tensile strained (on InP)

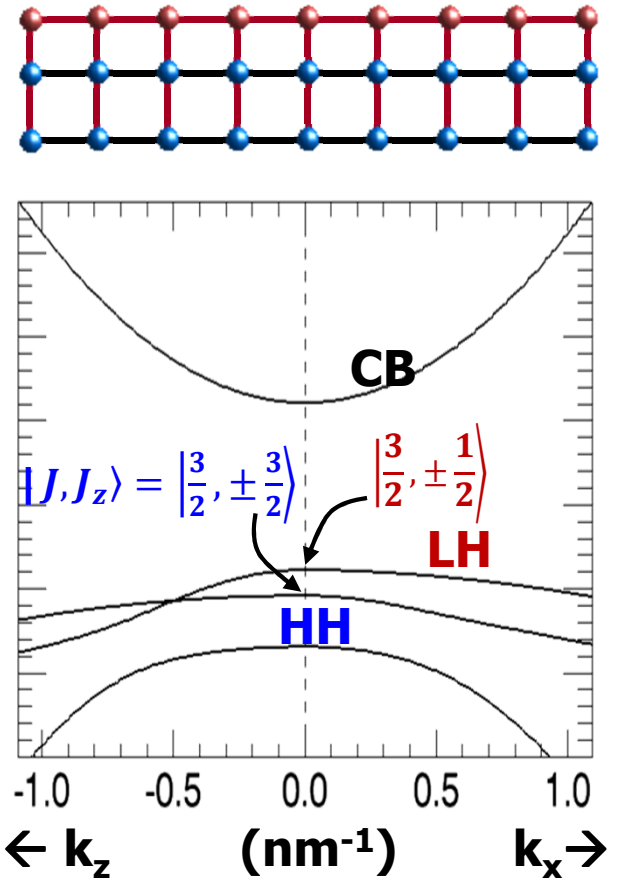

Calculation based on k.p method (see, e.g. S.L. Chuang, *Physics of photonic devices*, Wiley, 2009)

3.3 QD tuning via piezoelectric-induced strain fields

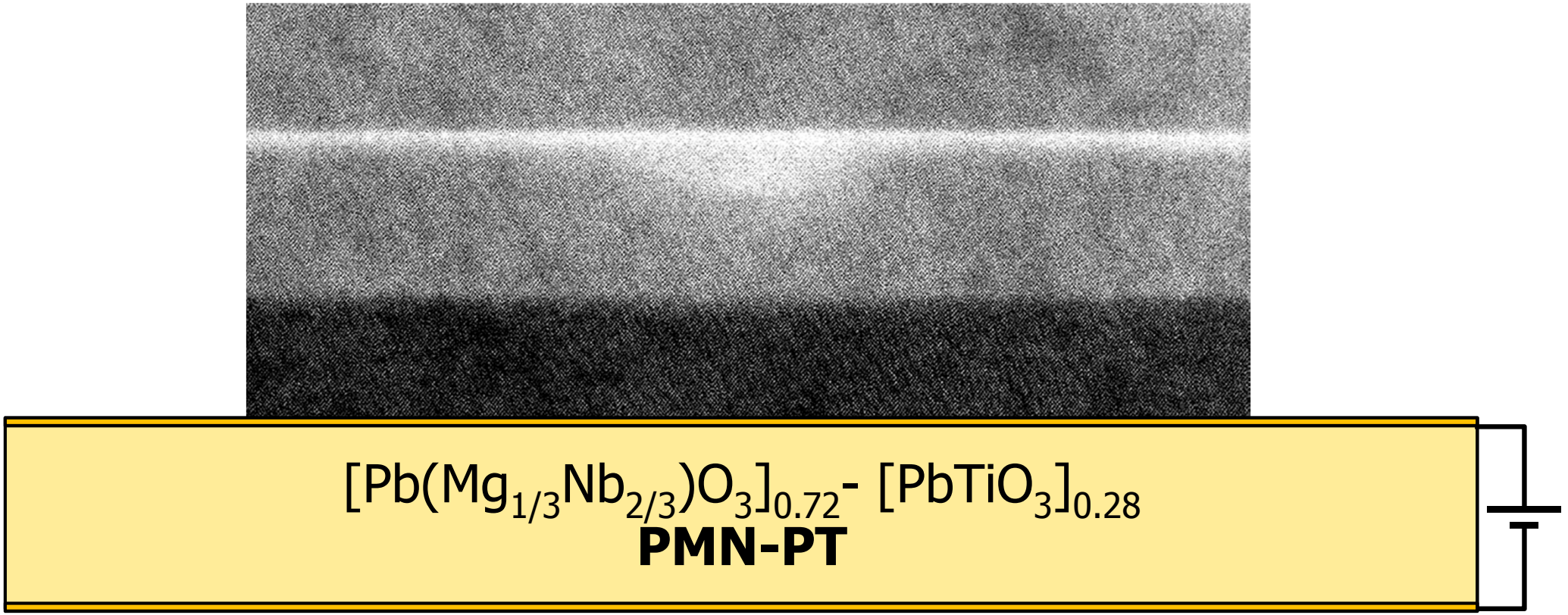

Reversible biaxial strains up to ~ ±0.2 % at low temperatures

First work with QDs and PMN-PT: T. Zander *et al.,* Optics Express **17,** 22452 (2009)
Review: AR *et al.* Phys. Status Solidi 249, 687 (2012)
Previous works using PZT (strain limited to ~0.02% - S. Seidl, *et al.*, APL **88,** 203113 (2006))

Replacing GaAs substrate with PMN-PT

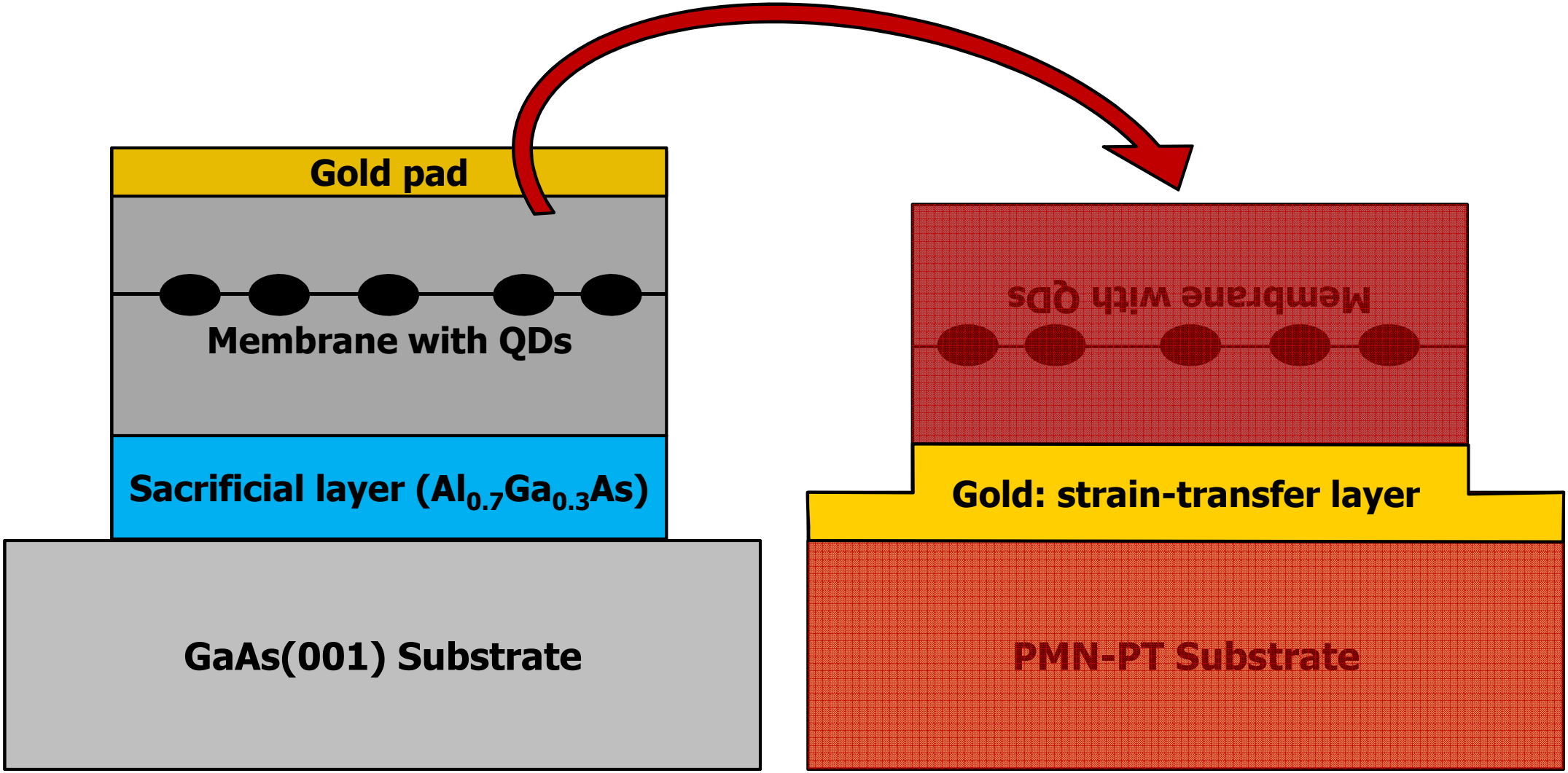

Thermocompression bonding @ 300°C

R. Trotta *et al*. Adv. Mater. 24, 2668 (2012)

Hybrid semiconductor-piezoelectric devices

JKU
JOHANNES KEPLER
UNIVERSITÄT LINZ

SEM after focused ion beam cut

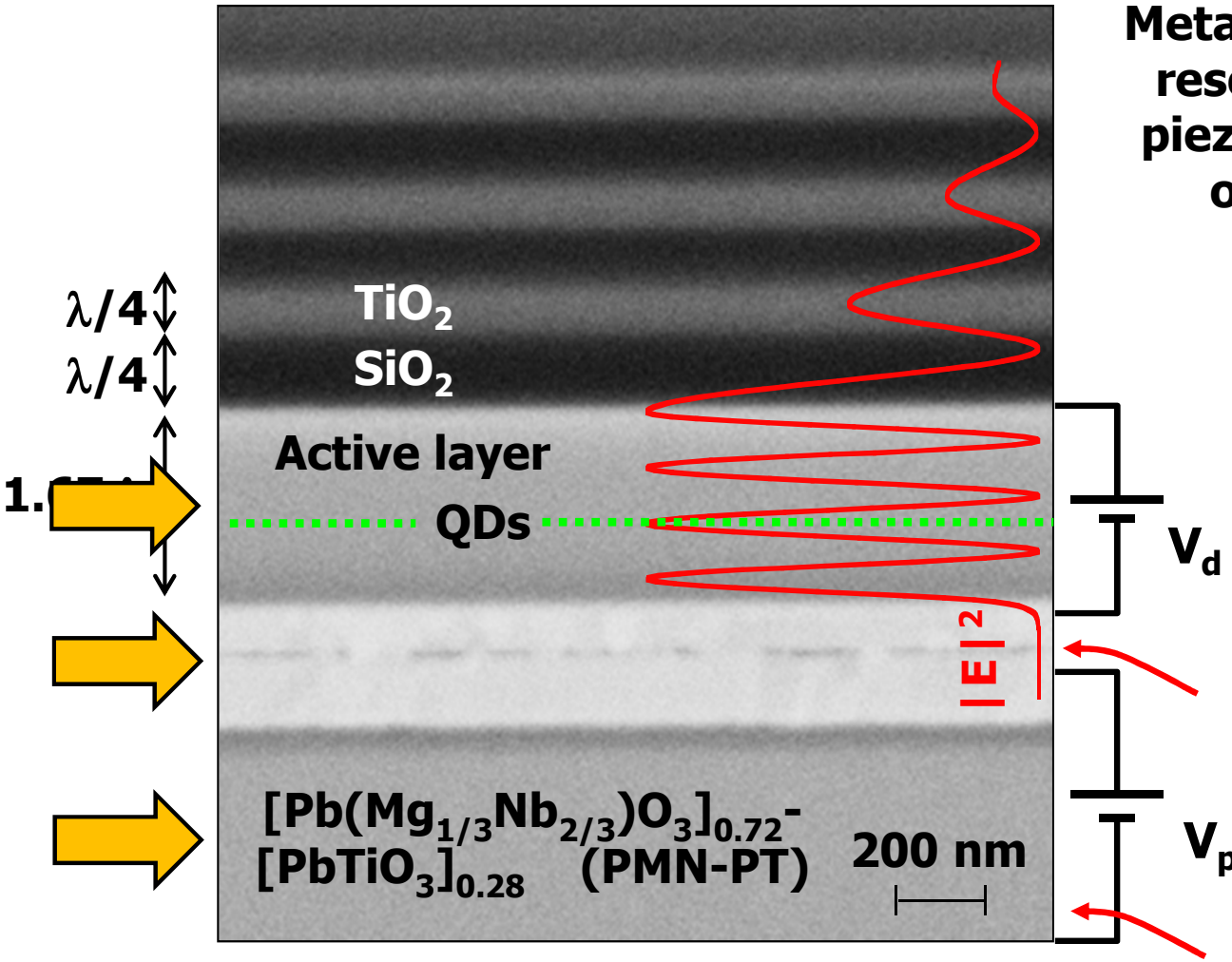

Metal-semiconductor-dielectric resonant-cavity structure on piezo (~10-20x enhancement of extraction efficiency)

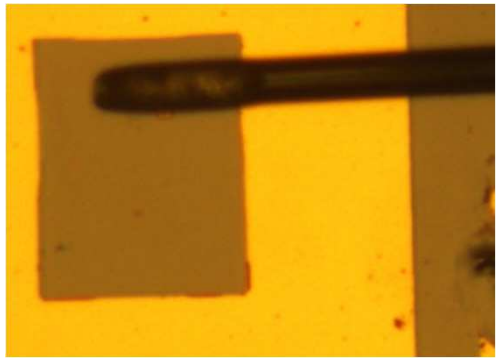

Optical microscopy view of 100x120 μm² membrane diode

Au bonding layer / mirror / electrical contact

Induces (slightly anisotropic) biaxial strain in QDs

R. Trotta *et al*. Adv. Mater. 24, 2668 (2012)

An energy-tunable InGaAs QD RC-LED

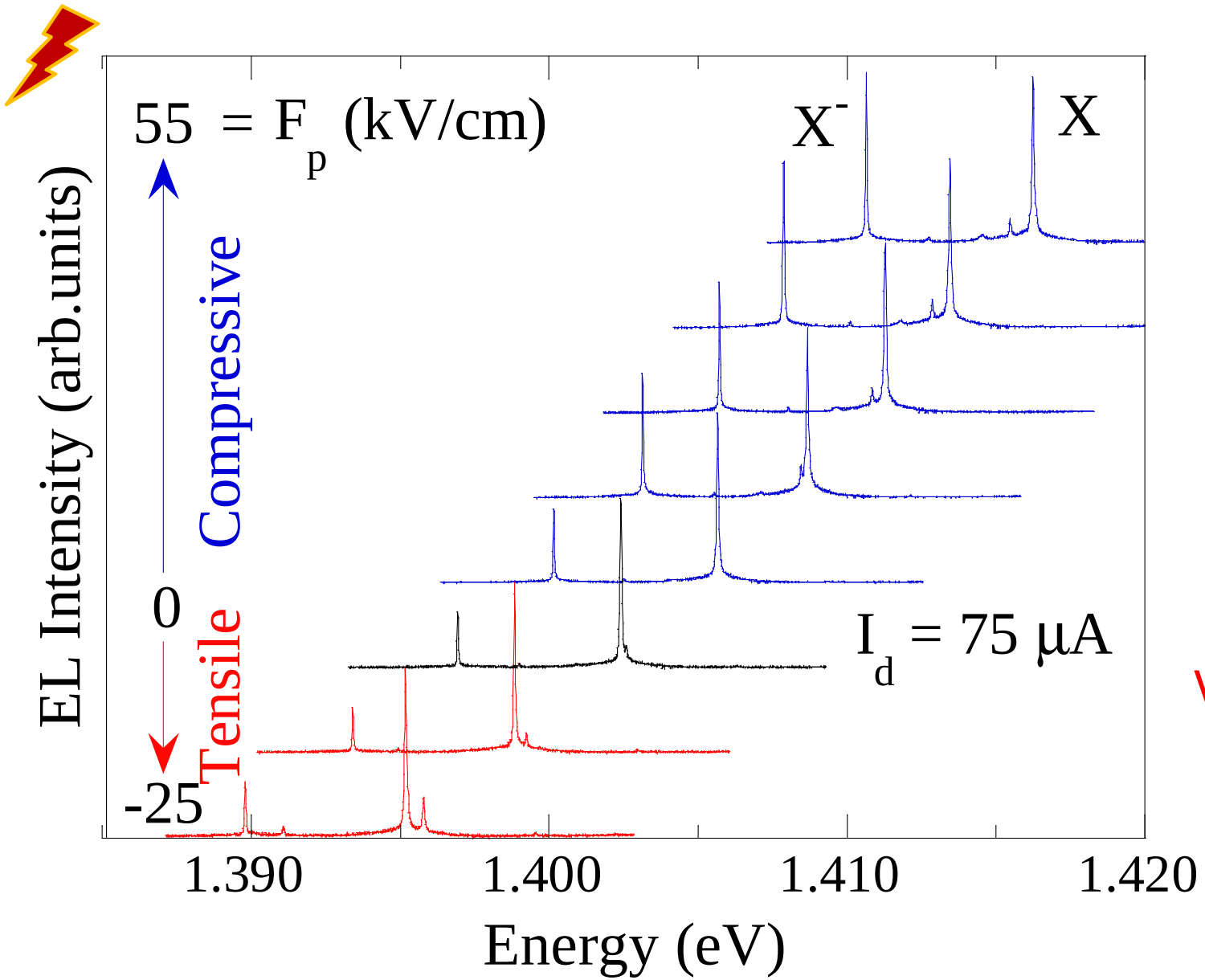

InGaAs/GaAs QD in ~500 nm thick n-i-p diode membrane
→ DC Electroluminescence spectra

V_d used to control current I_d in diode (→EL intensity)

V_p controls emission energy shift (>20 meV, strain change ~0.4%)

R. Trotta *et al*. Adv. Mater. 24, 2668 (2012)

Energy-tunable QD-single-photon source

Spectrally selected X emission

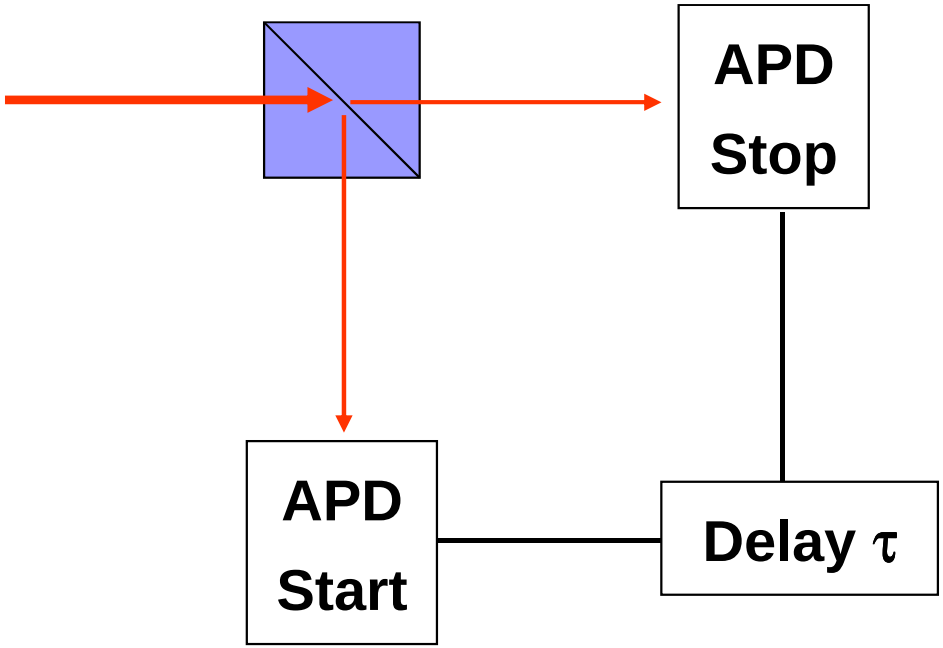

← Hambury-Brown and Twiss setup

See P. Michler et al., Science 290, 2282 (2000) and Refs. therein

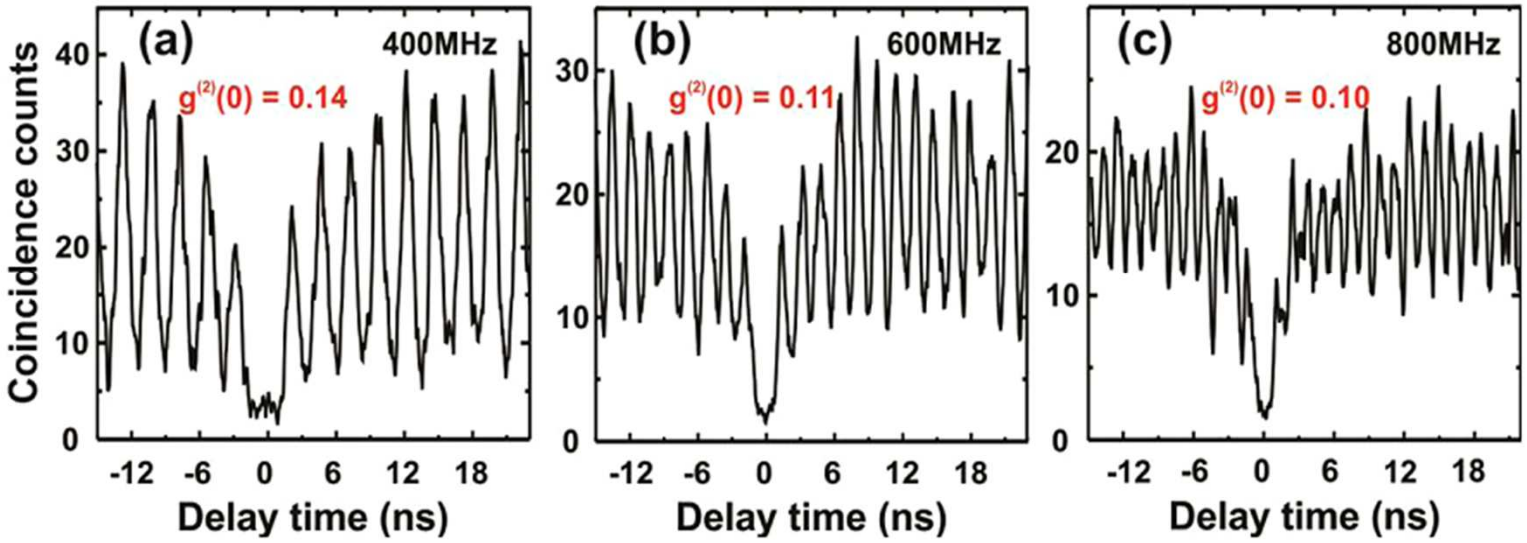

Modulation up to 800 MHz achieved

J. Zhang, et al, Nano Letters, 13, 5808 (2013)

QD-LEDs with same emission energy

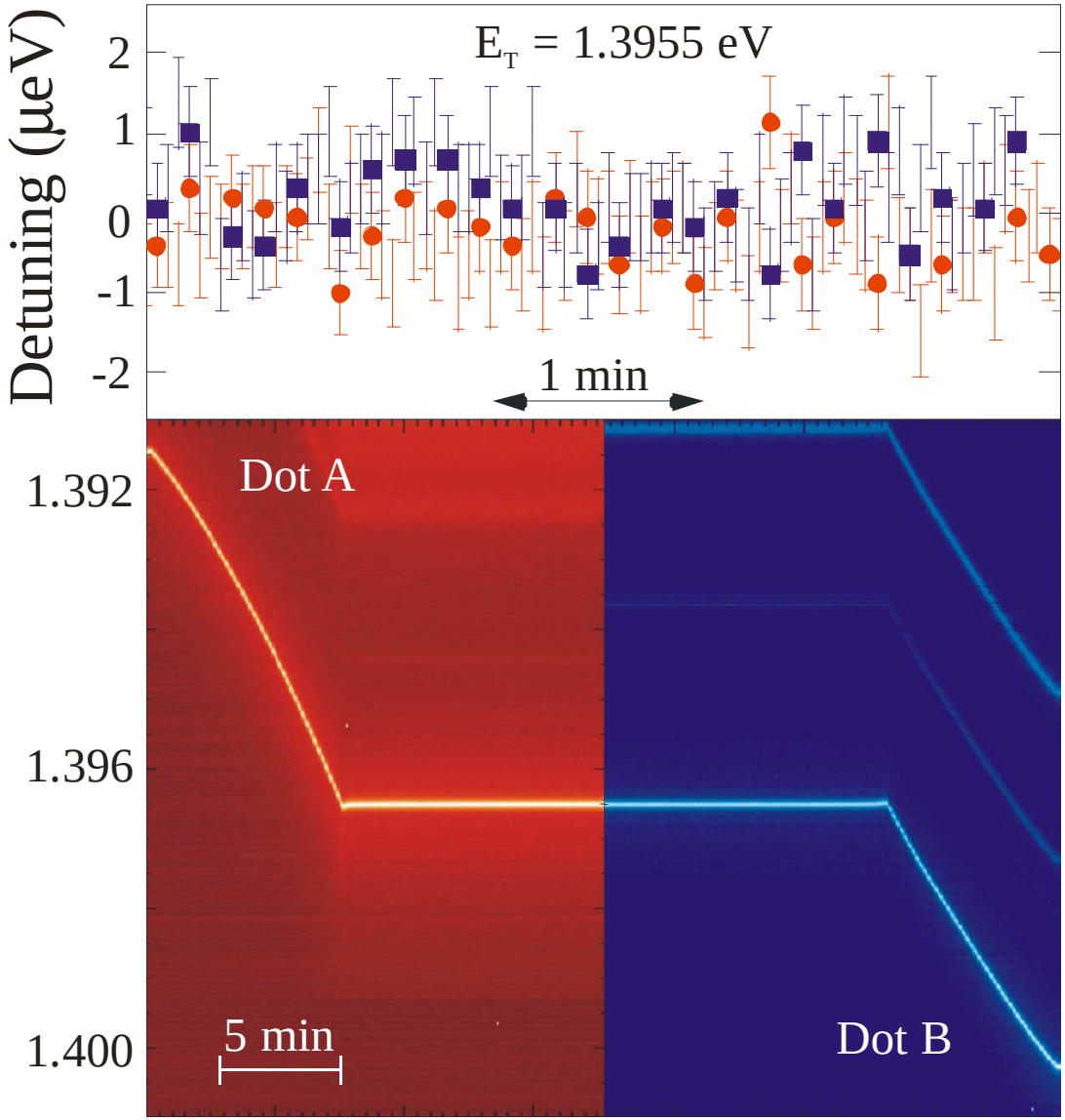

μeV stabilization reached with spectrometer (25 μeV res.) +real-time fitting + feedback

$$\frac{\text{Range}}{\text{Precision}} \sim 20.000$$

Note:

ΔE=1 μeV (~natural linewidth)

↔ Δσ ~10 kPa ↔ $\Delta\varepsilon_{//}$ ~$8 \cdot 10^{-8}$

↔ Δ bond lengths ~20 am

↔ Δ membrane thickness ~40 fm

Problem: with strain one can tune only one emission line of the QD

R. Trotta *et al*. Adv. Mater. 24, 2668 (2012)

Problem with as-grown QDs

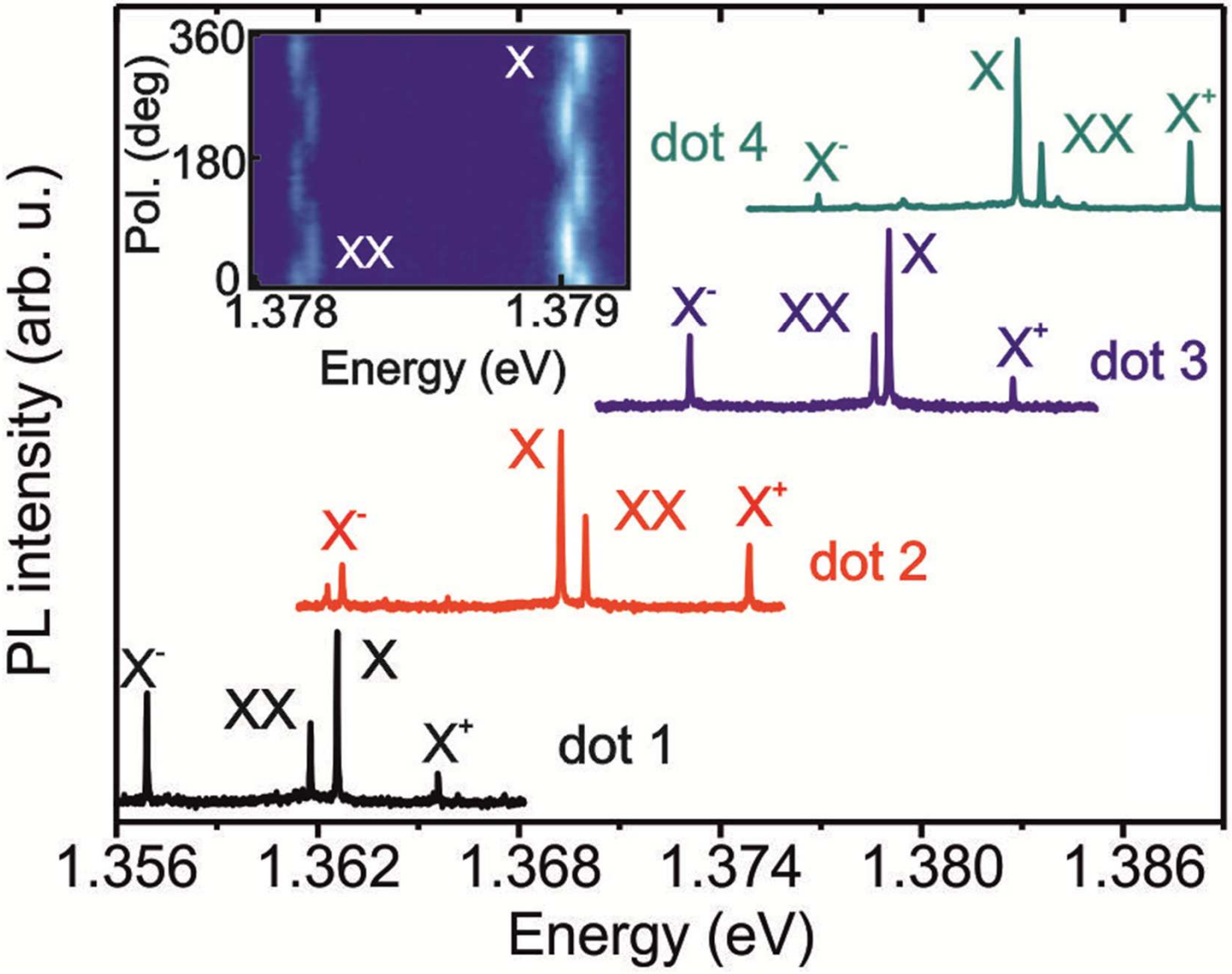

QD spectrum varies from QD to QD

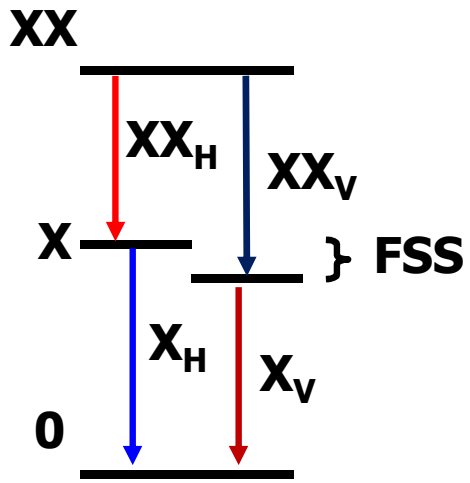

FSS, induced by QD **anisotropy**, prevents using most QDs as sources of entangled photons

Longstanding problem… M. Bayer, et al., Phys. Rev. B 65, 195315 (2002)
R. Trotta, E. Zallo, E. Magerl, O. G. Schmidt, A. Rastelli, Phys. Rev. B (2013)

3.4 Combination of strain and electric fields

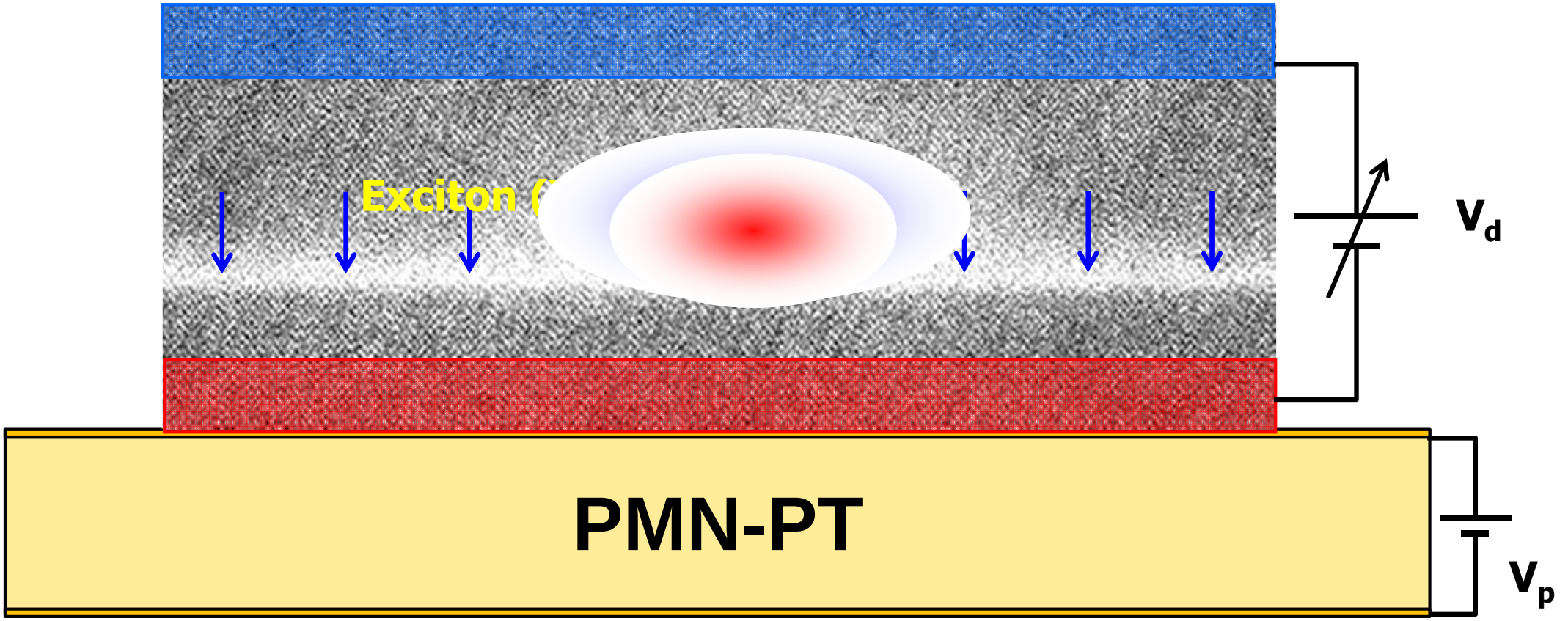

Diode membrane operated in reverse bias → QD in electric field

Independent control of X and XX energy

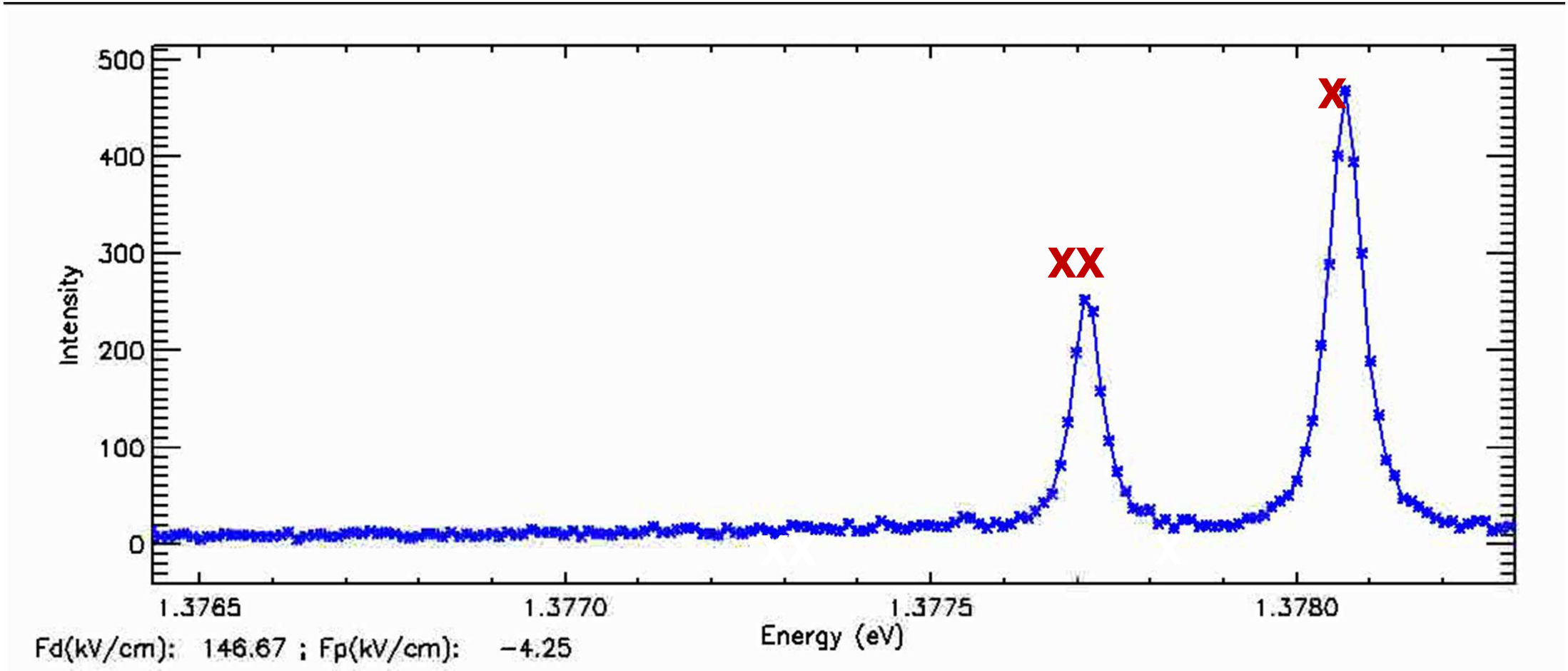

1) Drive X to predefined energy and lock with feedback on piezo
2) Ramp electric field in diode to decrease E_B(XX) while compensating X shift via piezo

R. Trotta, E. Zallo, E. Magerl, O. G. Schmidt, A. Rastelli, Phys. Rev. B (2013)

Independent control of X and XX energy

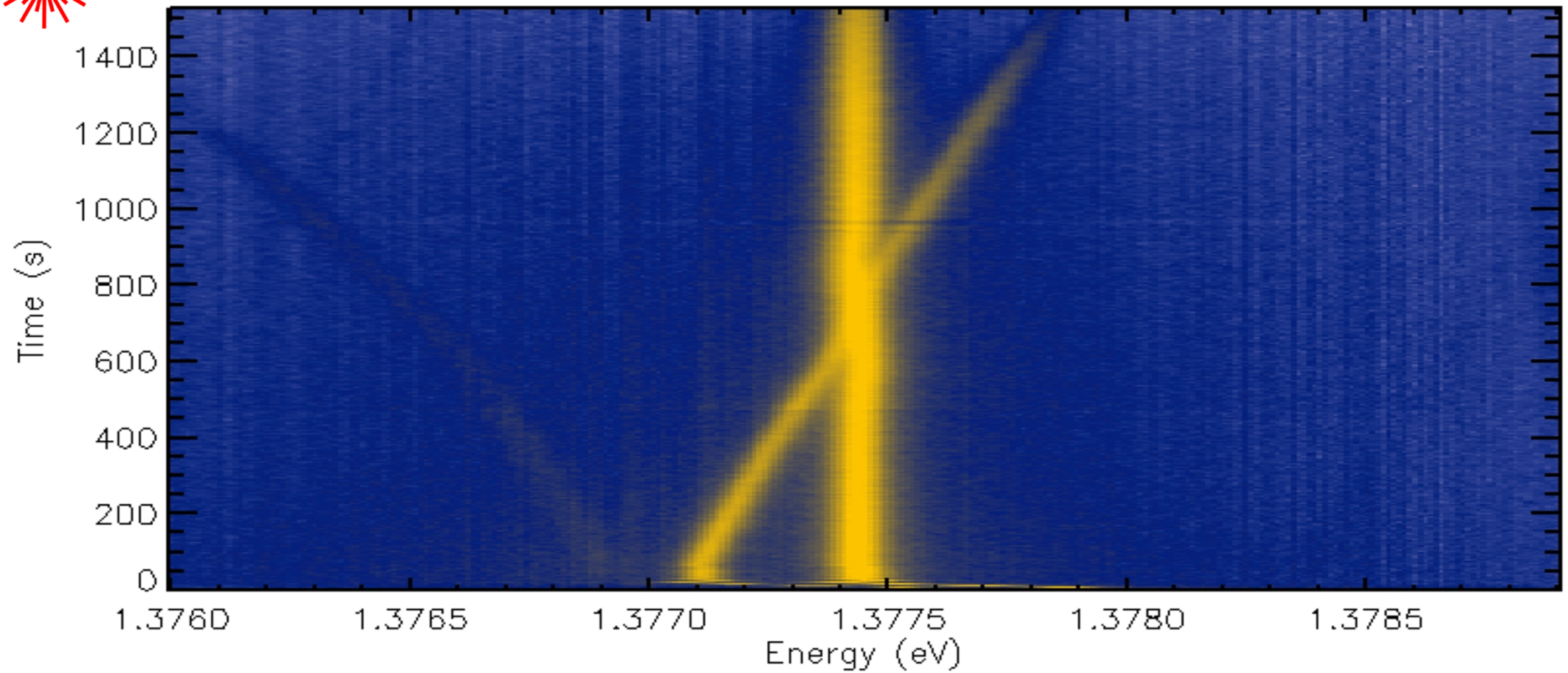

Two „tuning knobs" → Two QD parameters can be controlled independently
What about FSS? We would need anisotropic strain...

R. Trotta, E. Zallo, E. Magerl, O. G. Schmidt, A. Rastelli, Phys. Rev. B (2013)

Conclusions

- Semiconductor epitaxy gives the chance to create nanostructures enabling us to play with (and perhaps make us of) quantum mechanics

- Tight (but gentle) control on the properties of such nanostructures is unavoidable to keep playing

→ Site-control (by growth) and electronic structure control (after growth) seem the way to go.
→ Site-control via top-down + bottom-up is promising, but material quality is still an issue. Good ideas are welcome!
→ For optical properties control, stress application after growth is very promising and some miniaturization (down to the μm scale) appears feasible.

Realistic situation – quantum relay?!

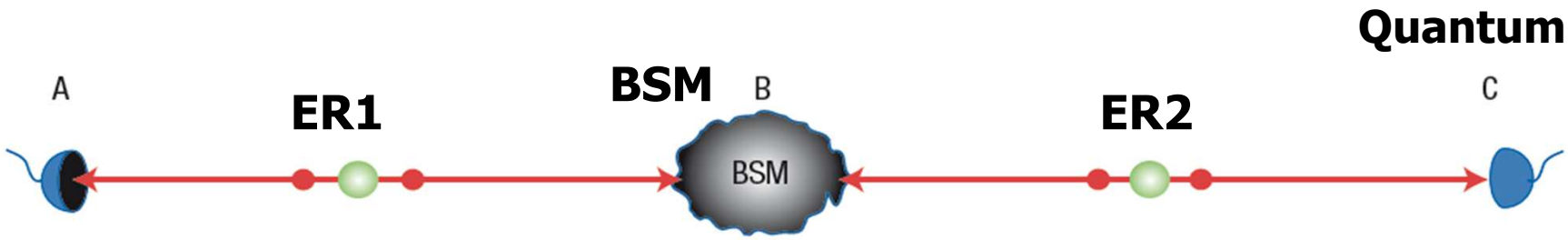

Required elements: Entanglement resources (ER) Bell-State-Measurement (BSM)

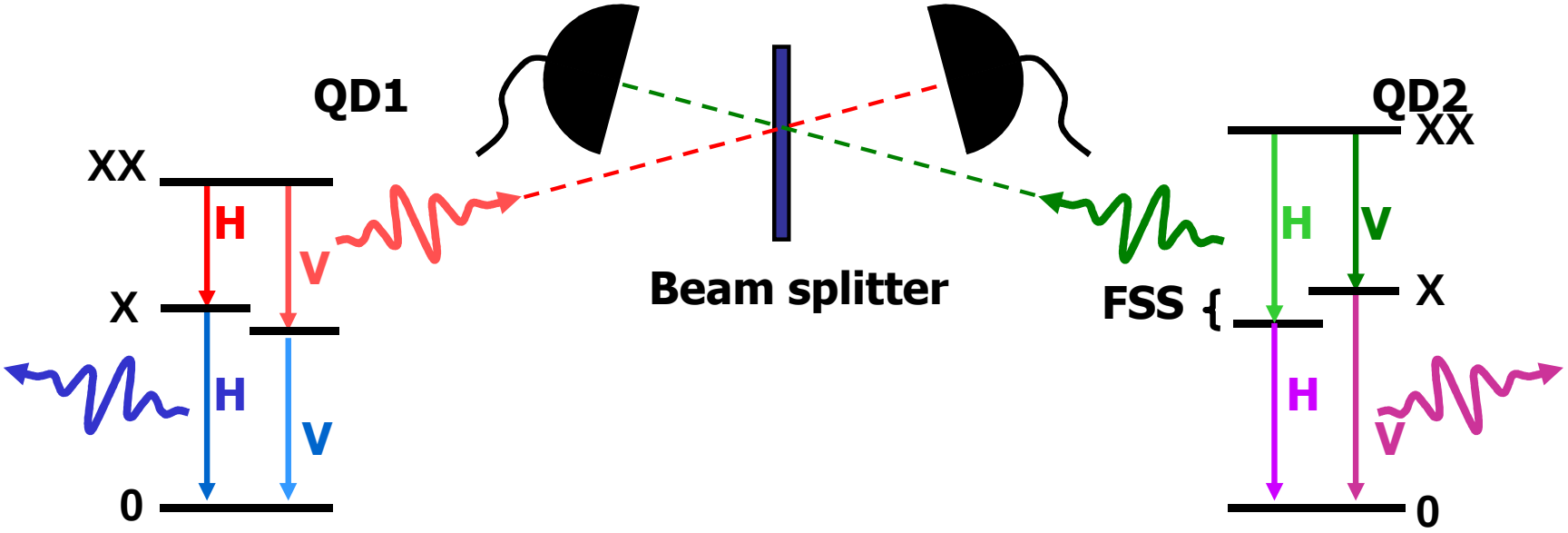

We need methods to tune emission energies of XX→X, X→0 and fine structure splitting (FSS)

Classical strain engineering

Example: $In_{0.25}Ga_{0.75}As$

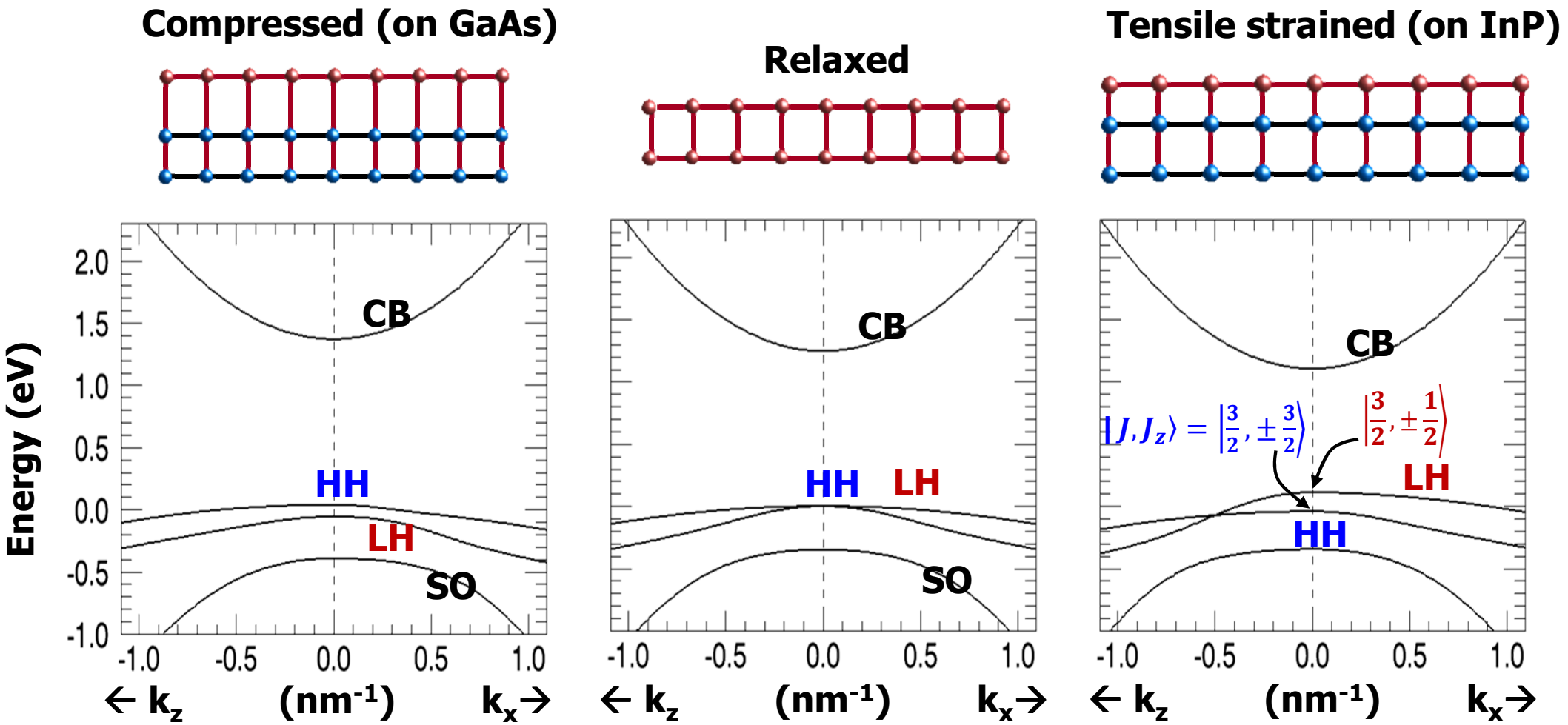

Calculation based on k.p method (see, e.g. S.L. Chuang, *Physics of photonic devices*, Wiley, 2009)

Electronic structure of optically-active QDs

Sketch of potential profiles and confined states in a InGaAs or GaAs QD (simplified picture

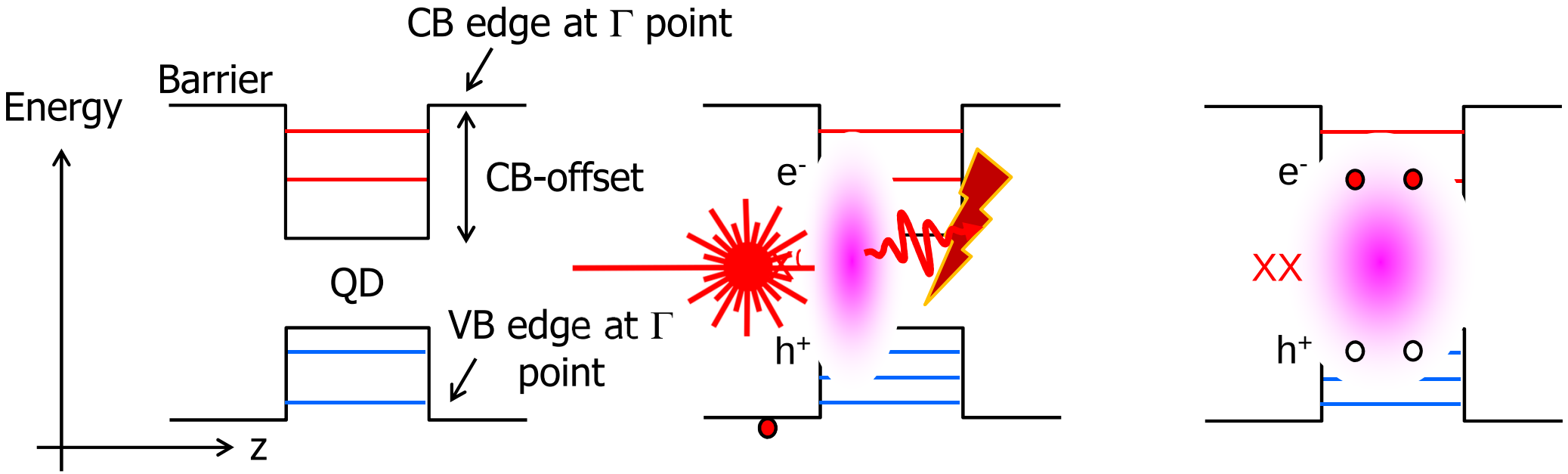

Crystal ground state: all valence band (VB) states are fully occupied and conduction band (CB) states empty

Neutral exciton X^0: one electron e^- is excited (optically or <u>electrically</u>) to CB leaving a single hole h^+ in VB. e^- & h^+ bond by Coulomb attraction (similar to positronium). Radiative recombination leads to emission of a single photon

Neutral biexciton XX: 2 e^- excited to CB leaving 2 h^+ in VB. Radiative recombination leads to 2 photon cascade (usually with different energy due to interactions)

QDs as sources of entangled photons on demand

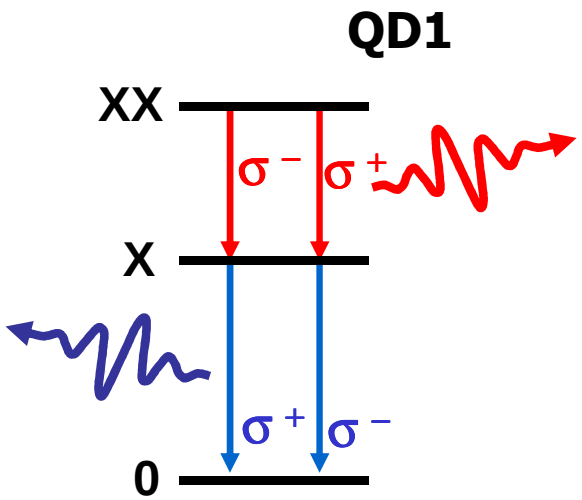

XX (biexciton) has two decay paths to X. If they are degenerate in energy a polarization-entangled photon pair can be produced

$$|\psi\rangle = \frac{1}{\sqrt{2}}\left(|\sigma^+\rangle_{XX}|\sigma^-\rangle_X + |\sigma^-\rangle_{XX}|\sigma^+\rangle_X\right)$$

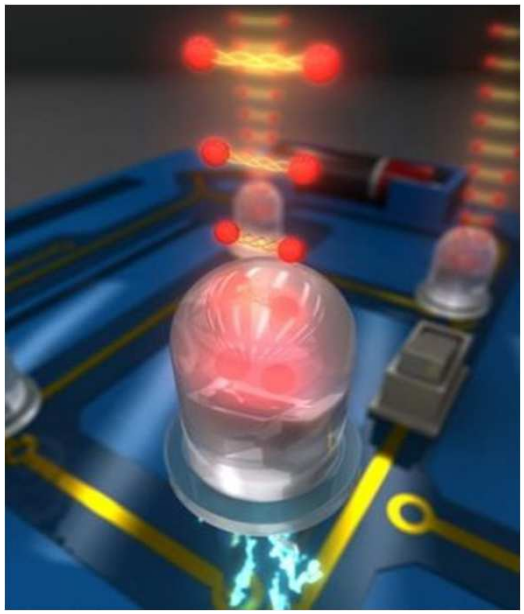

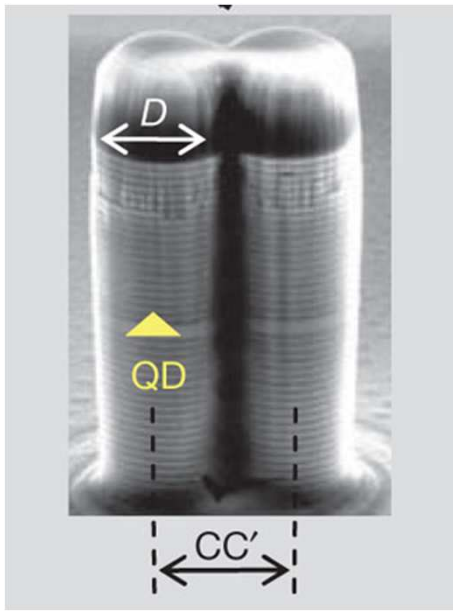

- ✓ Electrical excitation
- ✓ Compatible with photonic processing
- ✓ On demand emission
- ✓ Time stability
- - Cooling needed (4 K)

Salter et al, Nature 465, 594 (2010)
Dousse et al. Nature 466, 217 (2010)

Concept: O. Benson et al PRL 84, 2513 (2000)
First demonstration: R. M. Stevenson *et al*, Nature **439**, 179 (2006)

A quantum relay with QDs?

N. Gisin, R. Thew, Nature Photon. **1,** 165 (2007)

Quantum Relay

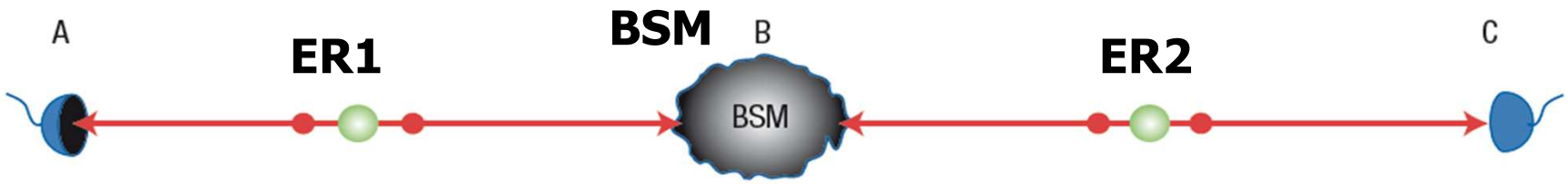

Entanglement resource (ER): XX→X→0 cascade in QD

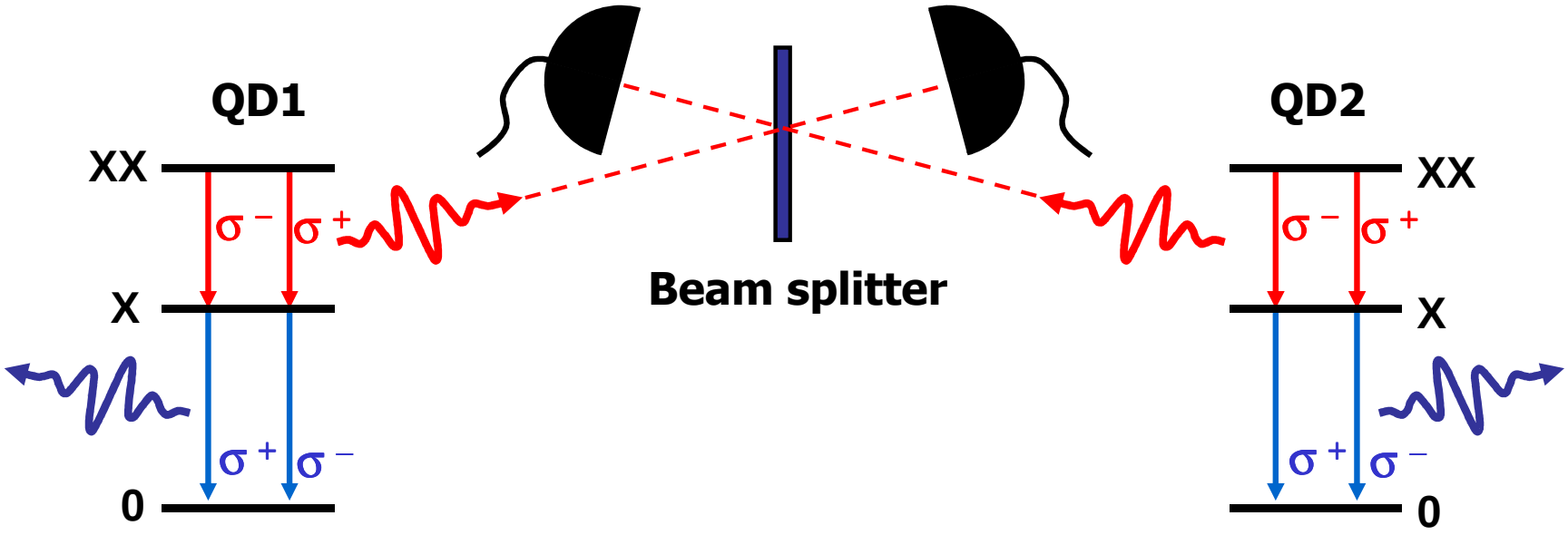

See Mark Fox, Introduction to quantum optics

Classical strain engineering and its limitations

Example: $In_{0.25}Ga_{0.75}As$

Strain effects:

- Changes in bond-lengths → Change of energy bandgap → change in emission energy
- Changes in crystal symmetry → Lifting of band degeneracies → Changes in emission and polarization properties
- …

Limitations of classical strain engineering:

- Limited choice of substrates
- Strain affects growth
- Fine tuning?

Tensile strained (on InP)

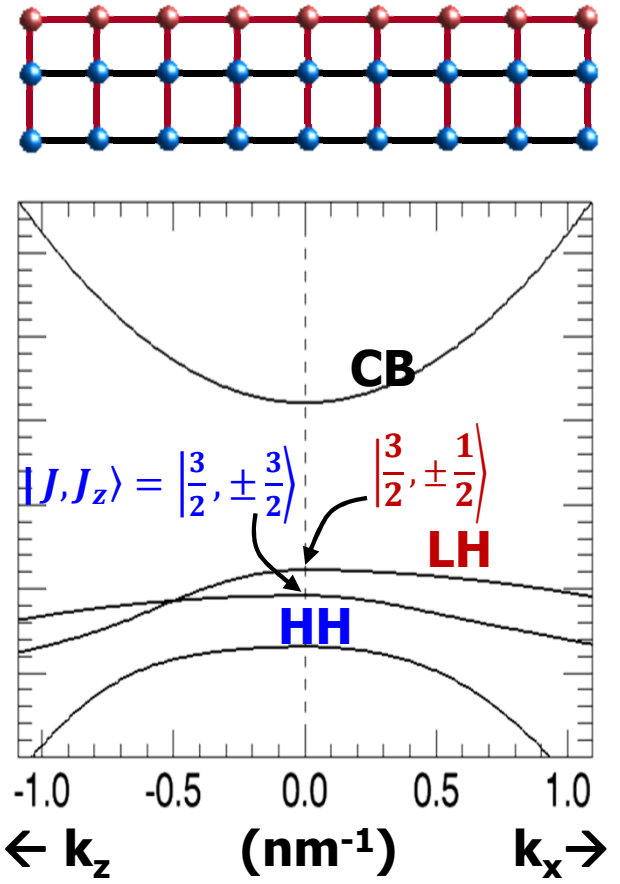

Calculation based on k.p method (see, e.g. S.L. Chuang, *Physics of photonic devices*, Wiley, 2009)

Example of top-down + bottom-up + top-down

J.-N. Aqua and X. Xu Surface Science 639 (2015) 20–24